

EXPERIMENTAL AND NUMERICAL ANALYSIS OF COMPRESSION  
ON A FORGING PRESS

A THESIS SUBMITTED  
TO THE GRADUATE SCHOOL OF NATURAL AND APPLIED SCIENCES OF  
MIDDLE EAST TECHNICAL UNIVERSITY

BY

GÖKHAN BİÇER

IN PARTIAL FULLFILMENT OF THE REQUIREMENTS  
FOR  
THE DEGREE OF MASTER OF SCIENCE  
IN  
MECHANICAL ENGINEERING

JUNE 2010

Approval of the thesis:

**EXPERIMENTAL AND NUMERICAL ANALYSIS OF COMPRESSION ON A  
FORGING PRESS**

submitted by **GÖKHAN BİÇER** in partial fulfillment of the requirements for the degree of **Master of Science in Mechanical Engineering, Middle East Technical University** by,

Prof. Dr. Canan Özgen  
Dean, Graduate School of **Natural and Applied Sciences** \_\_\_\_\_

Prof. Dr. Süha Oral  
Head of the Department, **Mechanical Engineering** \_\_\_\_\_

Prof. Dr. Mustafa İlhan Gökler  
Supervisor, **Mechanical Engineering Dept., METU** \_\_\_\_\_

Prof. Dr. Haluk Darendeliler  
Co-Supervisor, **Mechanical Engineering Dept., METU** \_\_\_\_\_

**Examining Committee Members:**

Prof. Dr. Bülent Doyum  
Mechanical Engineering Dept., METU \_\_\_\_\_

Prof. Dr. Mustafa İlhan Gökler  
Mechanical Engineering Dept., METU \_\_\_\_\_

Prof. Dr. Haluk Darendeliler  
Mechanical Engineering Dept., METU \_\_\_\_\_

Prof. Dr. Suat Kadioğlu  
Mechanical Engineering Dept., METU \_\_\_\_\_

Prof. Dr. Can Çoğun  
Mechanical Engineering Dept., Gazi Uni. \_\_\_\_\_

**Date:** June 18<sup>th</sup>, 2010

**I hereby declare that all information in this document has been obtained and presented in accordance with academic rules and ethical conduct. I also declare that, as required by these rules and conduct, I have fully cited and referenced all material and results that are not original to this work.**

Name, Last name: Gökhan Biçer

Signature:

## ABSTRACT

### EXPERIMENTAL AND NUMERICAL ANALYSIS OF COMPRESSION ON A FORGING PRESS

Biçer, Gökhan

M. Sc., Department of Mechanical Engineering

Supervisor: Prof. Dr. Mustafa İlhan Gökler

Co-Supervisor: Prof. Dr. Haluk Darendeliler

June 2010, 108 Pages

Forging is a metal forming process which involves non-linear deformations. Finite element and finite volume software programs are commonly used to simulate the process. In these simulations, material properties are required. However, stress-strain relations of the materials at some elevated temperatures are not available in the material libraries of the related software programs. In this study, the stress-strain curves have been obtained by applying the Cook and Larke Simple Compression Test to AISI 1045 steel at several temperatures on a forging press with a capacity of 1000 tons. The stress-strain curves have also been determined by simulating the processes in a commercial finite element software. It is observed that experimental results are consistent with the numerical ones. A modular die set has been designed and manufactured to conduct the Cook and Larke Simple Compression Test. It has been shown that the forging press with data acquisition system can be used as a material testing equipment to obtain stress-strain curves.

**Keywords:** Cook and Larke Simple Compression Test, Hot Forging, AISI 1045

## ÖZ

### DÖVME PRESİNDEKİ BASMANIN DENEYSEL VE SAYISAL OLARAK İNCELENMESİ

Biçer, Gökhan

Yüksek Lisans, Makina Mühendisliği Bölümü  
Tez Yöneticisi: Prof. Dr. Mustafa İlhan Gökler  
Ortak Tez Yöneticisi: Prof. Dr. Haluk Darendeliler

Haziran 2010, 108 Sayfa

Dövme, doğrusal olmayan şekil değiştirmeleri içeren bir metal şekillendirme işlemidir. Sonlu elemanlar ve sonlu hacim yazılım programları bu işlemin benzetiminde kullanılırlar. Benzetimler için malzeme özellikleri gereklidir. Ancak malzemelerin bazı yüksek sıcaklıklardaki gerilim-gerinim ilişkileri ilgili yazılım programlarının malzeme kütüphanelerinde mevcut değildir. Bu çalışmada, 1000 tonluk bir dövme presinde Cook ve Larke basit basma deneyinin uygulanması ile AISI 1045 çeliği için gerilim-gerinim eğrileri elde edilmiştir. Gerilim-gerinim eğrileri ticari bir sonlu elemanlar yazılımı kullanılarak da belirlenmiştir. Deneysel sonuçların, sayısal sonuçlar ile uyumlu oldukları gözlenmiştir. Cook ve Larke basit basma deneyini gerçekleştirmek için modüler bir kalıp seti hazırlanmıştır. Veri alma sistemine sahip dövme presinin, gerilim-gerinim eğrilerini elde etmek için bir malzeme test cihazı gibi kullanılabilceği gösterilmiştir.

**Anahtar Kelimeler:** Cook ve Larke Basit Basma Deneyi, Sıcak Dövme, AISI 1045

## ACKNOWLEDGEMENTS

I express sincere appreciation to my supervisor Prof. Dr. Mustafa İlhan Gökler who is the director of METU-BILTIR Center and my co-supervisor Prof. Dr. Haluk Darendeliler, head of the Metal Forming Unit of the same research and application center at METU.

I would like to thank to METU-BILTIR Center for facilities provided to me throughout this study.

I also wish to thank to Mr. Cevat Kömürcü who is the general manager of AKSAN Steel Forging Company for his support.

I wish to thank to my senior colleagues Hüseyin Öztürk and Arda Özgen, and my colleagues at the moment Sinem Demirkaya, Ulaş Göçmen, and Boray Dişbudak for their valuable support, encouragement and assistance in METU-BILTIR Center.

Also thanks to the technical staff of METU-BILTIR Center; Halit Şahin, Ali Demir, Hüseyin Ali Atmaca for their dedicated efforts. And I also wish to thank to Servet Şehirli from Mechanical Engineering Department and Atalay Özdemir from Metallurgical and Materials Engineering Department of METU.

Further, thanks go to other personnel of METU-BILTIR Center, Filiz Güngör Sütekin, Tuğba Ertürk, Arzu Öztürk, Tanık Öden, Osman Mumcu, Halime Küçük and Mehmet Ali Sarıhan for their efforts and aids.

I would like to thank to my friends Doğan Kıvanç Aksungur from BIAS Engineering and Celalettin Yumuş from ASELSAN for their encouragements and assistance.

I am deeply indebt to my parents, my sister and my wife for their encouragement and faith in me.

## TABLE OF CONTENTS

ABSTRACT.....	iv
ÖZ .....	v
ACKNOWLEDGEMENTS .....	vi
TABLE OF CONTENTS .....	viii
LIST OF FIGURES .....	ix
LIST OF TABLES .....	xviii
CHAPTERS	
1. INTRODUCTION.....	1
1.1 Forging Process .....	1
1.2 Computational Methods for Forging Process .....	3
1.3 Simple Compression Test .....	3
1.4 Cook and Larke Simple Compression Test.....	4
1.5 Literature Survey on Material Testing .....	6
1.6 Scope of the Thesis .....	7
2. DESIGN AND MANUFACTURING OF FORGING DIES FOR COOK AND LARKE SIMPLE COMPRESSION TEST ON FORGING PRESS .....	8
2.1 Conceptual Die Design .....	8
2.2 Modular Die Set Design.....	18
3. COMPUTATIONAL STUDY .....	23
3.1 Performing Analyses in Simufact.forming 8.1 .....	23
3.2 Numerical Results .....	25
4. EXPERIMENTAL STUDY .....	57
4.1 Preparation for the Experiments.....	57
4.1.1 Specimens .....	57
4.1.2 Forging Dies.....	59

4.1.3 Heating Equipment and the Forging Press.....	60
4.1.4 Other Equipment .....	61
4.2 Data Acquisition System for Recording Load versus Crank Angle Values.....	63
4.3 Conducting Experiments.....	66
4.4 Experimental Results .....	70
5. DISCUSSION AND CONCLUSION.....	78
5.1 Comparison of Experimental and Numerical Results.....	78
5.2 General Conclusion.....	93
5.3 Future Works.....	93
REFERENCES.....	94
APPENDICIES	
A. TECHNICAL DRAWINGS OF THE DIE SET .....	96
B. PROPERTIES OF AISI 1045 STEEL .....	103
C. TECHNICAL INFORMATION OF SMERAL BRNO LZK 1000 <sup>®</sup> HOT FORGING PRESS.....	104
D. MANUAL FOR THE APPLICATION OF THE COOK AND LARKE SIMPLE COMPRESSION TEST AT METU-BILTIR CENTER FORGING RESEARCH AND APPLICATION LABORATORY .....	105
D.1 Main Steps for the Test .....	105
D.2 Applying the Cook and Larke Simple Compression Test for Specimens with Initial Diameter of 50 mm and the Height of 100 mm. ....	106



## LIST OF FIGURES

### FIGURES

Figure 1.1 Illustration of Open Die Forging Process .....	2
Figure 1.2 Illustration of Closed Die Forging Process.....	2
Figure 1.3 Illustration of Simple Compression Test .....	4
Figure 1.4 Graphical Illustration of Derivation of Yield Stress Curve by the Cook and Larke Simple Compression Test in the Case of Constant Reduction Application.....	5
Figure 1.5 Graphical Illustration of Derivation of Yield Stress Curve by the Cook and Larke Simple Compression Test in the Case of Constant Load Application.....	5
Figure 2.1 Lower Die Spaces of the Forging Press.....	8
Figure 2.2 Schematic Drawing of the Specimens According to Their Aspect Ratios .....	9
Figure 2.3 Schematic Drawings of the Specimens for the Cook and Larke Simple Compression Test According to their Aspect and Reduction Ratios .....	10
Figure 2.4 Ram Adjustment Mechanism of the Forging Press .....	11
Figure 2.5 Different Configurations of the Die Set.....	17
Figure 2.6 3D Models of the Die Set .....	19
Figure 2.7 Technical Drawing of the Circular Die Housings of the Die Holder of the Forging Press .....	20
Figure 2.8 Dimensions of the Lower Die.....	21
Figure 2.9 Dimensions of the Upper Die .....	22

Figure 2.10 Schematic Drawing of the Lower Forging Die Showing the Opening in front of it .....	22
Figure 3.1 Axi-symmetric Problem Set Up for the Finite Element Analysis .....	24
Figure 3.2 Graphical Output of the Numerical Result for the Process with $r=5\%$ at $900^{\circ}\text{C}$ for the Specimen with $h_0=100$ mm.....	25
Figure 3.3 Graphical Output of the Numerical Result for the Process with $r=10\%$ at $900^{\circ}\text{C}$ for the Specimen with $h_0=100$ mm.....	26
Figure 3.4 Graphical Output of the Numerical Result for the Process with $r=20\%$ at $900^{\circ}\text{C}$ for the Specimen with $h_0=100$ mm.....	26
Figure 3.5 Graphical Output of the Numerical Result for the Process with $r=30\%$ at $900^{\circ}\text{C}$ for the Specimen with $h_0=100$ mm.....	27
Figure 3.6 Graphical Output of the Numerical Result for the Process with $r=40\%$ at $900^{\circ}\text{C}$ for the Specimen with $h_0=100$ mm.....	27
Figure 3.7 Graphical Output of the Numerical Result for the Process with $r=5\%$ at $1000^{\circ}\text{C}$ for the Specimen with $h_0=100$ mm.....	28
Figure 3.8 Graphical Output of the Numerical Result for the Process with $r=10\%$ at $1000^{\circ}\text{C}$ for the Specimen with $h_0=100$ mm.....	28
Figure 3.9 Graphical Output of the Numerical Result for the Process with $r=20\%$ at $1000^{\circ}\text{C}$ for the Specimen with $h_0=100$ mm.....	29
Figure 3.10 Graphical Output of the Numerical Result for the Process with $r=30\%$ at $1000^{\circ}\text{C}$ for the Specimen with $h_0=100$ mm.....	29
Figure 3.11 Graphical Output of the Numerical Result for the Process with $r=40\%$ at $1000^{\circ}\text{C}$ for the Specimen with $h_0=100$ mm.....	30
Figure 3.12 Graphical Output of the Numerical Result for the Process with $r=5\%$ at $1100^{\circ}\text{C}$ for the Specimen with $h_0=100$ mm.....	30
Figure 3.13 Graphical Output of the Numerical Result for the Process with $r=10\%$ at $1100^{\circ}\text{C}$ for the Specimen with $h_0=100$ mm.....	31
Figure 3.14 Graphical Output of the Numerical Result for the Process with $r=20\%$ at $1100^{\circ}\text{C}$ for the Specimen with $h_0=100$ mm.....	31

Figure 3.15 Graphical Output of the Numerical Result for the Process with r=30% at 1100°C for the Specimen with h <sub>0</sub> =100 mm.....	32
Figure 3.16 Graphical Output of the Numerical Result for the Process with r=40% at 1100°C for the Specimen with h <sub>0</sub> =100 mm.....	32
Figure 3.17 Graphical Output of the Numerical Result for the Process with r=5% at 900°C for the Specimen with h <sub>0</sub> =50 mm.....	33
Figure 3.18 Graphical Output of the Numerical Result for the Process with r=10% at 900°C for the Specimen with h <sub>0</sub> =50 mm.....	33
Figure 3.19 Graphical Output of the Numerical Result for the Process with r=20% at 900°C for the Specimen with h <sub>0</sub> =50 mm.....	34
Figure 3.20 Graphical Output of the Numerical Result for the Process with r=30% at 900°C for the Specimen with h <sub>0</sub> =50 mm.....	34
Figure 3.21 Graphical Output of the Numerical Result for the Process with r=40% at 900°C for the Specimen with h <sub>0</sub> =50 mm.....	35
Figure 3.22 Graphical Output of the Numerical Result for the Process with r=5% at 1000°C for the Specimen with h <sub>0</sub> =50 mm.....	35
Figure 3.23 Graphical Output of the Numerical Result for the Process with r=10% at 1000°C for the Specimen with h <sub>0</sub> =50 mm.....	36
Figure 3.24 Graphical Output of the Numerical Result for the Process with r=20% at 1000°C for the Specimen with h <sub>0</sub> =50 mm.....	36
Figure 3.25 Graphical Output of the Numerical Result for the Process with r=30% at 1000°C for the Specimen with h <sub>0</sub> =50 mm.....	37
Figure 3.26 Graphical Output of the Numerical Result for the Process with r=40% at 1000°C for the Specimen with h <sub>0</sub> =50 mm.....	37
Figure 3.27 Graphical Output of the Numerical Result for the Process with r=5% at 1100°C for the Specimen with h <sub>0</sub> =50 mm.....	38
Figure 3.28 Graphical Output of the Numerical Result for the Process with r=10% at 1100°C for the Specimen with h <sub>0</sub> =50 mm.....	38
Figure 3.29 Graphical Output of the Numerical Result for the Process with r=20% at 1100°C for the Specimen with h <sub>0</sub> =50 mm.....	39

Figure 3.30 Graphical Output of the Numerical Result for the Process with r=30% at 1100°C for the Specimen with h <sub>0</sub> =50 mm.....	39
Figure 3.31 Graphical Output of the Numerical Result for the Process with r=40% at 1100°C for the Specimen with h <sub>0</sub> =50 mm.....	40
Figure 3.32 Graphical Output of the Numerical Result for the Process with r=5% at 900°C for the Specimen with h <sub>0</sub> =25 mm.....	40
Figure 3.33 Graphical Output of the Numerical Result for the Process with r=10% at 900°C for the Specimen with h <sub>0</sub> =25 mm.....	41
Figure 3.34 Graphical Output of the Numerical Result for the Process with r=20% at 900°C for the Specimen with h <sub>0</sub> =25 mm.....	41
Figure 3.35 Graphical Output of the Numerical Result for the Process with r=30% at 900°C for the Specimen with h <sub>0</sub> =25 mm.....	42
Figure 3.36 Graphical Output of the Numerical Result for the Process with r=40% at 900°C for the Specimen with h <sub>0</sub> =25 mm.....	42
Figure 3.37 Graphical Output of the Numerical Result for the Process with r=5% at 1000°C for the Specimen with h <sub>0</sub> =25 mm.....	43
Figure 3.38 Graphical Output of the Numerical Result for the Process with r=10% at 1000°C for the Specimen with h <sub>0</sub> =25 mm.....	43
Figure 3.39 Graphical Output of the Numerical Result for the Process with r=20% at 1000°C for the Specimen with h <sub>0</sub> =25 mm.....	44
Figure 3.40 Graphical Output of the Numerical Result for the Process with r=30% at 1000°C for the Specimen with h <sub>0</sub> =25 mm.....	44
Figure 3.41 Graphical Output of the Numerical Result for the Process with r=40% at 1000°C for the Specimen with h <sub>0</sub> =25 mm.....	45
Figure 3.42 Graphical Output of the Numerical Result for the Process with r=5% at 1100°C for the Specimen with h <sub>0</sub> =25 mm.....	45
Figure 3.43 Graphical Output of the Numerical Result for the Process with r=10% at 1100°C for the Specimen with h <sub>0</sub> =25 mm.....	46
Figure 3.44 Graphical Output of the Numerical Result for the Process with r=20% at 1100°C for the Specimen with h <sub>0</sub> =25 mm.....	46

Figure 3.45 Graphical Output of the Numerical Result for the Process with r=30% at 1100°C for the Specimen with h <sub>0</sub> =25 mm.....	47
Figure 3.46 Graphical Output of the Numerical Result for the Process with r=40% at 1100°C for the Specimen with h <sub>0</sub> =25 mm.....	47
Figure 3.47 Graphical Output of the Numerical Result for the Process with r=5% at 900°C for the Specimen with h <sub>0</sub> =16,67 mm.....	48
Figure 3.48 Graphical Output of the Numerical Result for the Process with r=10% at 900°C for the Specimen with h <sub>0</sub> =16,67 mm.....	48
Figure 3.49 Graphical Output of the Numerical Result for the Process with r=20% at 900°C for the Specimen with h <sub>0</sub> =16,67 mm.....	49
Figure 3.50 Graphical Output of the Numerical Result for the Process with r=30% at 900°C for the Specimen with h <sub>0</sub> =16,67 mm.....	49
Figure 3.51 Graphical Output of the Numerical Result for the Process with r=40% at 900°C for the Specimen with h <sub>0</sub> =16,67 mm.....	50
Figure 3.52 Graphical Output of the Numerical Result for the Process with r=5% at 1000°C for the Specimen with h <sub>0</sub> =16,67 mm.....	50
Figure 3.53 Graphical Output of the Numerical Result for the Process with r=10% at 1000°C for the Specimen with h <sub>0</sub> =16,67 mm.....	51
Figure 3.54 Graphical Output of the Numerical Result for the Process with r=20% at 1000°C for the Specimen with h <sub>0</sub> =16,67 mm.....	51
Figure 3.55 Graphical Output of the Numerical Result for the Process with r=30% at 1000°C for the Specimen with h <sub>0</sub> =16,67 mm.....	52
Figure 3.56 Graphical Output of the Numerical Result for the Process with r=40% at 1000°C for the Specimen with h <sub>0</sub> =16,67 mm.....	52
Figure 3.57 Graphical Output of the Numerical Result for the Process with r=5% at 1100°C for the Specimen with h <sub>0</sub> =16,67 mm.....	53
Figure 3.58 Graphical Output of the Numerical Result for the Process with r=10% at 1100°C for the Specimen with h <sub>0</sub> =16,67 mm.....	53
Figure 3.59 Graphical Output of the Numerical Result for the Process with r=20% at 1100°C for the Specimen with h <sub>0</sub> =16,67 mm.....	54

Figure 3.60 Graphical Output of the Numerical Result for the Process with r=30% at 1100°C for the Specimen with $h_0=16,67$ mm.....	54
Figure 3.61 Graphical Output of the Numerical Result for the Process with r=40% at 1100°C for the Specimen with $h_0=16,67$ mm.....	55
Figure 4.1 Grinding of the Specimens .....	58
Figure 4.2 Turning Operation of the Lower Die .....	59
Figure 4.3 CNC Milling of the Lower Die .....	59
Figure 4.4 Inserts of the Die Set after Machining Operations .....	60
Figure 4.5 (a) 125 kVA Induction Heater (b) 1000 Ton Capacity Forging Press....	61
Figure 4.6 Fixed Pyrometer.....	62
Figure 4.7 (a) LPG Tube with Flame Gun for Preheating the Dies (b) Tong for Holding Hot Specimens .....	62
Figure 4.8 Portable Pyrometer .....	63
Figure 4.9 Picture Showing the Elements of the Data Acquisition System.....	64
Figure 4.10 (a) One of the Strain Gages Attached to the Forging Press (b) Encoder of the Data Acquisition System.....	64
Figure 4.11 DECADE 260 <sup>®</sup> Unit (a) Screen on the Front Side (b) View of the Hardware when the Back Cover is Opened .....	65
Figure 4.12 Schematic View Showing the Working Principle of the Data Acquisition System .....	66
Figure 4.13 Preheating of the Forging Dies .....	67
Figure 4.14 (a) Heated Specimen Leaving the Induction Heater (b) Measuring the Temperature of a Specimen by a Pyrometer Before Forging Process.....	67
Figure 4.15 A Specimen Waiting to be Forged Between the Dies .....	68
Figure 4.16 Grouped Specimens Waiting for Cooling.....	68
Figure 4.17 Measuring the Final Height of a Specimen .....	69

Figure 4.18 Grouped Specimens after Measurement .....	69
Figure 5.1 Plotting and Curve Fitting of True Stress vs. $d_0/h_0$ for the Experimental Study at 900°C .....	79
Figure 5.2 True Stress vs. True Strain Curve for the Experimental Study at 900°C .....	80
Figure 5.3 Plotting and Curve Fitting of True Stresses versus Aspect Ratios for the Experimental Study at 1000°C .....	81
Figure 5.4 True Stress versus True Strain Curve for Experimental Study at 1000°C .....	82
Figure 5.5 Plotting and Curve Fitting of True Stress versus $d_0/h_0$ for the Experimental Study at 1100°C .....	83
Figure 5.6 True Stress versus True Strain Curve for Experimental Study at 1100°C .....	84
Figure 5.7 Plotting and Curve Fitting of True Stress versus $d_0/h_0$ for the Numerical Study at 900°C .....	85
Figure 5.8 True Stress versus True Strain Curve for Numerical Study at 900°C .....	86
Figure 5.9 Plotting and Curve Fitting of True Stress versus $d_0/h_0$ for the Numerical Study at 1000°C .....	87
Figure 5.10 True Stress versus True Strain Curve for Numerical Study at 1000°C .....	88
Figure 5.11 Plotting and Curve Fitting of True Stress versus $d_0/h_0$ for the Numerical Study at 1100°C .....	89
Figure 5.12 True Stress versus True Strain Curve for Numerical Study at 1100°C .....	90
Figure 5.13 True Stress versus True Strain Curves Obtained from all Numerical and Experimental Studies .....	91
Figure 5.14 True Stress versus True Strain Values Obtained from Numerical and Experimental Studies with the Ones Obtained from Material Tests at Room Temperature .....	92

Figure A.1 Technical Drawing of the Upper Die.....	97
Figure A.2 Technical Drawing of the Lower Die .....	98
Figure A.3 Technical Drawing of the Insert with 10 mm Height .....	99
Figure A.4 Technical Drawing of the Insert with 20 mm Height .....	100
Figure A.5 Technical Drawing of the Insert with 30 mm Height .....	101
Figure A.6 Technical Drawing of the Insert with 40 mm Height .....	102



## LIST OF TABLES

### TABLES

Table 2.1 Dimensions for the Specimens with Initial Diameter 50 mm .....	12
Table 2.2 Dimensions for the Specimens with Initial Diameter 45 mm .....	13
Table 2.3 Dimensions for the Specimens with Initial Diameter 40 mm .....	14
Table 2.4 Dimensions for the Specimens with Initial Diameter 35 mm .....	15
Table 2.5 Dimensions for the Specimens with Initial Diameter 30 mm .....	16
Table 2.6 Die Set Configuration for the Application of the Cook and Larke Simple Compression Test to the Specimens with Initial Diameter 50 mm .....	18
Table 3.1 Number of the Mesh Elements According to the Geometries of the Specimens .....	24
Table 3.2 Maximum Force Values (kN) of the Processes at 900°C .....	55
Table 3.3 Maximum Force Values (kN) of the Processes at 1000°C .....	56
Table 3.4 Maximum Force Values (kN) of the Processes at 1100°C .....	56
Table 4.1 Specimen Dimensions According to Selected Aspect Ratios .....	57
Table 4.2 The Dimensions, Temperatures and Force Values Measured in the Experiments .....	70
Table 5.1 True Stress Values Obtained from the Graph in Figure 5.1 and Calculated True Strains .....	80
Table 5.2 True Stress Values Obtained from the Graph in Figure 5.3 and Calculated True Strains .....	81

Table 5.3 True Stress Values Obtained from the Graph in Figure 5.5 and Calculated True Strains .....	83
Table 5.4 True Stress Values Obtained from the Graph in Figure 5.7 and Calculated True Strains .....	85
Table 5.5 True Stress Values Obtained from the Graph in Figure 5.9 and Calculated True Strains .....	87
Table 5.6 True Stress Values Obtained from the Graph in Figure 5.11 and Calculated True Strains .....	89

## CHAPTER 1

### INTRODUCTION

#### 1.1 Forging Process

Forging could simply be defined as shaping an object by applying compressive forces. This process is generally classified according to the type of the die set used, temperature and material of the workpiece.

According to the type of the die set, forging can be classified as open die forging and closed die or impression die forging.

Open die forging gets its name from the fact that the dies do not enclose the workpiece, allowing it to flow except where contacted by the dies. The dies are usually flat in shape [1]. An illustrative example of open die forging is shown in Figure 1.1. In impression die forging, metal is placed in a die resembling a mold, which is attached to the anvil. The ram squeezes on the workpiece, causing the metal to flow and fill the cavities. Excess metal is squeezed out of the die cavities, forming what is referred to as flash shown in Figure 1.2. The flash forces the metal to completely fill the die cavity. After forging process, the flash is removed by trimming process [1]. Both open die and closed die stages may be used subsequently in forging a product.

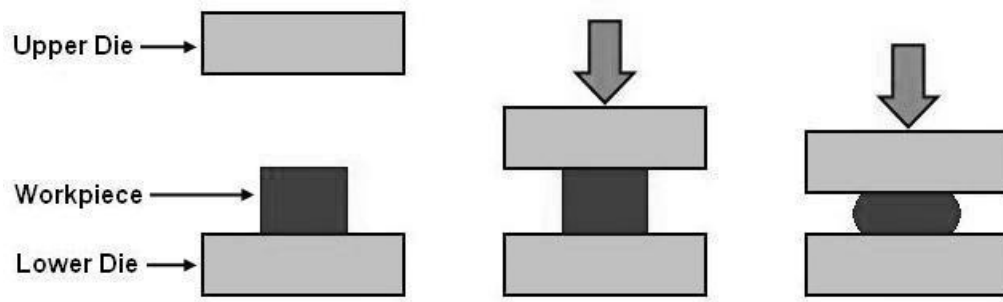


**Figure 1.1 Illustration of Open Die Forging Process**

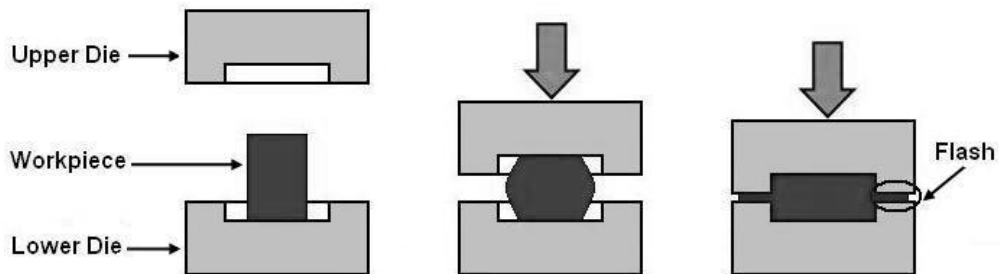


**Figure 1.2 Illustration of Closed Die Forging Process**

According to temperature of the workpiece to be formed, forging processes are classified as hot forging, warm forging and cold forging. If the temperature is above the material's recrystallization temperature, it is deemed "hot forging"; if the temperature is below the material's recrystallization temperature but above  $3/10^{\text{th}}$  of recrystallization temperature (in Kelvin) it is deemed "warm forging"; if below  $3/10^{\text{th}}$  of the recrystallization temperature (usually room temperature) then it is deemed "cold forging". The main advantage of hot forging is that the metal is deformed with less energy, and work hardening effects are negated due to the recrystallization process. Cold forging typically results in work hardening of the piece and it can be applied generally for simple geometries [1].

Another classification can be done according to the type of the workpiece material. This classification can be done as forging of ferrous metals and non-ferrous metals.

But practically processes are named as with the name of the workpiece material to be forged i.e. steel forging, aluminum forging etc.

## **1.2 Computational Methods for Forging Processes**

Forging processes can be simulated and analyzed by using the numerical methods such as finite element or finite volume analyses [2-13]. Several studies have been completed by the help of computer analysis programs. In these studies, the material properties of the workpiece to be formed are needed. It is possible to determine the material properties from the library of the software. However, in these libraries, there are limited materials and a few temperatures. In the analyses, the properties of a selected material may be necessary at a temperature other than the available ones in the software library. Also due to the variations in the material production, it may be necessary to determine the properties by using the actual material or verify these properties.

The mechanical properties of the materials can be obtained by using either the tension test or the compression test. In general, mechanical properties of materials obtained from the simple tension test are available in the material libraries of the software.

## **1.3 Simple Compression Test**

In the simple compression test, a specimen is subjected to load between the upper and lower dies of a test machine as shown in Figure 1.3. If there were no friction between the ends of the specimen, one should hope the specimen's diameter in every circular cross section enlarge by the same value while the height decreases. However, homogenous compression is difficult to achieve because of friction between the ends of the specimen and the deforming tools. This causes barreling of the specimen with increasing load as shown in Figure 1.3 [14].

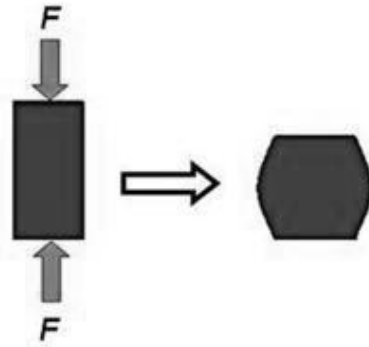


**Figure 1.3 Illustration of Simple Compression Test**

#### **1.4 Cook and Larke Simple Compression Test**

Cook and Larke Simple Compression Test can be conducted in two ways [15]; using constant reduction or constant load for various specimens. These specimens have the same diameters but different heights. Typical height/diameter ratios are 3, 2, 1 and  $\frac{1}{2}$ . In the constant reduction test, the specimens are compressed and the mean stress is calculated from the load and the current cross-sectional area on the assumption of uniform diameter and with constant volume. A graph of apparent yield stress versus the aspect ratio,  $d_0/h_0$ , is plotted for various percentage reductions  $r=[(h_0-h)/h_0]*100$  where  $d_0$  and  $h_0$  are the original diameter and height, respectively, while  $h$  is the current height. Extrapolation to zero  $d_0/h_0$  ratio (i.e to infinite length) is used to give the true yield stress. Figure 1.4 shows this method of deriving the results.

In the constant load application method, the cylinders of different heights, but of the same initial diameter are all subjected to the same load in succession, then the taller the cylinder the more it will deform for a given load, because of the small interference from friction at the ends. In the incremental loading technique, the test piece is removed from the testing machine so that the height can be measured accurately. All specimens are successively subjected to the same load, and the percentage reduction in height is calculated. Extrapolation of percentage reduction

against  $d_0/h_0$  ratio gives the percentage reduction that would have occurred with an infinitely long test piece [15] (Figure 1.5)

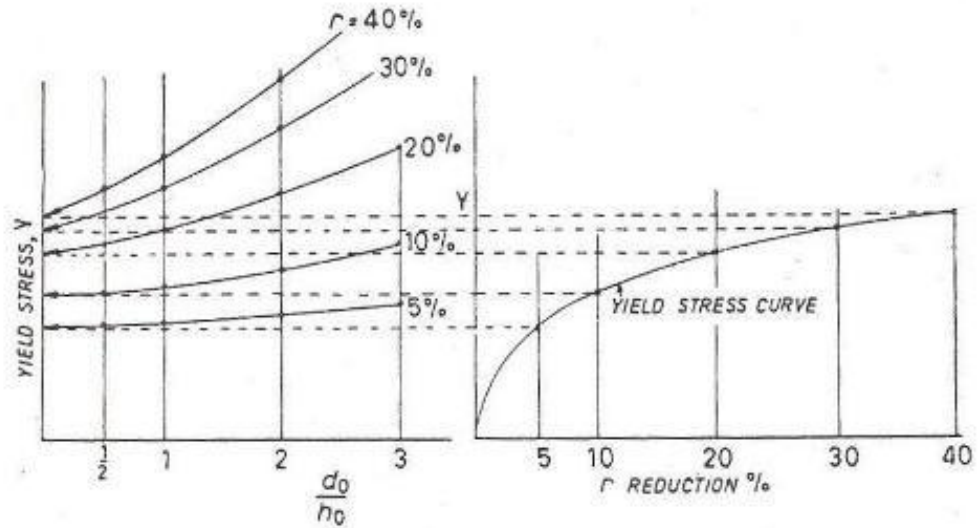


**Figure 1.4 Graphical Illustration of Derivation of Yield Stress Curve by the Cook and Larke Simple Compression Test in the Case of Constant Reduction Application [15]**

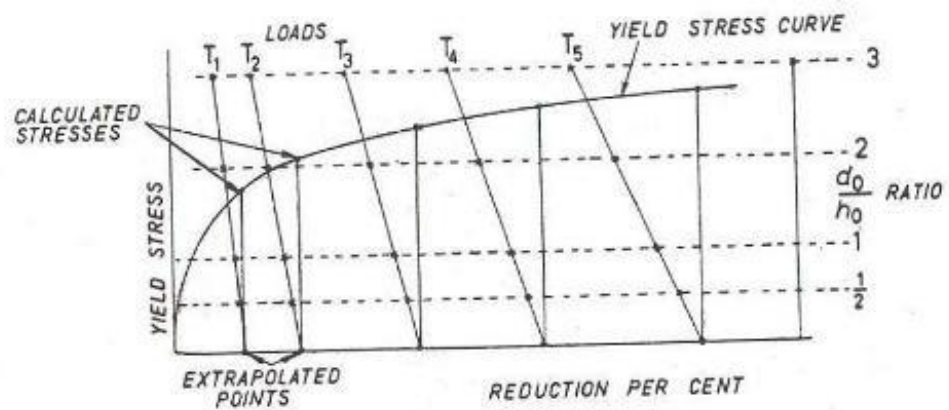


**Figure 1.5 Graphical Illustration of Derivation of Yield Stress Curve by the Cook and Larke Simple Compression Test in the Case of Constant Load Application [15]**

## 1.5 Literature Survey on Material Testing

Singh *et al.* [16] used solid aluminum, steel, lead and tin-lead eutectic alloy cylinders of 12.7 mm and of different heights to get the compressive yield stress of these materials. Steel specimens were tested on a 60 ton universal testing machine and non-ferrous ones compressed on a 5 ton universal testing machine. The experiments are performed at the room temperature.

Banarjee [17] used solid aluminum cylinders of 1 inch and of different heights corresponding to a set of aspect ratios (height/diameter = 2, 1.5, 1, 0.75 and 0.5) on the way to get true stress-strain curves. In the experiments, an electrohydraulic press is used. The load applied by the machine can be controlled and five or six load increments are applied by increasing the axial compressive pressure of the testing machine during each loading. These experiments are also performed at the room temperature.

Singh *et al.* [18] prepared another study to observe the behaviors of materials in more rapid loading conditions and this time only aluminum and steel cylinders are used. Steel cylinders with 20 mm diameters and  $d_0/h_0$  ratios of 1.0, 0.8 and 0.67 were prepared while aluminum ones were with 1 inch diameter and at the same  $d_0/h_0$  ratios. The screw press had an electronic data acquisition system. Ram travel was recorded using a linear variable differential transducer (LVDT). The load measurements were made using a standard electrical resistance strain gauge dynamometer.

Chen *et al.* [19] made a computational study using a commercial finite element software. The study was not based on the Cook and Larke Simple Compression Test but specimens of 10 mm diameter and 1.5 and 1  $d_0/h_0$  ratios are examined.



## **1.6 Scope of the Thesis**

The material libraries of the commercial software programs include mechanical properties of limited materials at the room temperature or a few elevated temperatures. However, different forging temperatures may be required in applications. The material properties at the temperatures which are especially applied in semi hot forging process are not available in the library of the software programs. Therefore, the material properties must be determined by testing. On the other hand it may also be necessary to conduct the test by using the actual material used in the forging processes at different temperatures to verify them even if the necessary data is available in the library of the software programs.

In this study, a forging press is used as a material testing equipment for elevated temperatures of the specimens. By this study, the stress-strain relations of AISI 1045 steel at the elevated temperatures are obtained by performing experiments on a 1000 ton forging press with a data acquisition system integrated at METU-BILTIR Center Forging Research and Application Laboratory. The dimensions of the test specimens and the reduction ratios are determined according to the Cook and Larke Simple Compression Test. In this way, it is also aimed to obtain a procedure to determine the mechanical properties of the materials by using the mentioned forging press.

Design of forging dies to apply the Cook and Larke Simple Compression Test on the forging press are described in Chapter 2.

Chapter 3 consists of the computational study performed by a commercial software which is available in METU-BILTIR Center. The experiments performed with the manufactured die set and prepared specimens are presented in Chapter 4.

In Chapter 5, the experimental and numerical results are compared and the study is concluded with the recommended further works.

## CHAPTER 2

### DESIGN OF FORGING DIES FOR THE COOK AND LARKE SIMPLE COMPRESSION TEST ON FORGING PRESS

#### 2.1 Conceptual Die Set Design

A die set is required to prepare for the application of Cook and Larke Simple Compression Test on the 1000 ton forging press in METU-BILTIR Center Forging Research and Application Laboratory. Dies are mounted into the die holders of the forging press. The lower die holder of the forging press is shown in Figure 2.1 with die housings and clamping elements on anvil. The upper die holder is attached to the ram of the forging press. The dimensions of circular die housings in the upper die holder are the same with those in the lower die holder.

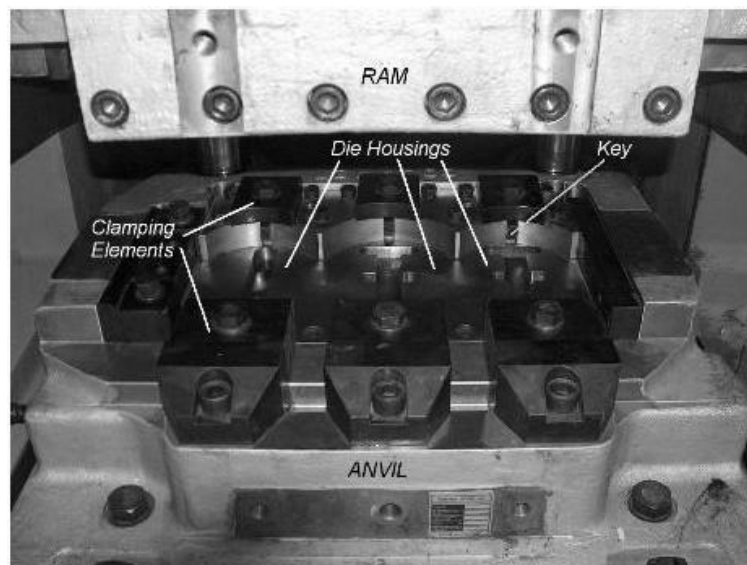


**Figure 2.1 Lower Die Spaces of the Forging Press**

In this thesis study, specimens with aspect ratios,  $d_0/h_0$ , 3, 2, 1 and 0,5 are selected to be used as suggested in the Cook and Larke Simple Compression Test [15]. Schematic views of these specimens according to their aspect ratios are given in Figure 2.2

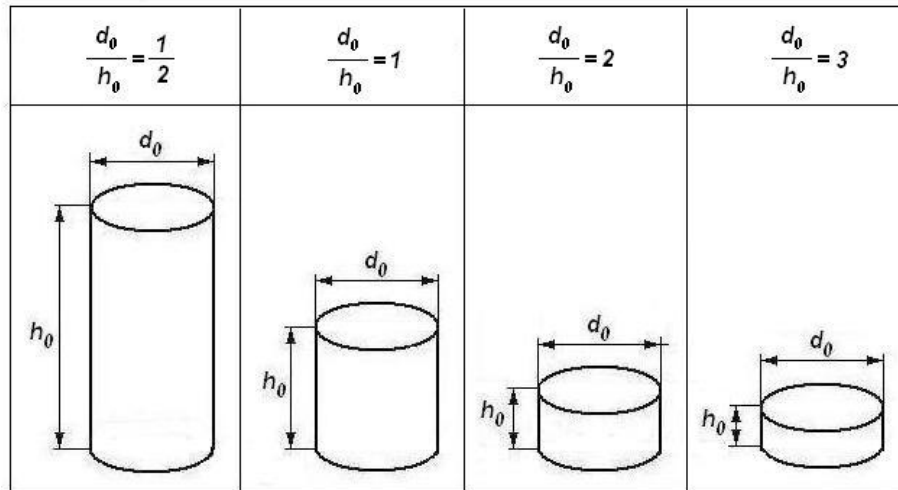


**Figure 2.2 Schematic Views of the Specimens According to Their Aspect Ratios**

The height of each type of specimens shown in Figure 2.2 will be reduced by 5%, 10%, 20%, 30% and 40%. The changes in the geometry of the specimens are shown schematically in Figure 2.3 with respect to the four aspect ratios and the five reduction ratios,  $r$ , without considering the barreling effect. Therefore, twenty forging operations are conducted. In the die set design, the constraints due to the forging press should also be taken into account. The final height value to be obtained in each configuration is the distance between the upper and the lower dies when the ram of the forging press is at the bottom dead point.

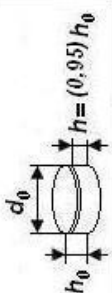
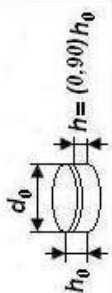
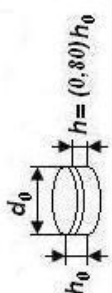
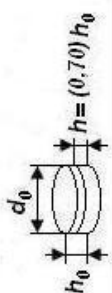
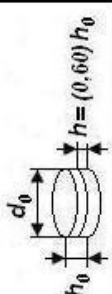
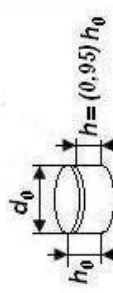
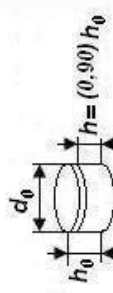
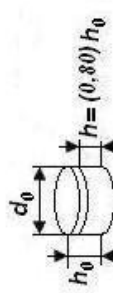
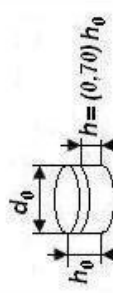
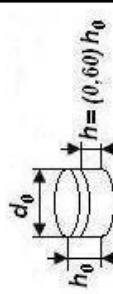
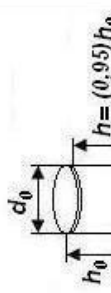
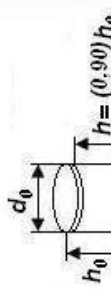
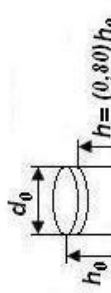
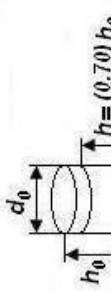
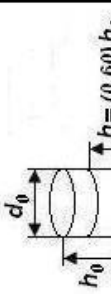
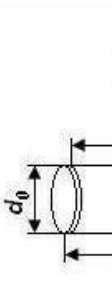
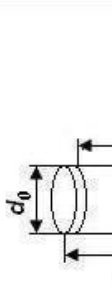
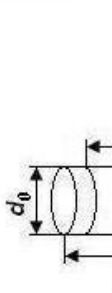
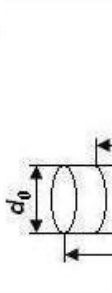
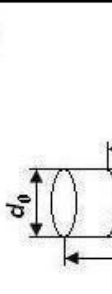
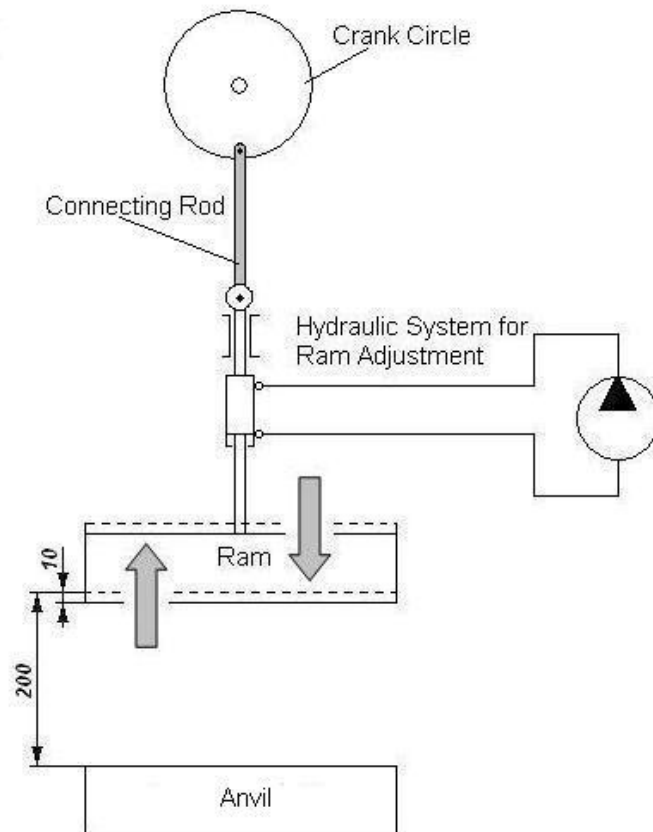
$r$ $d_0/h_0$	5 %	10 %	20 %	30 %	40 %
3					
2					
1					
$\frac{1}{2}$					

Figure 2.3 Schematic Drawings of the Specimens for the Cook and Larke Simple Compression Test According to their Aspect and Reduction Ratios

The ram adjustment mechanism of the forging press is schematically shown in Figure 2.4. The distance between the ram and the anvil is 200 mm when the ram is at its bottom dead center. However, the position can be adjusted by 10 mm. On the other hand, the stroke of the press is 220 mm.



**Figure 2.4 Ram Adjustment Mechanism of the Forging Press**

The induction heater to be used for heating the specimens is adequate to heat the specimens with the diameter of 30 mm-50mm. By considering this possible range for the specimen diameter, the dimensions of the specimens according to the Cook and Larke Simple Compression Test are given in Tables 2.1-2.5 for the specimen diameter of 50 mm, 45 mm, 40 mm, 35 mm and 30 mm, respectively.

**Table 2.1 Dimensions for the Specimens with Initial Diameter 50 mm**

$d_0$ (mm)	$h_0$ (mm)	$d_0/h_0$	$r$ (%)	$h$ (mm)
50	100,00	0,5	5	95,00
50	100,00	0,5	10	90,00
50	100,00	0,5	20	80,00
50	100,00	0,5	30	70,00
50	100,00	0,5	40	60,00
50	50,00	1	5	47,50
50	50,00	1	10	45,00
50	50,00	1	20	40,00
50	50,00	1	30	35,00
50	50,00	1	40	30,00
50	25,00	2	5	23,75
50	25,00	2	10	22,50
50	25,00	2	20	20,00
50	25,00	2	30	17,50
50	25,00	2	40	15,00
50	16,67	3	5	15,83
50	16,67	3	10	15,00
50	16,67	3	20	13,33
50	16,67	3	30	11,67
50	16,67	3	40	10,00

**Table 2.2 Dimensions for the Specimens with Initial Diameter 45 mm**

$d_0$ (mm)	$h_0$ (mm)	$d_0/h_0$	$r$ (%)	$h$ (mm)
------------	------------	-----------	---------	----------

45	90,00	0,5	5	85,50
45	90,00	0,5	10	81,00
45	90,00	0,5	20	72,00
45	90,00	0,5	30	63,00
45	90,00	0,5	40	54,00

45	45,00	1	5	42,75
45	45,00	1	10	40,50
45	45,00	1	20	36,00
45	45,00	1	30	31,50
45	45,00	1	40	27,00

45	22,50	2	5	21,38
45	22,50	2	10	20,25
45	22,50	2	20	18,00
45	22,50	2	30	15,75
45	22,50	2	40	13,50

45	15,00	3	5	14,25
45	15,00	3	10	13,50
45	15,00	3	20	12,00
45	15,00	3	30	10,50
45	15,00	3	40	9,00

**Table 2.3 Dimensions for the Specimens with Initial Diameter 40 mm**

$d_0$ (mm)	$h_0$ (mm)	$d_0/h_0$	$r$ (%)	$h$ (mm)
------------	------------	-----------	---------	----------

40	80,00	0,5	5	76,00
40	80,00	0,5	10	72,00
40	80,00	0,5	20	64,00
40	80,00	0,5	30	56,00
40	80,00	0,5	40	48,00

40	40,00	1	5	38,00
40	40,00	1	10	36,00
40	40,00	1	20	32,00
40	40,00	1	30	28,00
40	40,00	1	40	24

40	20,00	2	5	19,00
40	20,00	2	10	18,00
40	20,00	2	20	16,00
40	20,00	2	30	14,00
40	20,00	2	40	12,00

40	13,33	3	5	12,67
40	13,33	3	10	12,00
40	13,33	3	20	10,67
40	13,33	3	30	9,33
40	13,33	3	40	8,00



**Table 2.4 Dimensions for the Specimens with Initial Diameter 35 mm**

$d_0$ (mm)	$h_0$ (mm)	$d_0/h_0$	$r$ (%)	$h$ (mm)
35	70,00	0,5	5	66,50
35	70,00	0,5	10	63,00
35	70,00	0,5	20	56,00
35	70,00	0,5	30	49,00
35	70,00	0,5	40	42,00
35	35,00	1	5	33,25
35	35,00	1	10	31,50
35	35,00	1	20	28,00
35	35,00	1	30	24,50
35	35,00	1	40	21,00
35	17,50	2	5	16,62
35	17,50	2	10	15,75
35	17,50	2	20	14,00
35	17,50	2	30	12,25
35	17,50	2	40	10,50
35	11,67	3	5	11,08
35	11,67	3	10	10,50
35	11,67	3	20	9,33
35	11,67	3	30	8,17
35	11,67	3	40	7,00

**Table 2.5 Dimensions for the Specimens with Initial Diameter 30 mm**

$d_0$ (mm)	$h_0$ (mm)	$d_0/h_0$	$r$ (%)	$h$ (mm)
30	60,00	0,5	5	57,00
30	60,00	0,5	10	54,00
30	60,00	0,5	20	48,00
30	60,00	0,5	30	42,00
30	60,00	0,5	40	36,00

30	30,00	1	5	28,50
30	30,00	1	10	27,00
30	30,00	1	20	24,00
30	30,00	1	30	21,00
30	30,00	1	40	18,00

30	15,00	2	5	14,25
30	15,00	2	10	13,50
30	15,00	2	20	12,00
30	15,00	2	30	10,50
30	15,00	2	40	9,00

30	10,00	3	5	9,50
30	10,00	3	10	9,00
30	10,00	3	20	8,00
30	10,00	3	30	7,00
30	10,00	3	40	6,00

In Figure 2.5, the die set configurations are shown to satisfy the required distance between upper and lower dies when the ram is at bottom dead point. The broken lines below the upper die represent the 10 mm distance by the ram adjustment. The upper die is fixed to the upper die holder and the lower die is fixed to the lower die holder. The heights of the upper die and the base thickness of lower die are 50 mm and 54 mm, respectively. Considering the final height of the specimens, the inserts with

height of 10 mm, 20 mm, 30 mm and 40 mm are required to satisfy the reduction in height by the aid of the ram adjustment. In this study, it is decided to use specimens with initial nominal diameter of  $d_0=50$  mm. The final heights of these specimens are given with respect to different reduction ratios and aspect ratios in Table 2.6.

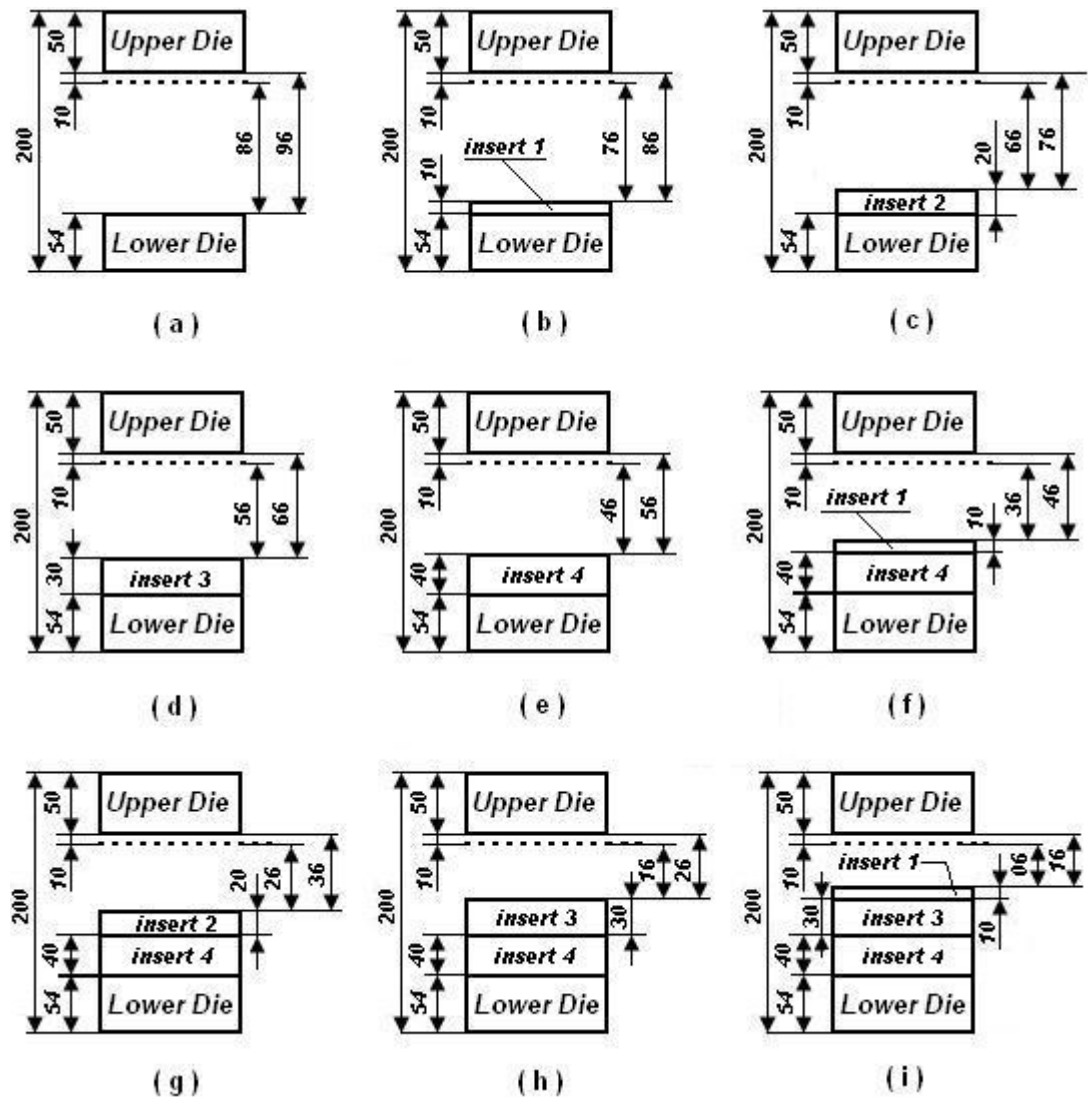


Figure 2.5 Different Configurations of the Die Set

**Table 2.6 Die Set Configuration for the Application of the Cook and Larke Simple Compression Test to the Specimens with Initial Diameter 50 mm**

$d_0$ (mm)	$h_0$ (mm)	$d_0/h_0$	$r$ (%)	$h$ (mm)	Die Set Configuration	Calculated Ram Movement by Adjustment (mm)
50	100,00	0,5	5	95,00	Figure 2.7 (a)	1,00
50	100,00	0,5	10	90,00	Figure 2.7 (a)	6,00
50	100,00	0,5	20	80,00	Figure 2.7 (b)	6,00
50	100,00	0,5	30	70,00	Figure 2.7 (c)	6,00
50	100,00	0,5	40	60,00	Figure 2.7 (d)	6,00
50	50,00	1	5	47,50	Figure 2.7 (e)	8,50
50	50,00	1	10	45,00	Figure 2.7 (e)	9,00
50	50,00	1	20	40,00	Figure 2.7 (f)	6,00
50	50,00	1	30	35,00	Figure 2.7 (g)	1,00
50	50,00	1	40	30,00	Figure 2.7 (g)	6,00
50	25,00	2	5	23,75	Figure 2.7 (h)	2,25
50	25,00	2	10	22,50	Figure 2.7 (h)	3,50
50	25,00	2	20	20,00	Figure 2.7 (h)	6,00
50	25,00	2	30	17,50	Figure 2.7 (h)	8,50
50	25,00	2	40	15,00	Figure 2.7 (i)	1,00
50	16,67	3	5	15,83	Figure 2.7 (i)	0,07
50	16,67	3	10	15,00	Figure 2.7 (i)	1,00
50	16,67	3	20	13,33	Figure 2.7 (i)	2,67
50	16,67	3	30	11,67	Figure 2.7 (i)	4,33
50	16,67	3	40	10,00	Figure 2.7 (i)	6,00

## 2.2 Modular Die Set Design

By taking the conceptual design into account, 3D models of the designed die set is shown in Figure 2.6. The technical drawings of the die set are given in Appendix A.

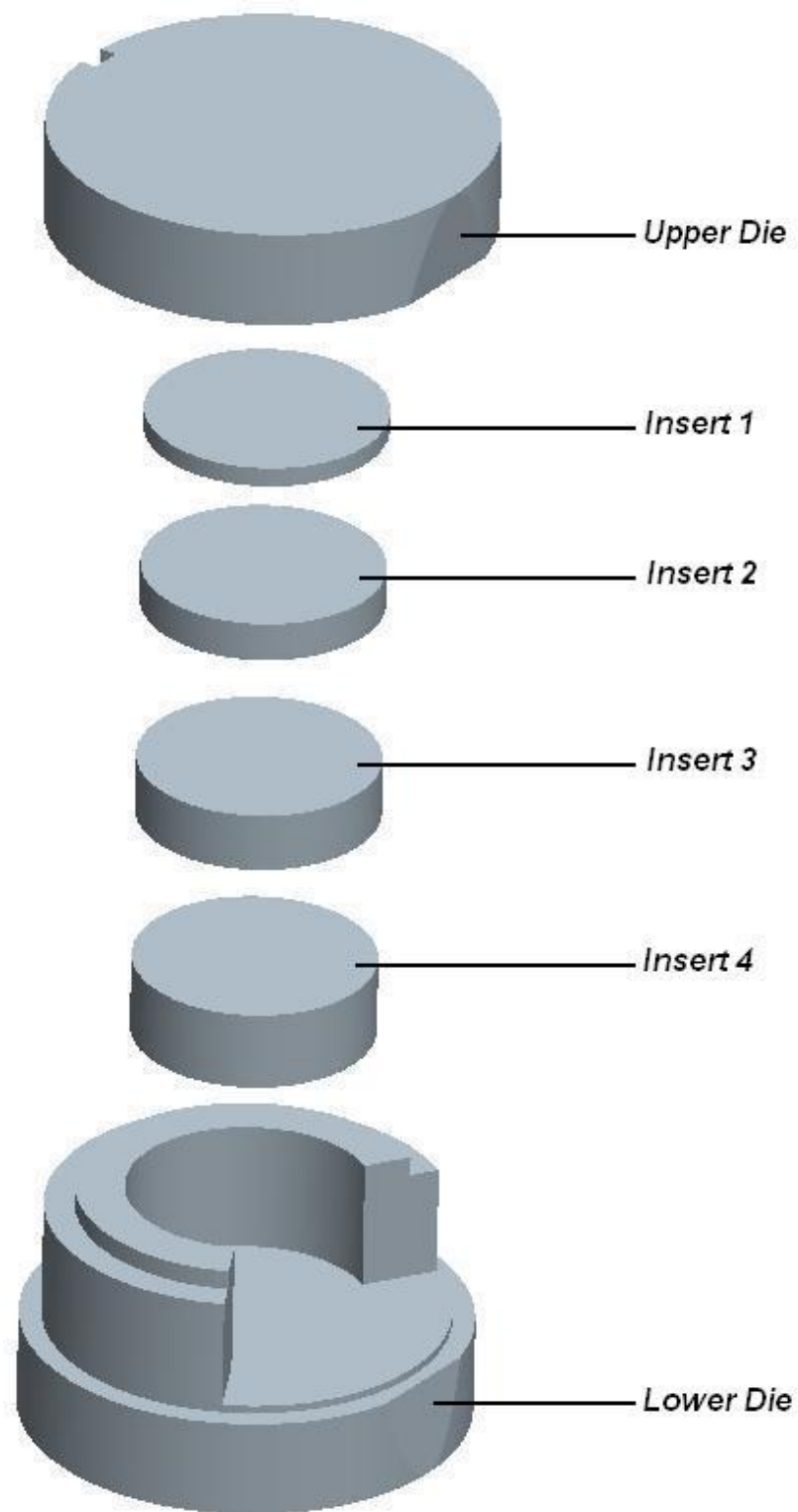


**Figure 2.6 3D Models of the Die Set**

In Figure 2.7, technical drawing of the circular die housings of the die holder of the forging press is shown [20]. The die set is decided to be located in the middle housing.

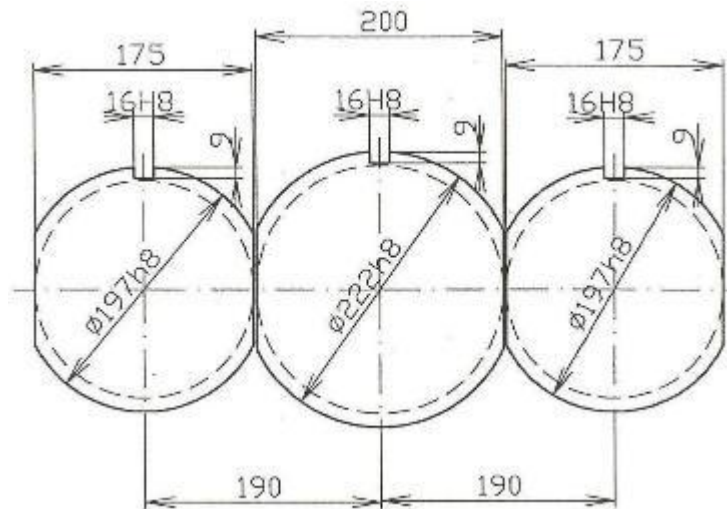


**Figure 2.7 Technical Drawing of the Circular Die Housings of the Die Holder of the Forging Press [20]**

The dimensions of the designed upper and lower dies are shown in Figure 2.8 and in Figure 2.9 respectively. The diameter at the bottom of the dies must be 222 mm according to Figure 2.7 and inclined surfaces with a taper angle of 5° must be provided on each die for clamping elements to fix them according to the instruction manual of the forging press [20]. In the lower die, there is a cavity for locating the inserts to restrain the horizontal motion of them. The diameter of the inserts are decided as 120 mm and the diameter of the cavity in the lower die is decided as 121,5 for locating in and taking out the inserts easily. The diameter has been decreased to 170 mm on the upper region of the lower die with a height of 20 mm to avoid collision of the clamping elements fixing the upper die and the lower die. It should be noted that, an opening in the lower die as shown in Figure 2.8 and Figure 2.10 is provided for putting the specimens into the lower die and taking them out easily. This opening also makes easy to put the inserts in it and take them out.

The upper die is has a diameter of 222 mm and a height of 50 mm. An inclined plane with a value of  $5^\circ$  is provided on the side of the upper die for clamping purposes .like the lower one for clamping purposes. Additionally, key cavities for both the upper and lower dies are needed to fix them to the die holders as seen in Figure 2.7.

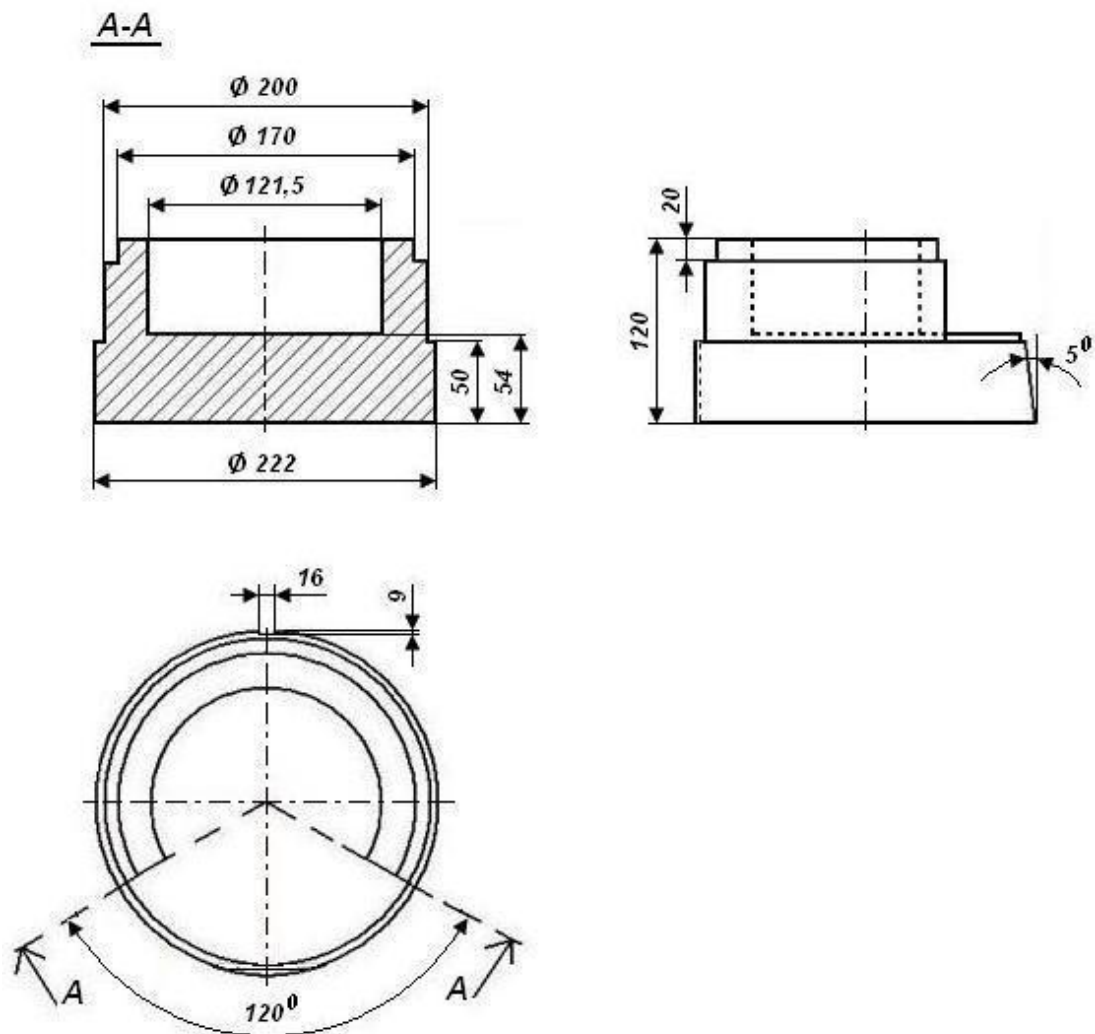


**Figure 2.8 Dimensions of the Lower Die**

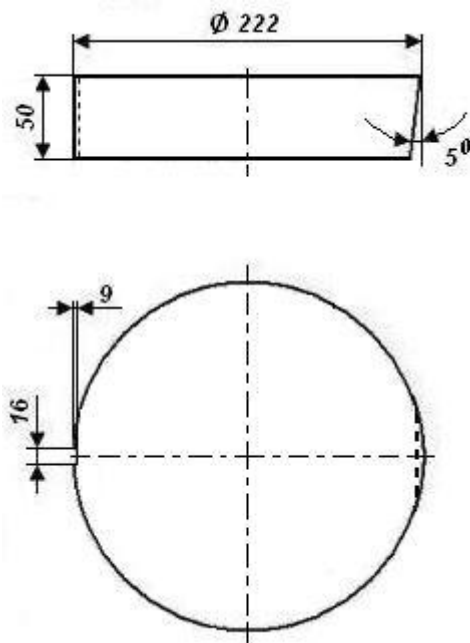


**Figure 2.9 Dimensions of the Upper Die**

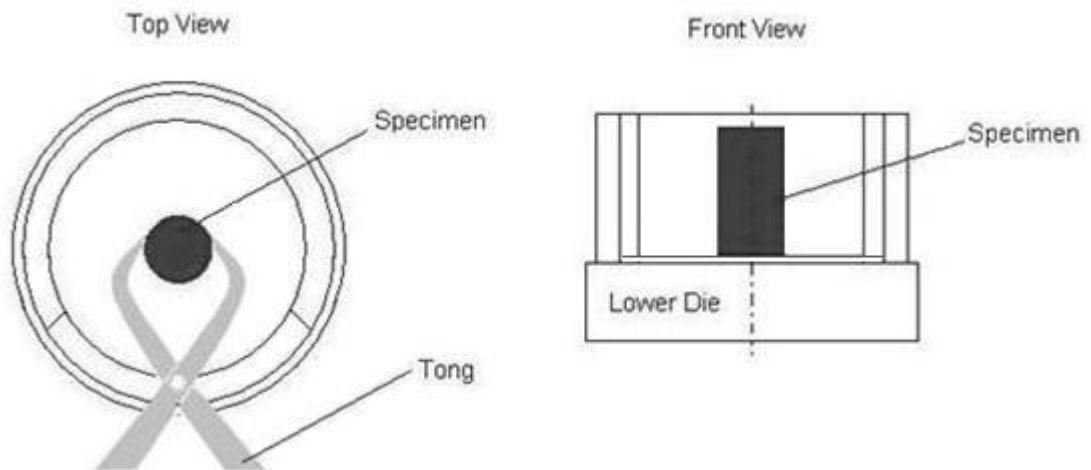


**Figure 2.10 Schematic Drawing of the Lower Forging Die Showing the Opening in front of it**



## CHAPTER 3

### COMPUTATIONAL STUDY

As mentioned in Chapter 2, twenty different configurations for each temperature value of the specimens due to four different heights of the specimens and five different reduction ratios are required to apply the Cook and Larke Simple Compression Test as shown in Figure 2.3. The Cook and Larke Simple Compression Tests for these twenty different cases have been simulated by using the finite element module of Simufact.forming 8.1<sup>®</sup> [22]. Simulations have been repeated for the temperatures for the specimens of 900°C, 1000°C and 1100°C.

#### 3.1 Performing Analyses in Simufact.forming 8.1<sup>®</sup>

In this thesis study, due to axi-symmetric specimens, axi-symmetric elements are used in which element type is four-node rectangular finite element shown in Figure 3.1. The number of the mesh elements created by the software due to the geometries of the specimens are given in Table 3.1

To set up a problem like this, the type of the process, “upsetting” is selected in the dialog box. Since the process is in hot working conditions, appropriate conditions are selected in the same dialog box. The appropriate dimensions for the Cook and Larke Simple Compression Test for this study are input from Table 2.1. Since the type of the press in METU-BILTIR Center Forging Research and Application Laboratory is a mechanical crank press, the choice of “Crank Press” is chosen in the related dialog box. The forging press Smeral Brno LZK 1000<sup>®</sup> which is used in the experiments has a crank radius of 110 mm and a connecting rod of 750 mm with the rotation

speed of 100 rpm. The coefficient of friction is taken as 0,2. In industry, the hot forging dies are heated about 200°C, so in the software this value is input for the dies. The workpiece temperatures are selected as 900°C, 1000°C and 1100°C as discussed previously. Reduction,  $r$ , is another factor in this study session, so the height to be deformed also should be input. The “Rigid Die with Heat Conduction” is selected for the forging dies in the software environment.

After doing other forming controls, the analysis can be started.

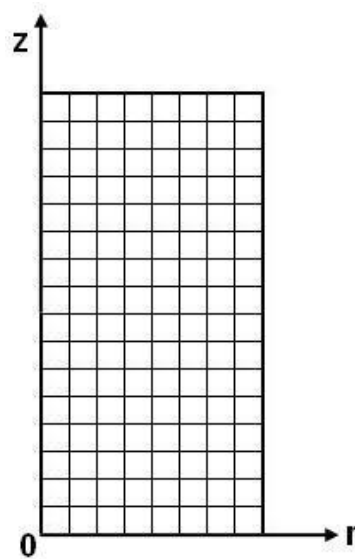


**Figure 3.1 Axi-symmetric Problem Set Up for the Finite Element Analysis**

**Table 3.1 Number of the Mesh Elements According to the Geometries of the Specimens**

$d_o$ (mm)	$h_o$ (mm)	$d_o/h_o$	Number of the Mesh Elements
50	100,00	0,5	885
50	50,00	1,0	882
50	25,00	2,0	841
50	16,67	3,0	864

### 3.2 Numerical Results

Graphical outputs of the results evaluated from the analyses performed by following the steps told in Section 3.1 are shown in Figures 3.2-3.61.

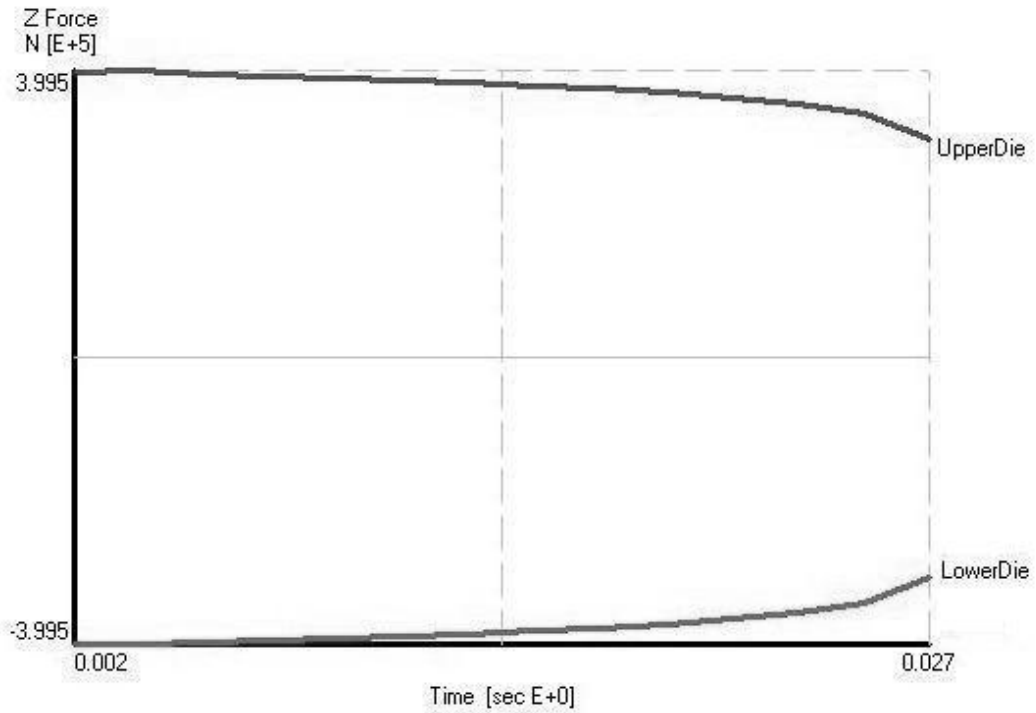


**Figure 3.2 Graphical Output of the Numerical Result for the Process with  $r=5\%$  at  $900^{\circ}\text{C}$  for the Specimen with  $h_0=100\text{ mm}$**

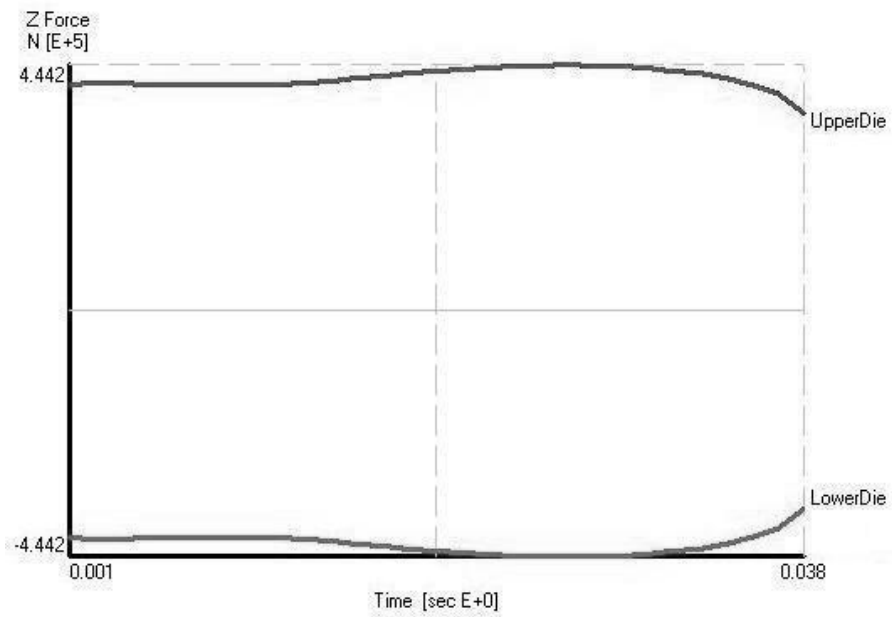


**Figure 3.3 Graphical Output of the Numerical Result for the Process with  $r=10\%$  at  $900^\circ\text{C}$  for the Specimen with  $h_0=100\text{ mm}$**

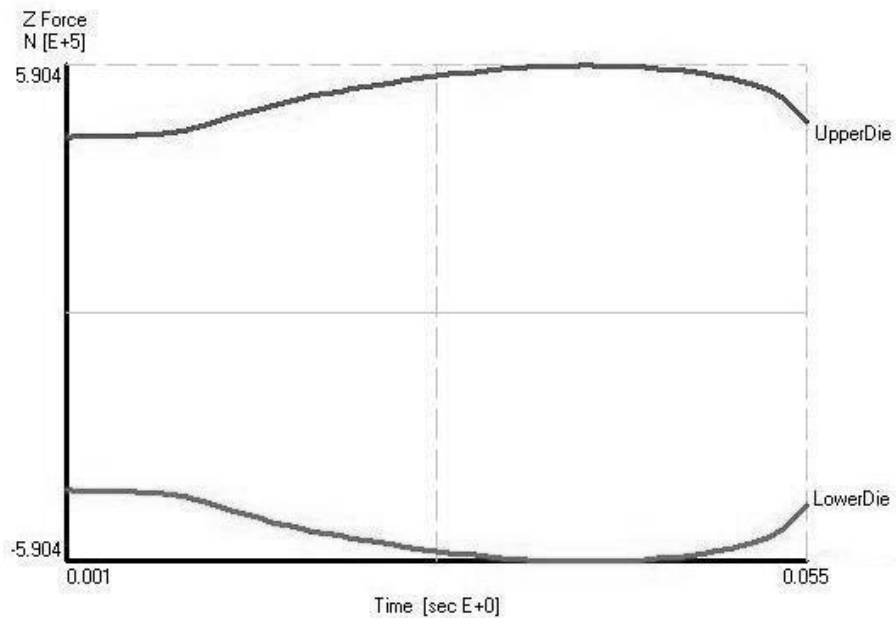


**Figure 3.4 Graphical Output of the Numerical Result for the Process with  $r=20\%$  at  $900^\circ\text{C}$  for the Specimen with  $h_0=100\text{ mm}$**

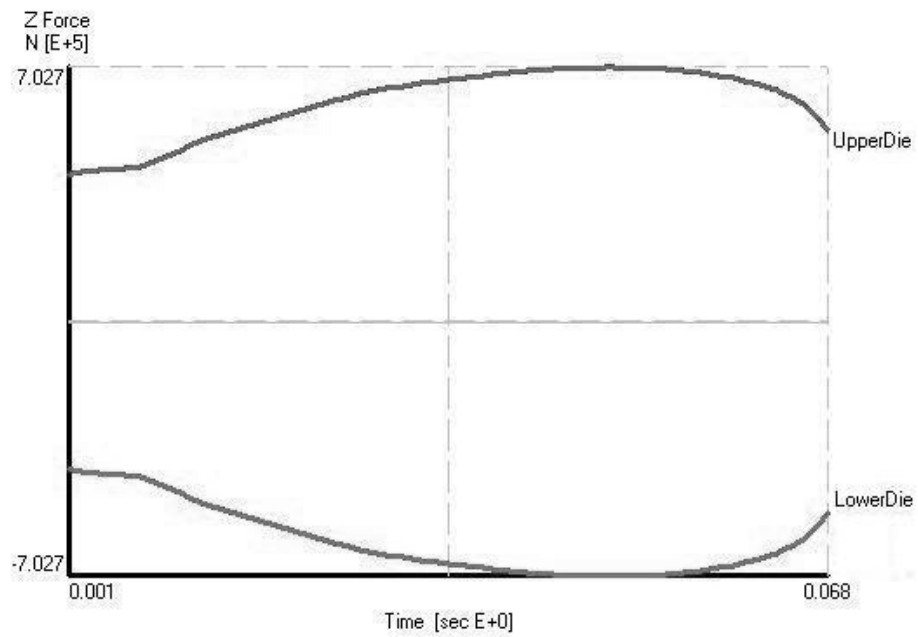


**Figure 3.5 Graphical Output of the Numerical Result for the Process with  $r=30\%$  at  $900^{\circ}\text{C}$  for the Specimen with  $h_0=100\text{ mm}$**

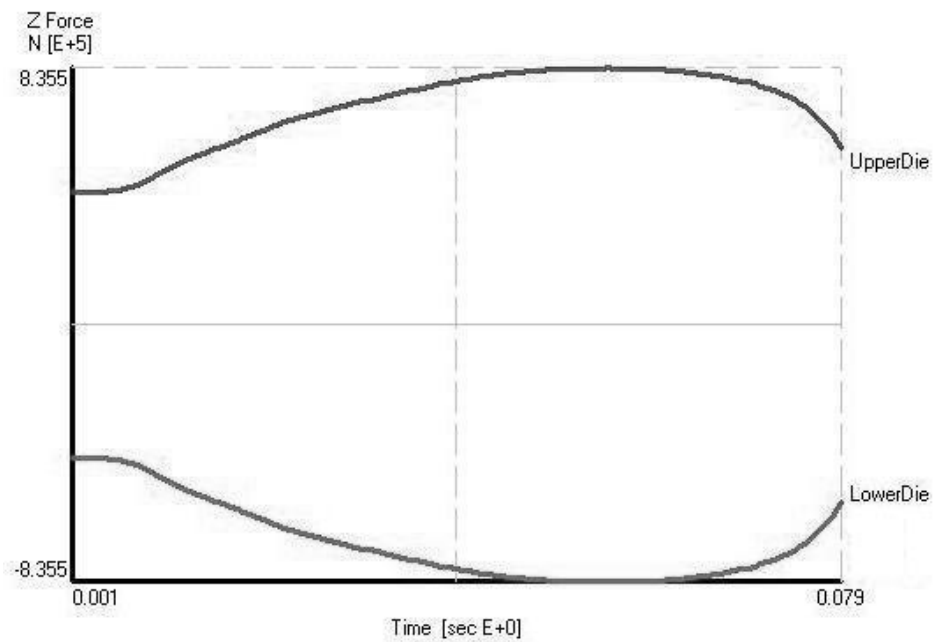


**Figure 3.6 Graphical Output of the Numerical Result for the Process with  $r=40\%$  at  $900^{\circ}\text{C}$  for the Specimen with  $h_0=100\text{ mm}$**

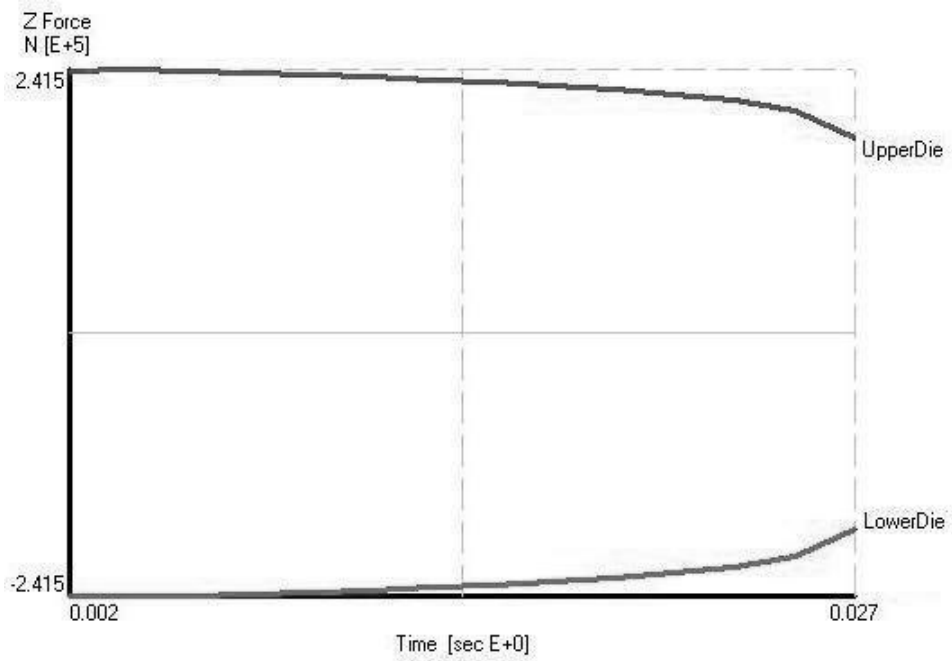


**Figure 3.7 Graphical Output of the Numerical Result for the Process with  $r=5\%$  at  $1000^{\circ}\text{C}$  for the Specimen with  $h_0=100$  mm**

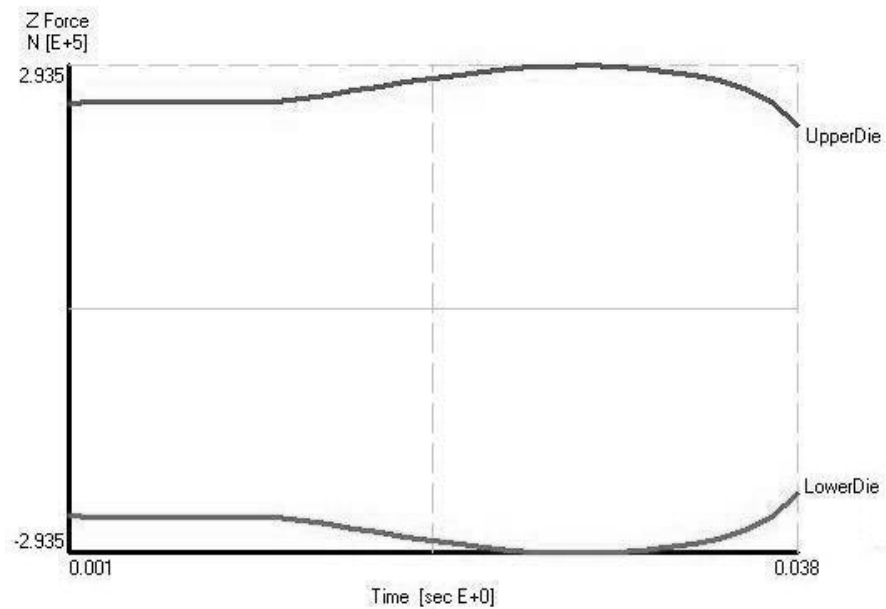


**Figure 3.8 Graphical Output of the Numerical Result for the Process with  $r=10\%$  at  $1000^{\circ}\text{C}$  for the Specimen with  $h_0=100$  mm**

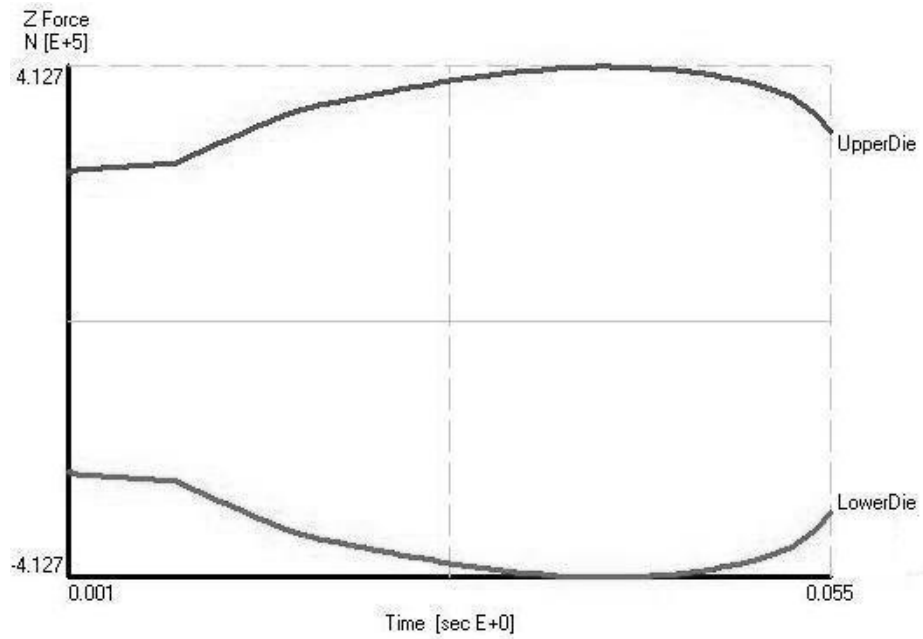


**Figure 3.9 Graphical Output of the Numerical Result for the Process with  $r=20\%$  at  $1000^\circ\text{C}$  for the Specimen with  $h_0=100$  mm**

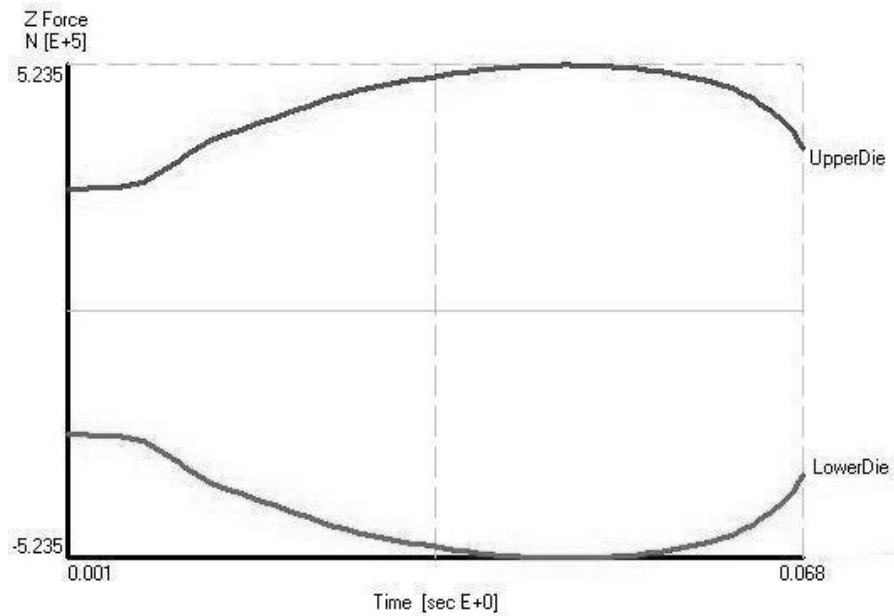


**Figure 3.10 Graphical Output of the Numerical Result for the Process with  $r=30\%$  at  $1000^\circ\text{C}$  for the Specimen with  $h_0=100$  mm**

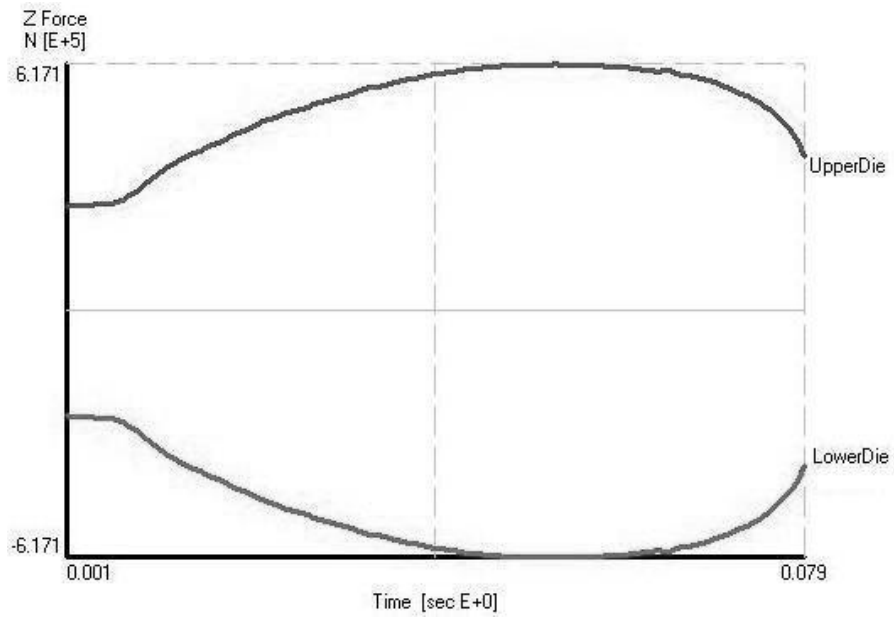


**Figure 3.11 Graphical Output of the Numerical Result for the Process with  $r=40\%$  at  $1000^\circ\text{C}$  for the Specimen with  $h_0=100$  mm**

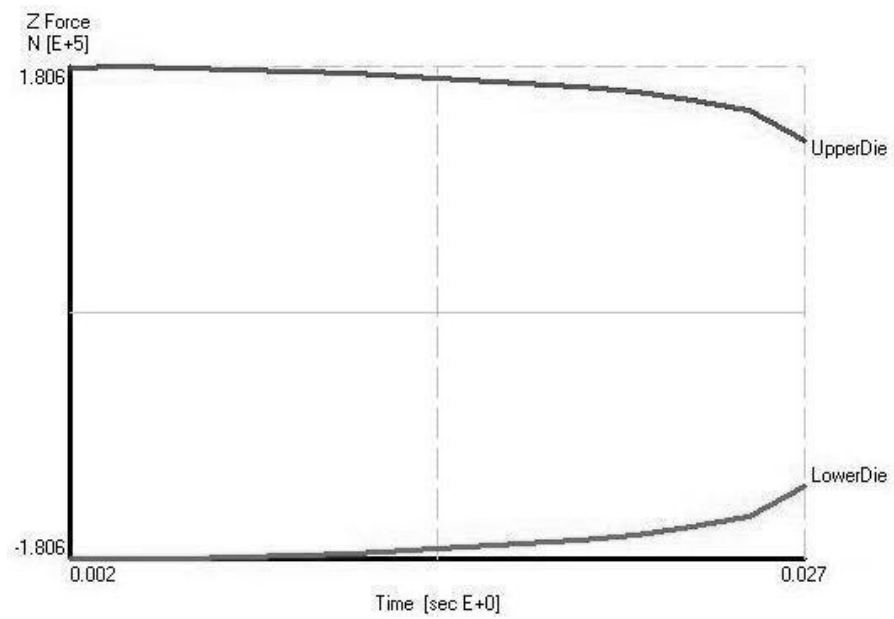


**Figure 3.12 Graphical Output of the Numerical Result for the Process with  $r=5\%$  at  $1100^\circ\text{C}$  for the Specimen with  $h_0=100$  mm**



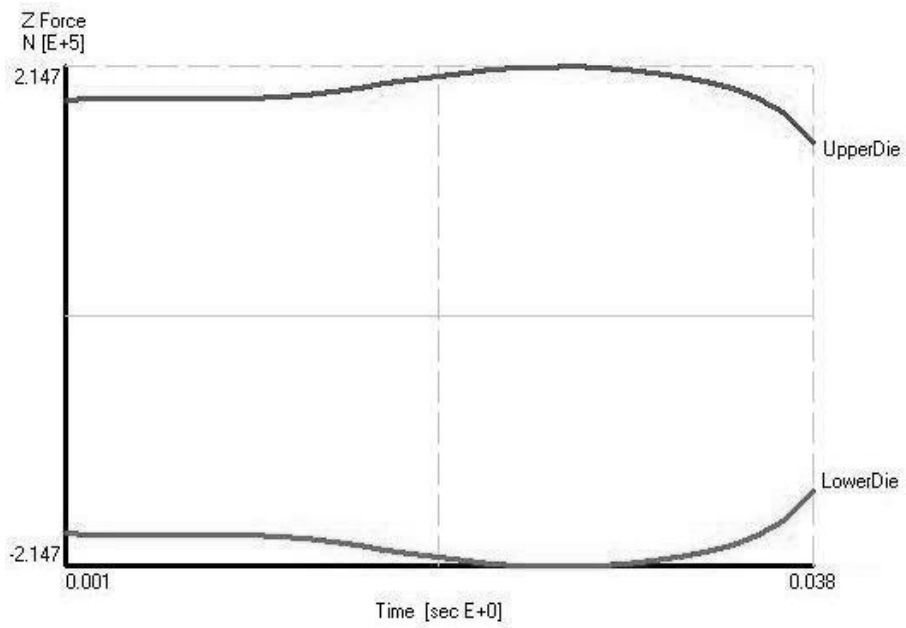


**Figure 3.13 Graphical Output of the Numerical Result for the Process with  $r=10\%$  at  $1100^{\circ}\text{C}$  for the Specimen with  $h_0=100$  mm**

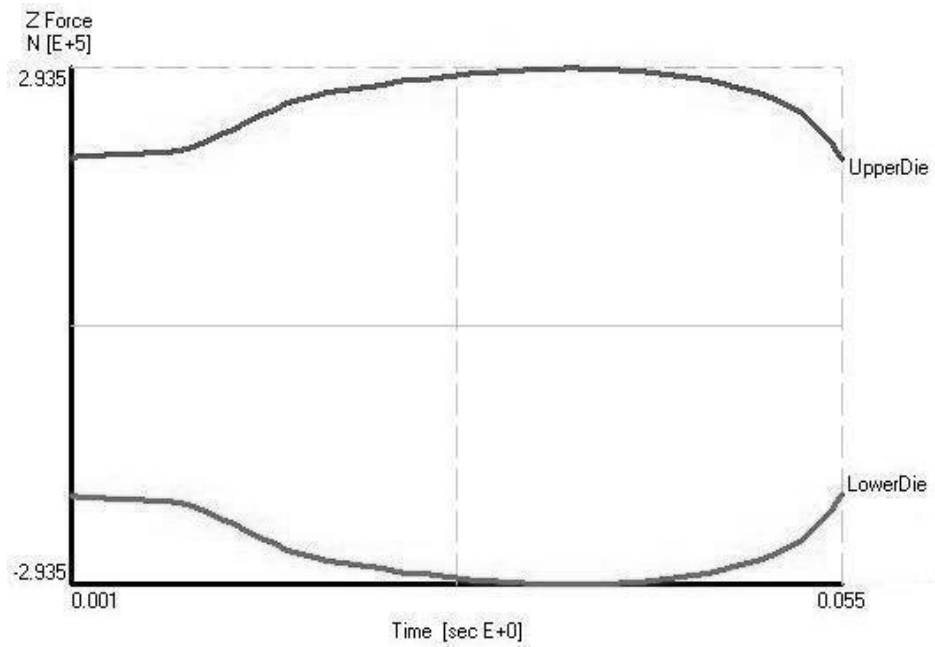


**Figure 3.14 Graphical Output of the Numerical Result for the Process with  $r=20\%$  at  $1100^{\circ}\text{C}$  for the Specimen with  $h_0=100$  mm**

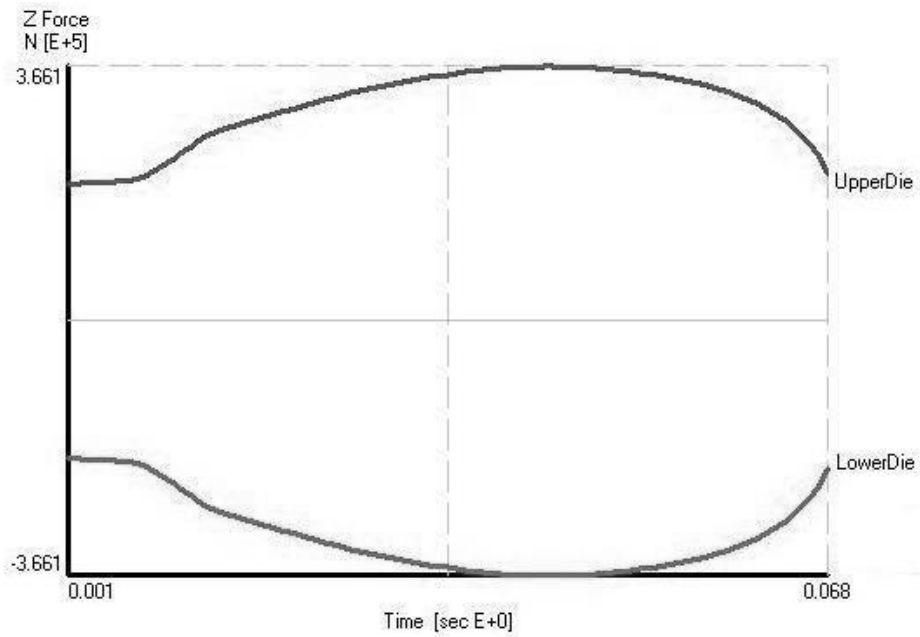


**Figure 3.15 Graphical Output of the Numerical Result for the Process with  $r=30\%$  at  $1100^\circ\text{C}$  for the Specimen with  $h_0=100$  mm**

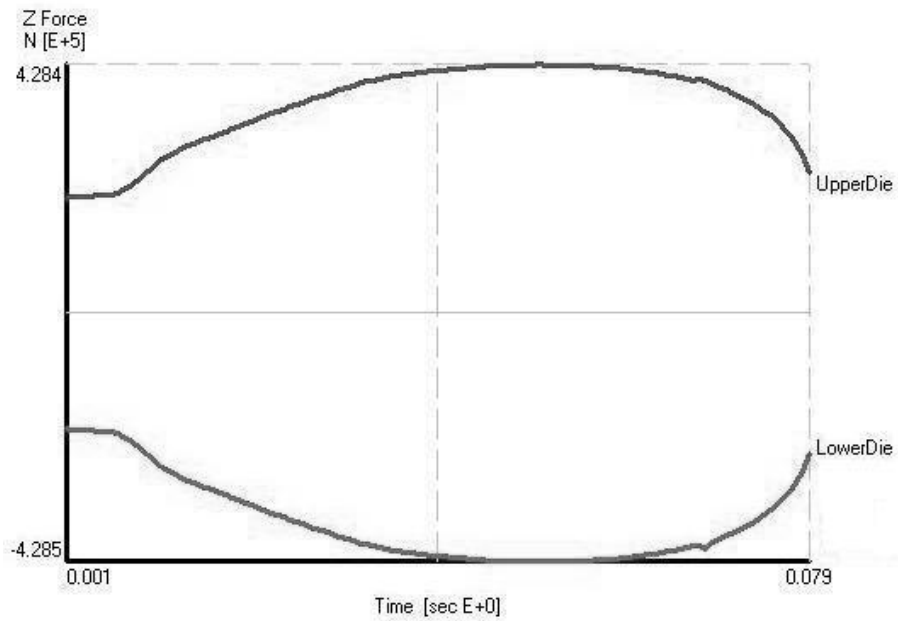


**Figure 3.16 Graphical Output of the Numerical Result for the Process with  $r=40\%$  at  $1100^\circ\text{C}$  for the Specimen with  $h_0=100$  mm**

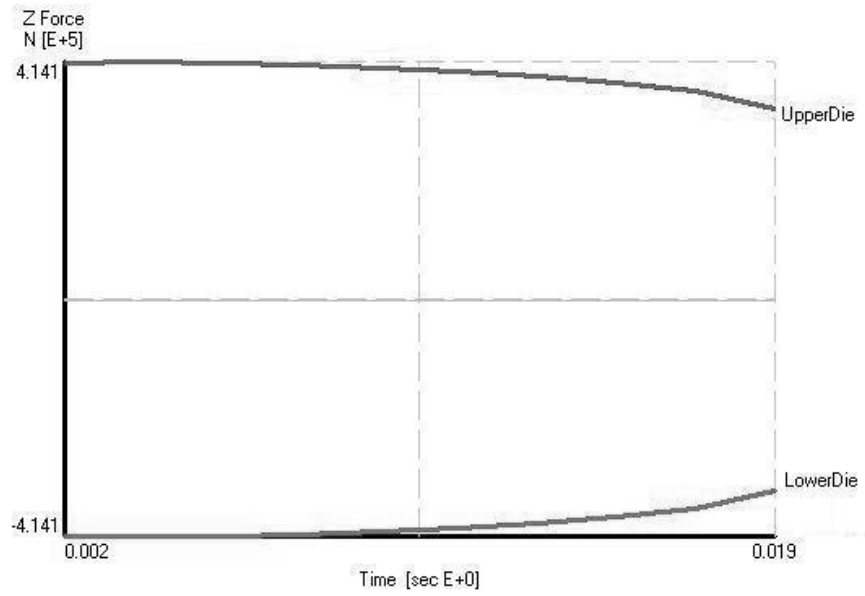


**Figure 3.17 Graphical Output of the Numerical Result for the Process with  $r=5\%$  at  $900^\circ\text{C}$  for the Specimen with  $h_0=50$  mm**

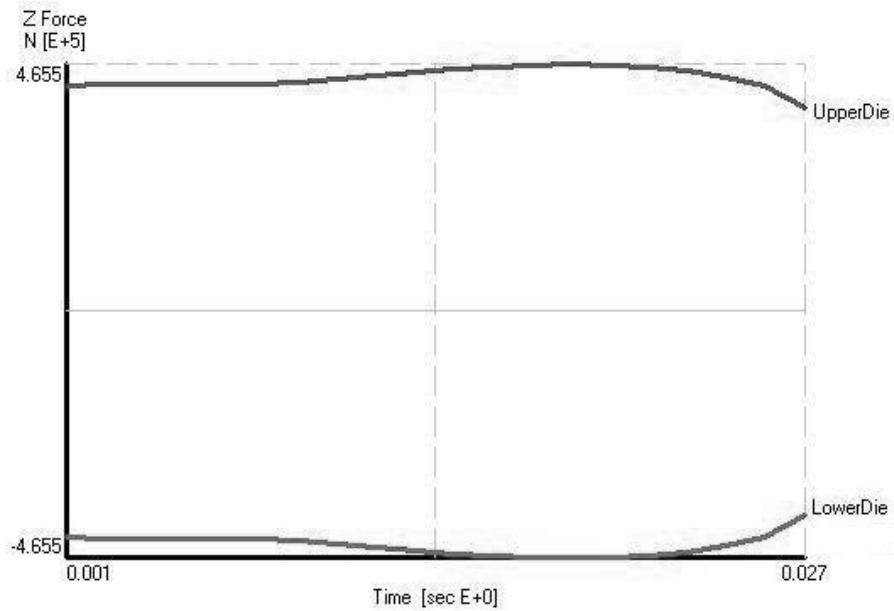


**Figure 3.18 Graphical Output of the Numerical Result for the Process with  $r=10\%$  at  $900^\circ\text{C}$  for the Specimen with  $h_0=50$  mm**

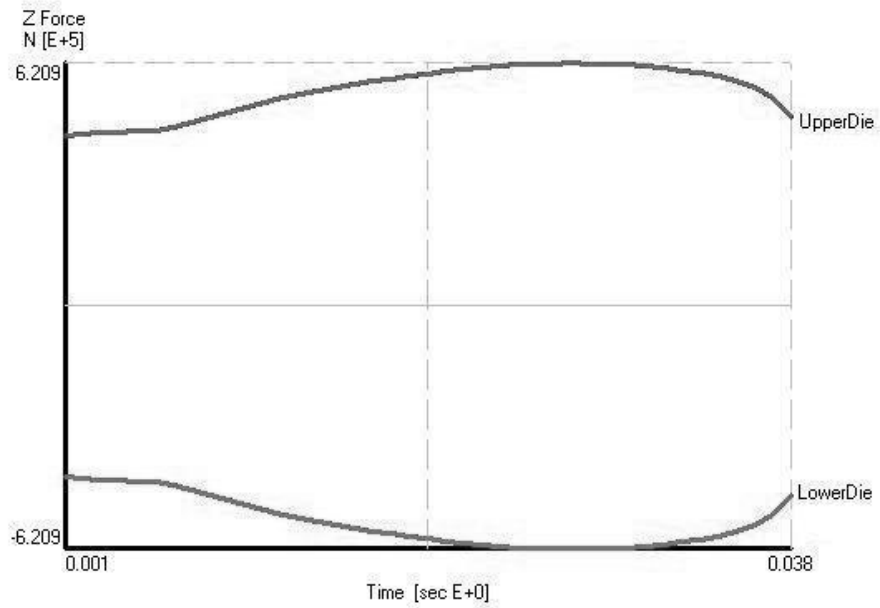


**Figure 3.19 Graphical Output of the Numerical Result for the Process with  $r=20\%$  at  $900^\circ\text{C}$  for the Specimen with  $h_0=50\text{ mm}$**

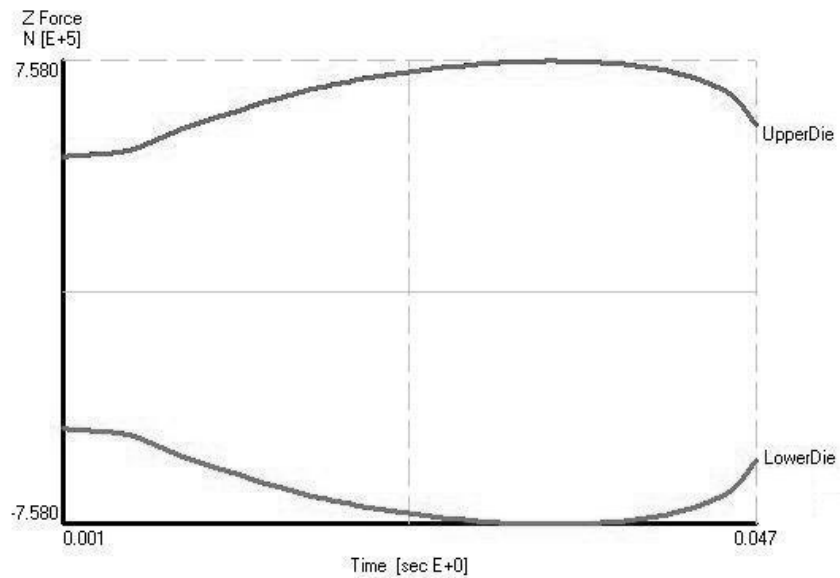


**Figure 3.20 Graphical Output of the Numerical Result for the Process with  $r=30\%$  at  $900^\circ\text{C}$  for the Specimen with  $h_0=50\text{ mm}$**

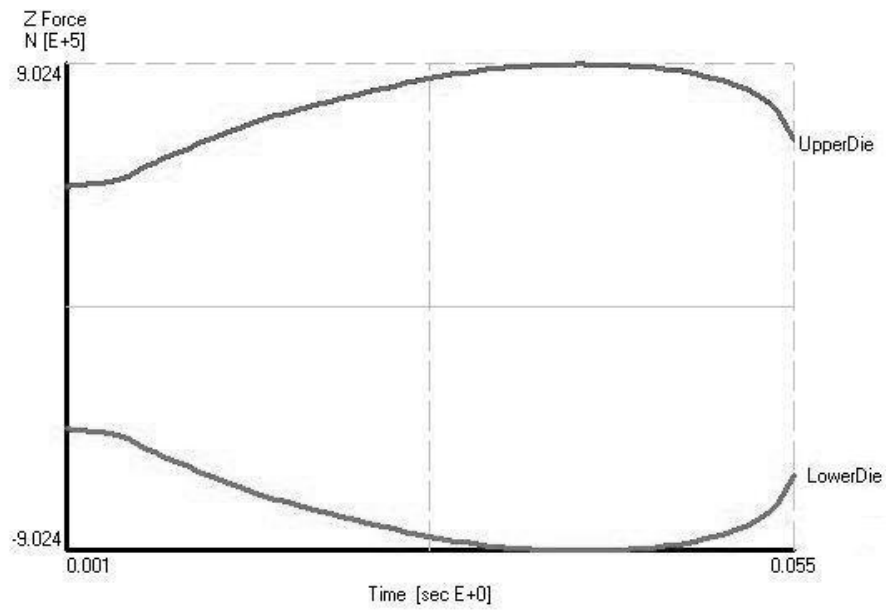


**Figure 3.21 Graphical Output of the Numerical Result for the Process with  $r=40\%$  at  $900^\circ\text{C}$  for the Specimen with  $h_0=50\text{ mm}$**

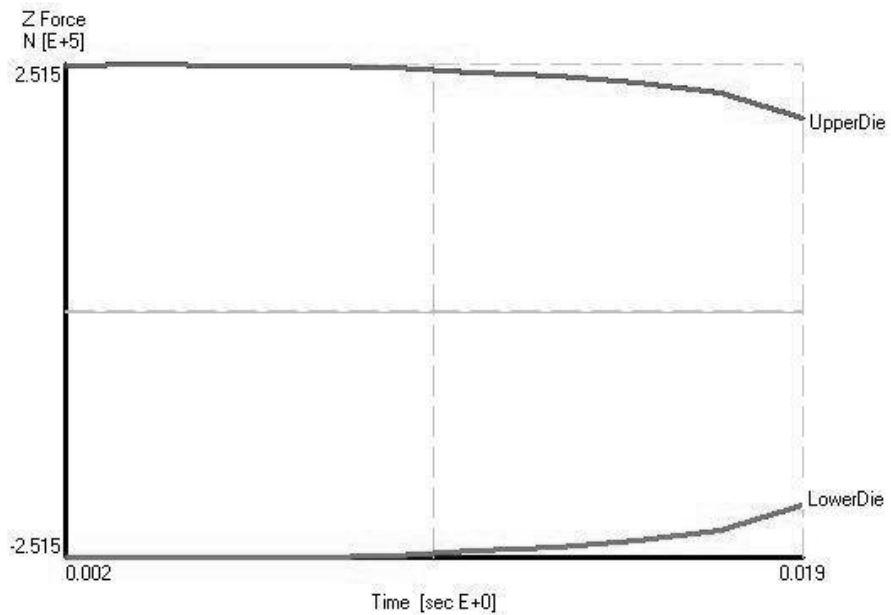


**Figure 3.22 Graphical Output of the Numerical Result for the Process with  $r=5\%$  at  $1000^\circ\text{C}$  for the Specimen with  $h_0=50\text{ mm}$**

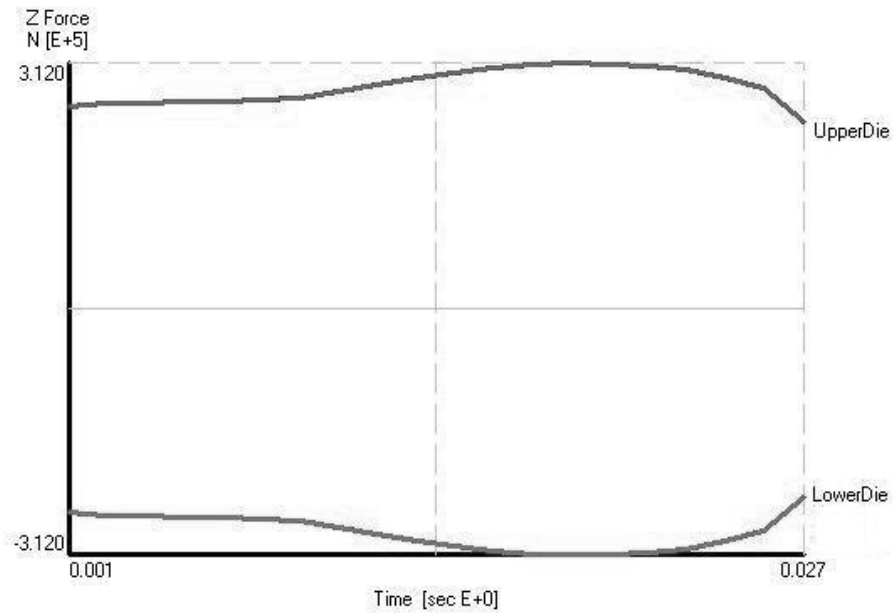


**Figure 3.23 Graphical Output of the Numerical Result for the Process with  $r=10\%$  at  $1000^{\circ}\text{C}$  for the Specimen with  $h_0=50\text{ mm}$**

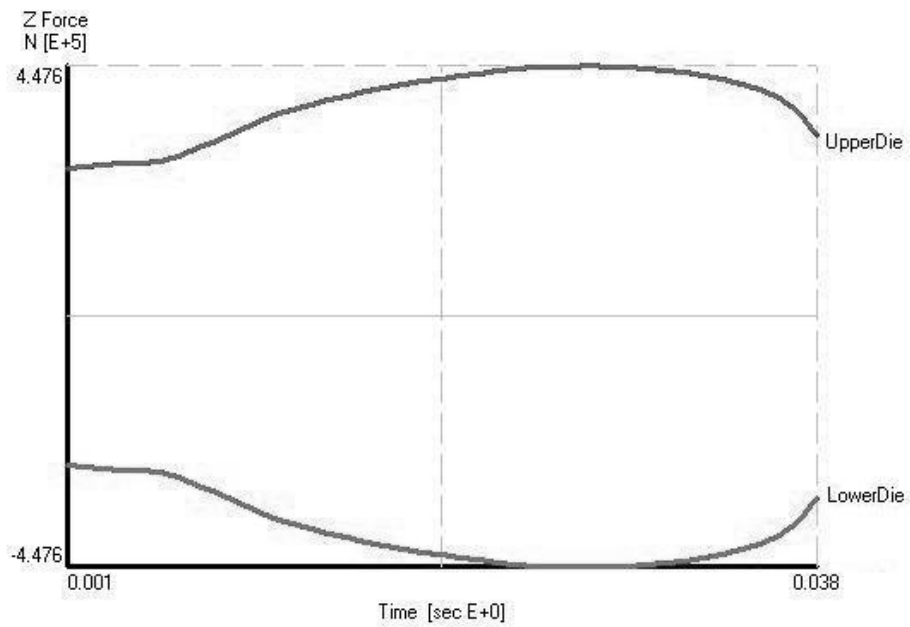


**Figure 3.24 Graphical Output of the Numerical Result for the Process with  $r=20\%$  at  $1000^{\circ}\text{C}$  for the Specimen with  $h_0=50\text{ mm}$**

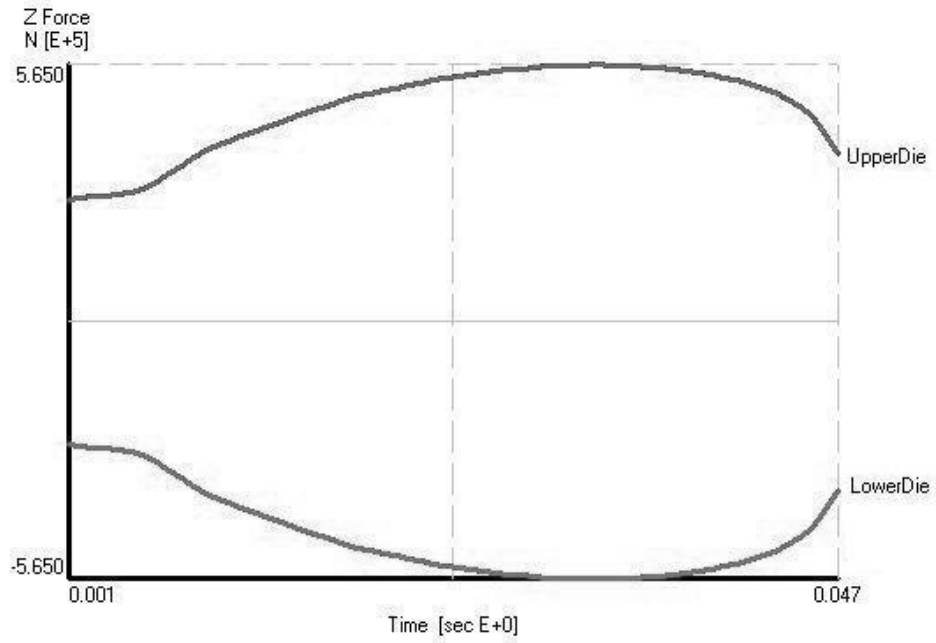


**Figure 3.25 Graphical Output of the Numerical Result for the Process with  $r=30\%$  at  $1000^{\circ}\text{C}$  for the Specimen with  $h_0=50$  mm**

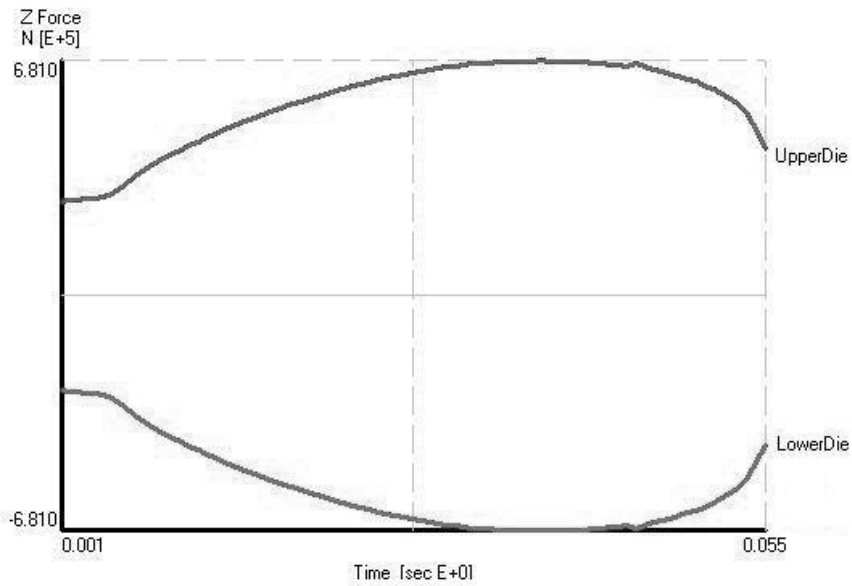


**Figure 3.26 Graphical Output of the Numerical Result for the Process with  $r=40\%$  at  $1000^{\circ}\text{C}$  for the Specimen with  $h_0=50$  mm**

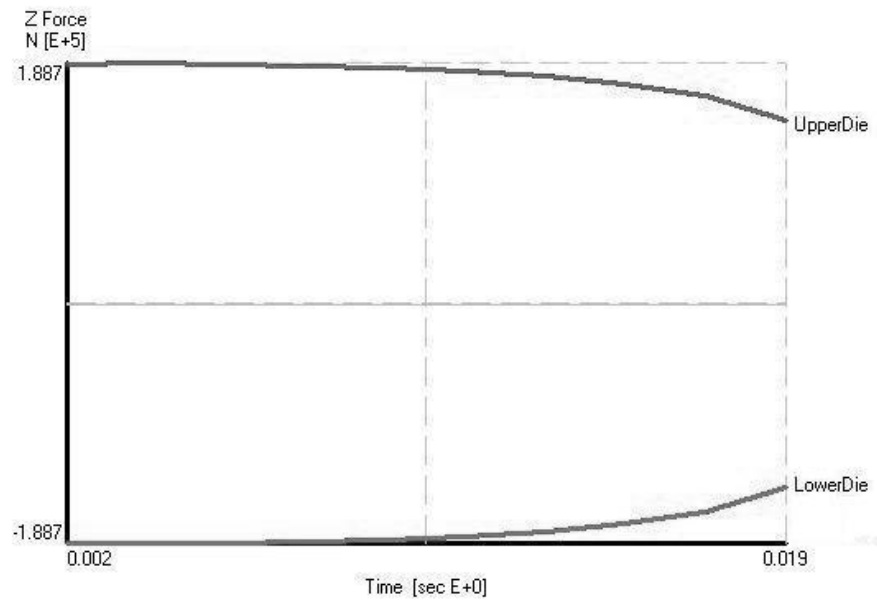


**Figure 3.27 Graphical Output of the Numerical Result for the Process with  $r=5\%$  at  $1100^{\circ}\text{C}$  for the Specimen with  $h_0=50\text{ mm}$**

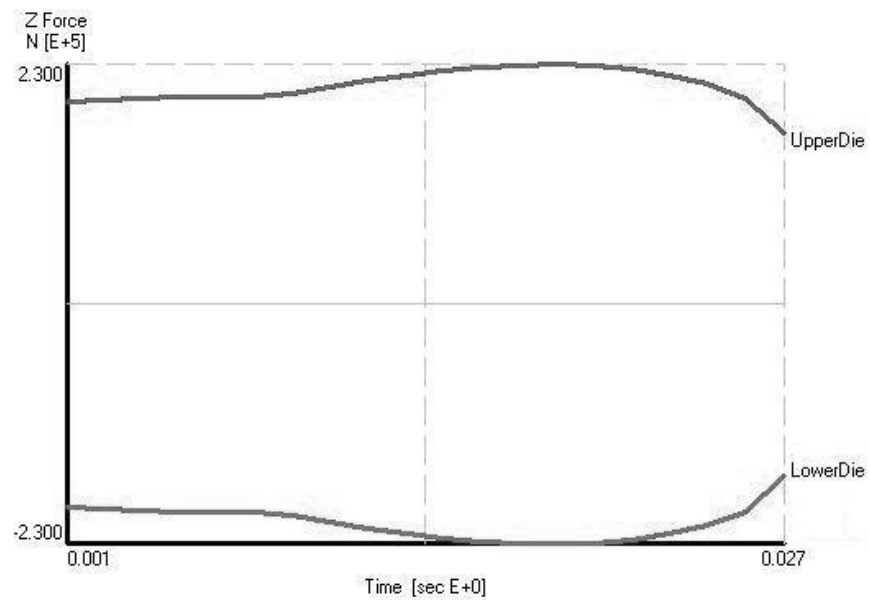


**Figure 3.28 Graphical Output of the Numerical Result for the Process with  $r=10\%$  at  $1100^{\circ}\text{C}$  for the Specimen with  $h_0=50\text{ mm}$**



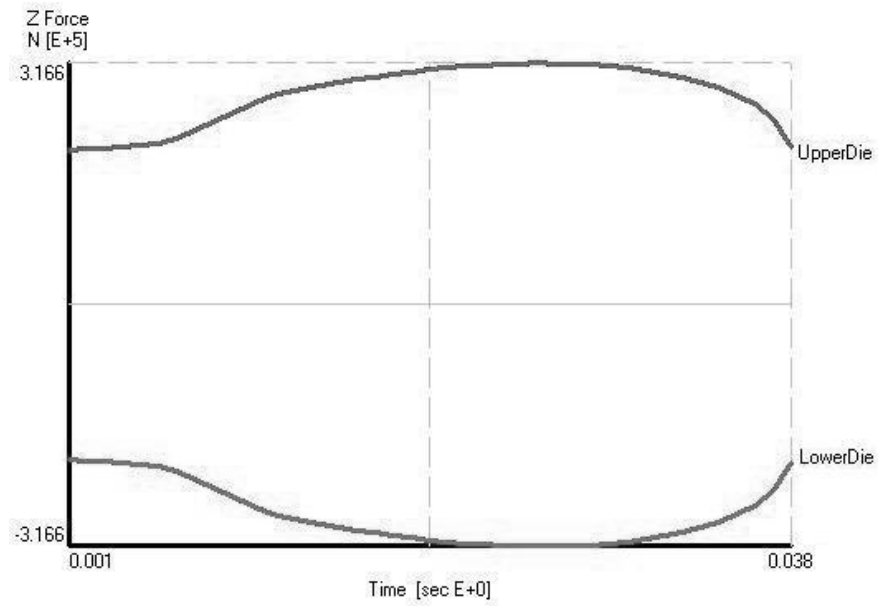


**Figure 3.29 Graphical Output of the Numerical Result for the Process with  $r=20\%$  at  $1100^{\circ}\text{C}$  for the Specimen with  $h_0=50\text{ mm}$**

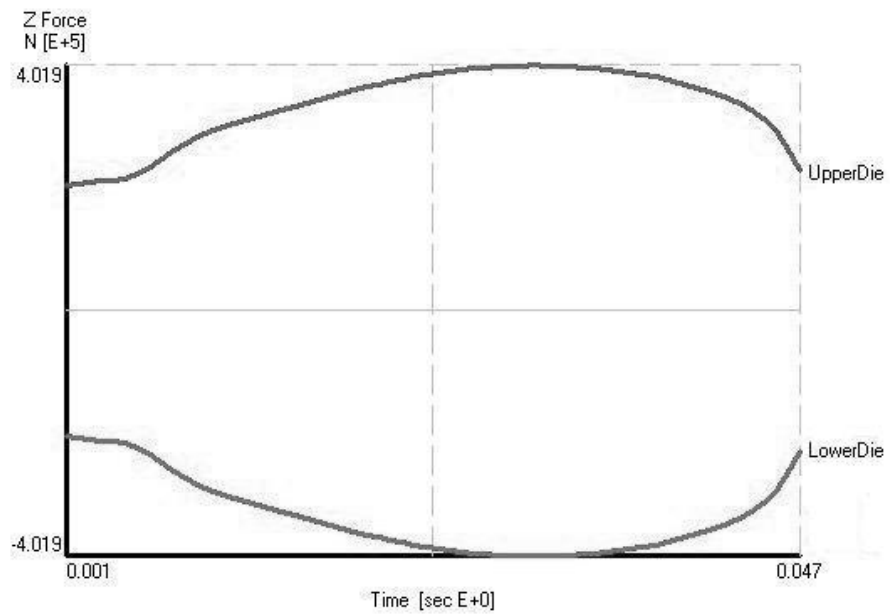


**Figure 3.30 Graphical Output of the Numerical Result for the Process with  $r=30\%$  at  $1100^{\circ}\text{C}$  for the Specimen with  $h_0=50\text{ mm}$**

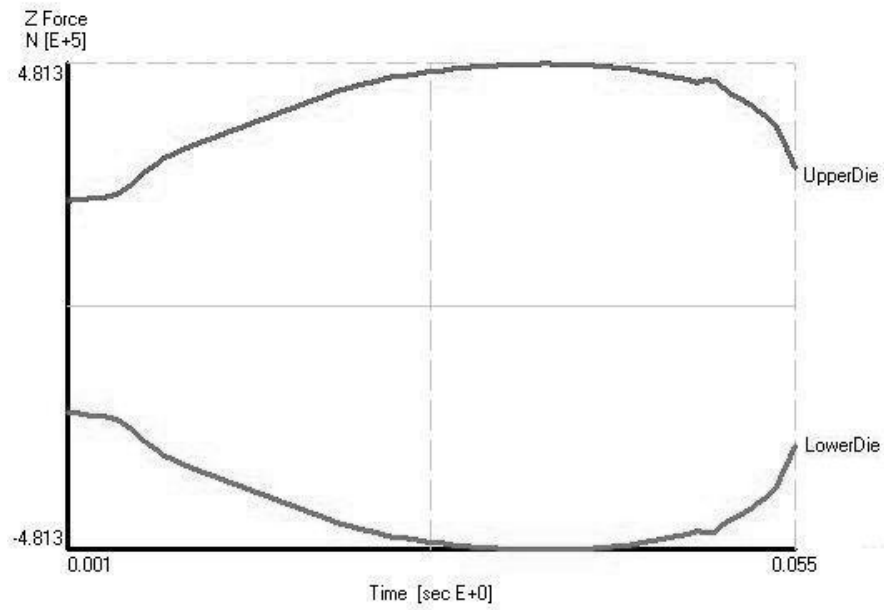


**Figure 3.31 Graphical Output of the Numerical Result for the Process with  $r=40\%$  at  $1100^\circ\text{C}$  for the Specimen with  $h_0=50$  mm**

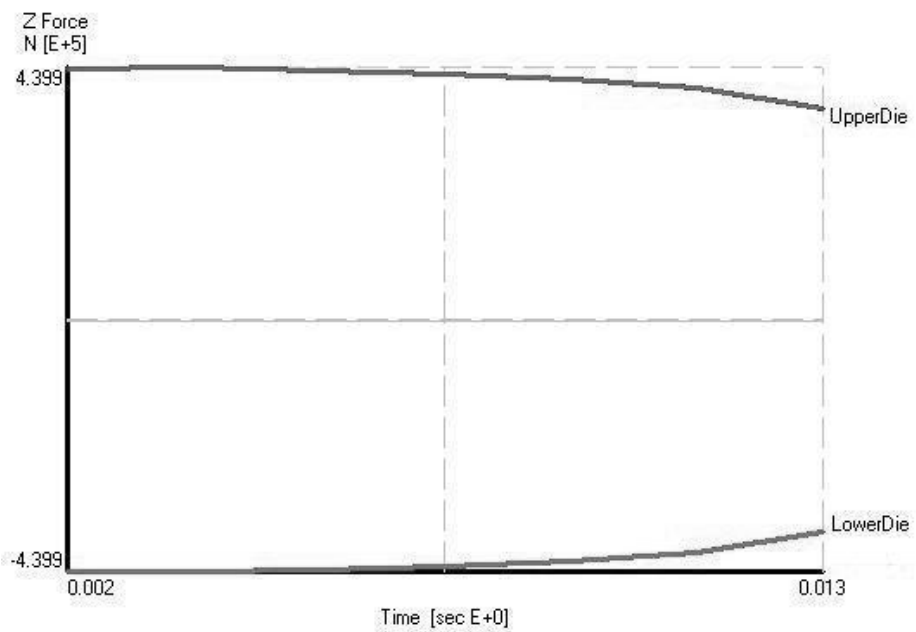


**Figure 3.32 Graphical Output of the Numerical Result for the Process with  $r=5\%$  at  $900^\circ\text{C}$  for the Specimen with  $h_0=25$  mm**

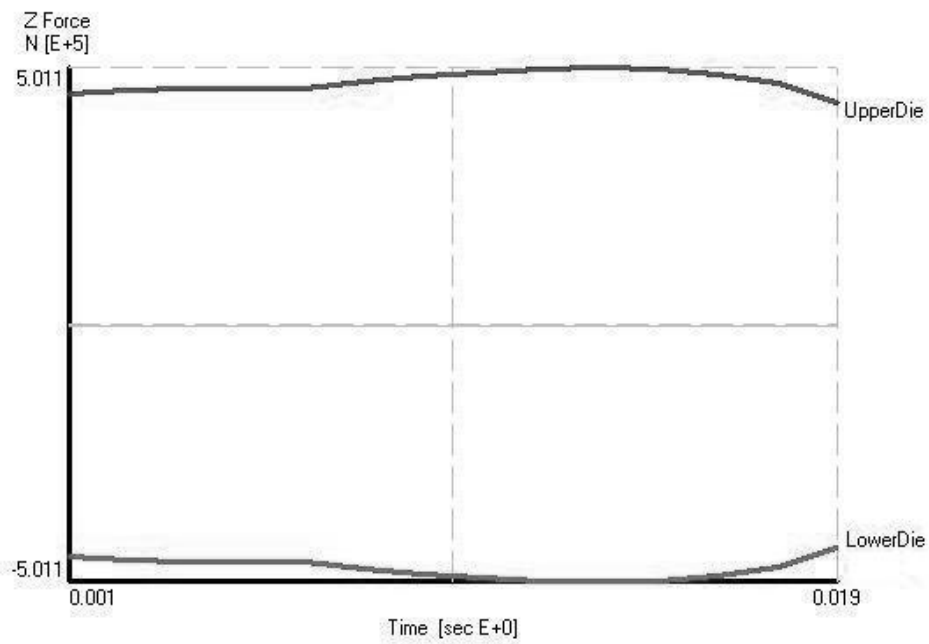


**Figure 3.33 Graphical Output of the Numerical Result for the Process with  $r=10\%$  at  $900^\circ\text{C}$  for the Specimen with  $h_0=25\text{ mm}$**

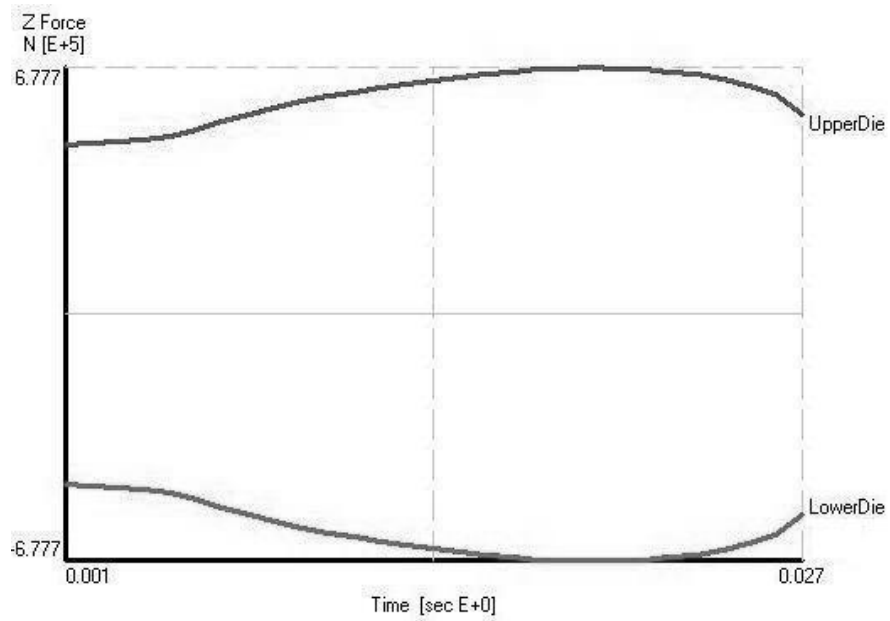


**Figure 3.34 Graphical Output of the Numerical Result for the Process with  $r=20\%$  at  $900^\circ\text{C}$  for the Specimen with  $h_0=25\text{ mm}$**

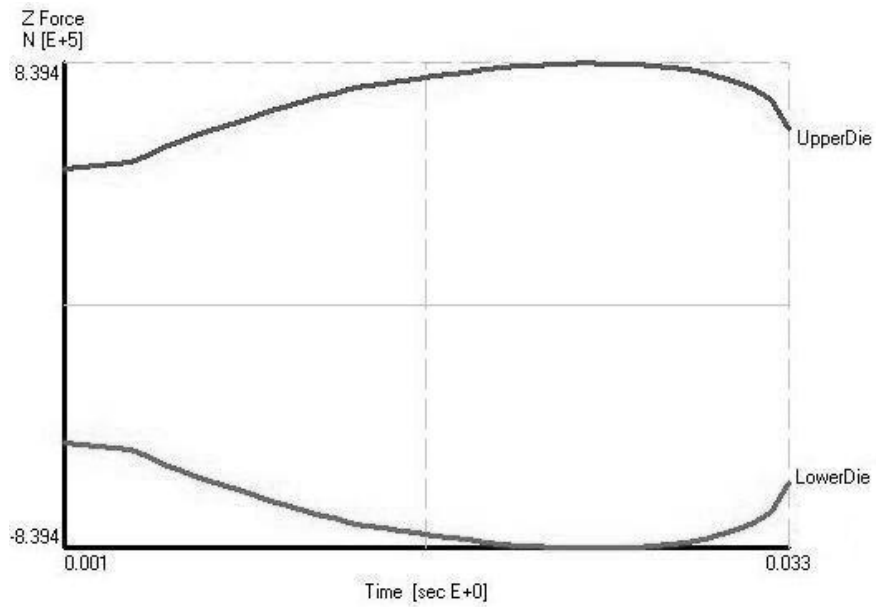


**Figure 3.35 Graphical Output of the Numerical Result for the Process with  $r=30\%$  at  $900^{\circ}\text{C}$  for the Specimen with  $h_0=25\text{ mm}$**

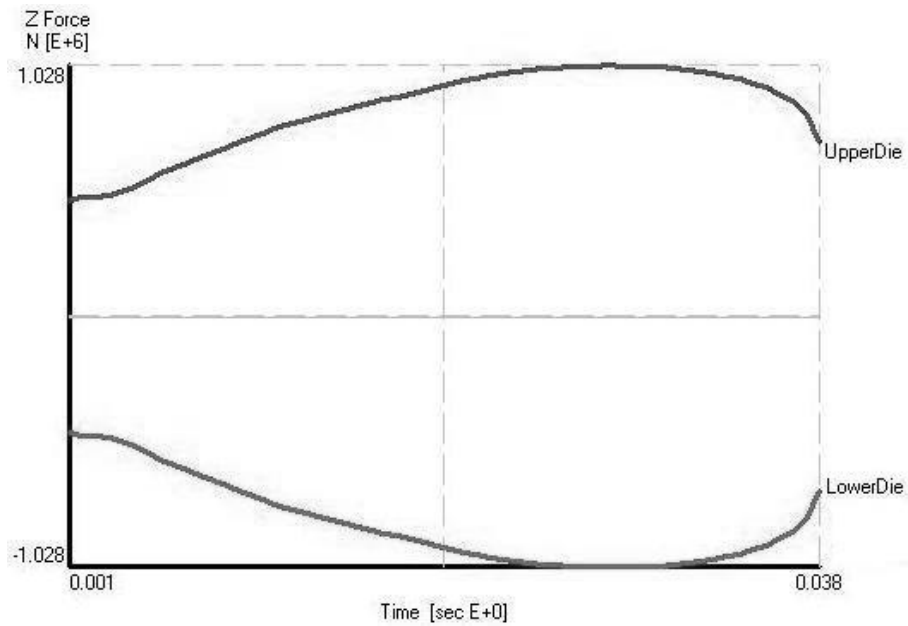


**Figure 3.36 Graphical Output of the Numerical Result for the Process with  $r=40\%$  at  $900^{\circ}\text{C}$  for the Specimen with  $h_0=25\text{ mm}$**

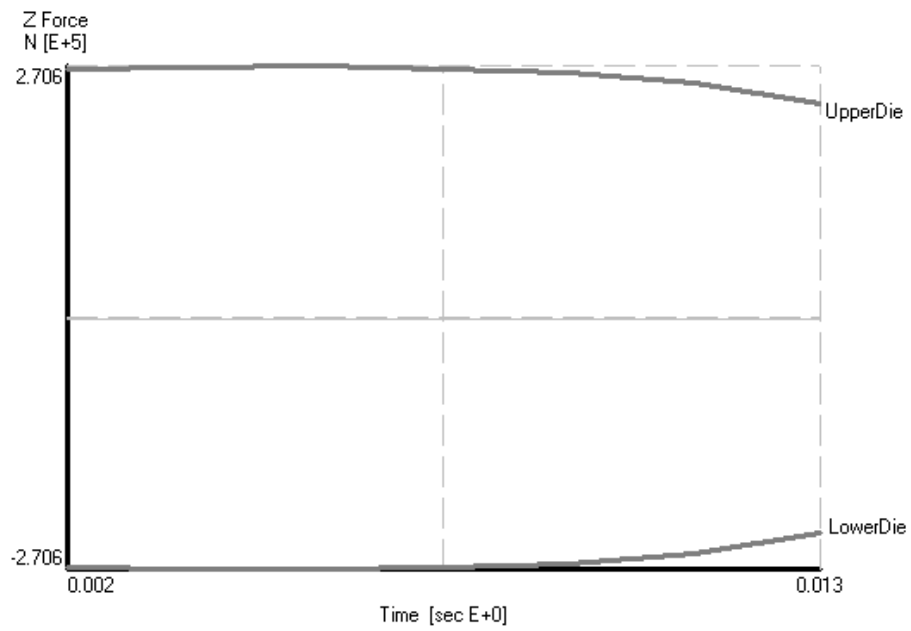


**Figure 3.37 Graphical Output of the Numerical Result for the Process with  $r=5\%$  at  $1000^{\circ}\text{C}$  for the Specimen with  $h_0=25\text{ mm}$**

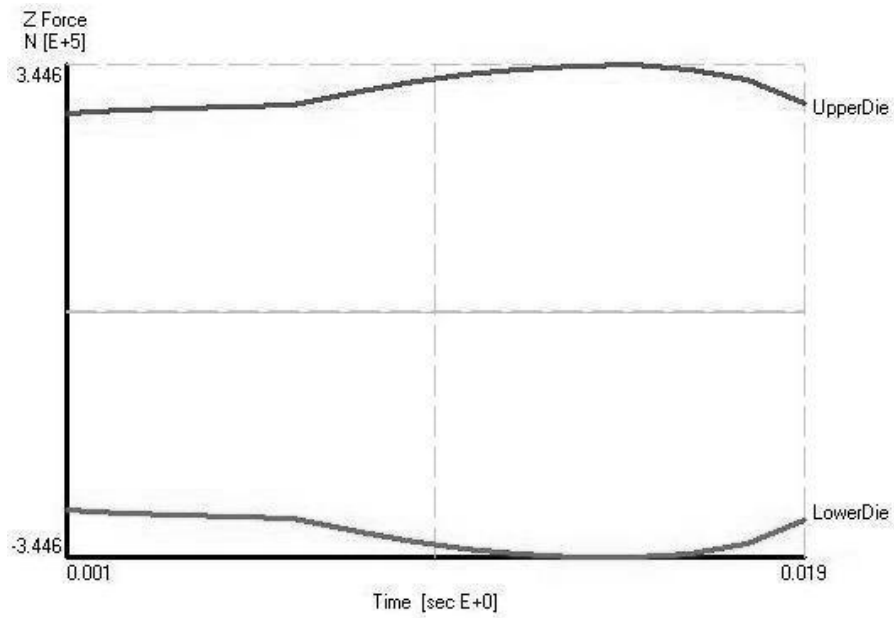


**Figure 3.38 Graphical Output of the Numerical Result for the Process with  $r=10\%$  at  $1000^{\circ}\text{C}$  for the Specimen with  $h_0=25\text{ mm}$**

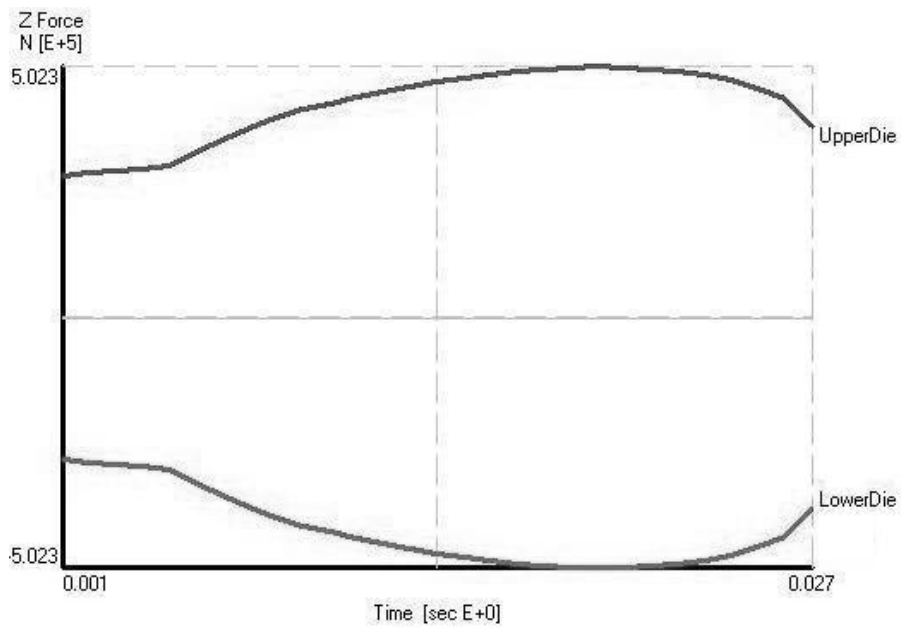


**Figure 3.39 Graphical Output of the Numerical Result for the Process with  $r=20\%$  at  $1000^\circ\text{C}$  for the Specimen with  $h_0=25$  mm**

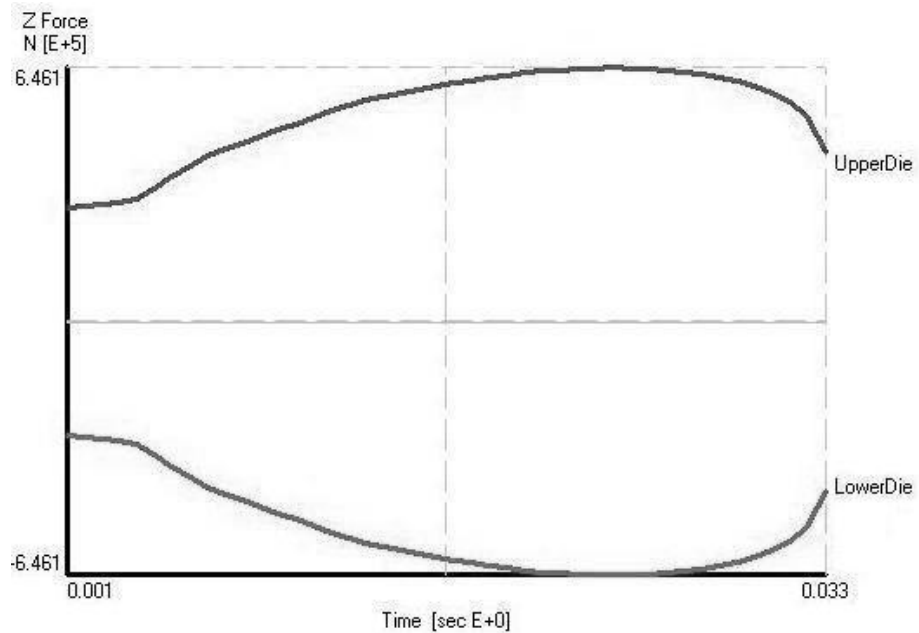


**Figure 3.40 Graphical Output of the Numerical Result for the Process with  $r=30\%$  at  $1000^\circ\text{C}$  for the Specimen with  $h_0=25$  mm**

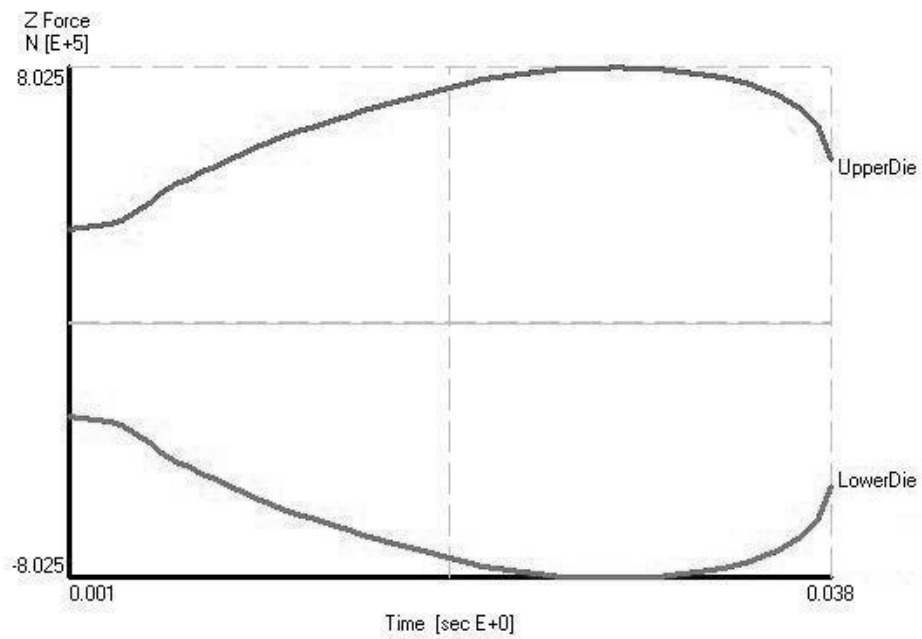


**Figure 3.41 Graphical Output of the Numerical Result for the Process with  $r=40\%$  at  $1000^{\circ}\text{C}$  for the Specimen with  $h_0=25\text{ mm}$**

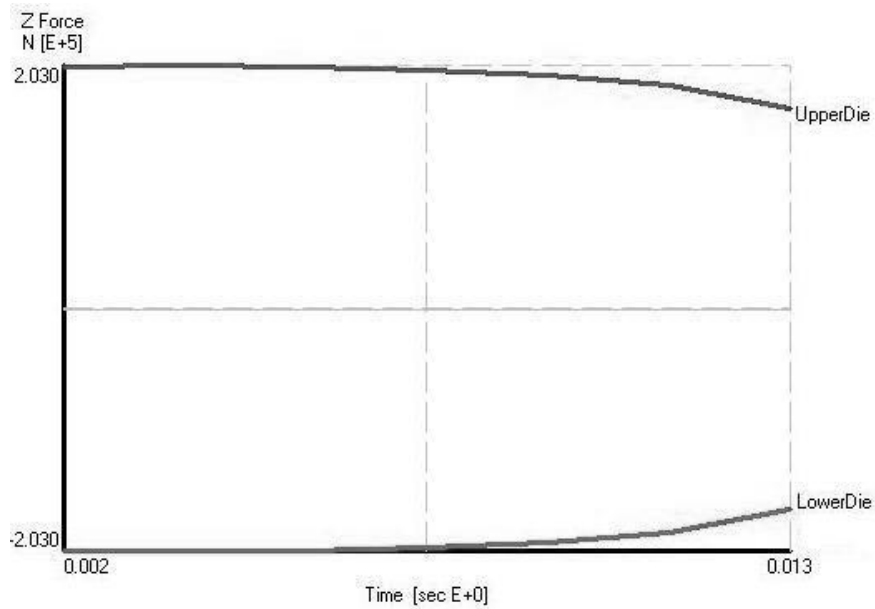


**Figure 3.42 Graphical Output of the Numerical Result for the Process with  $r=5\%$  at  $1100^{\circ}\text{C}$  for the Specimen with  $h_0=25\text{ mm}$**

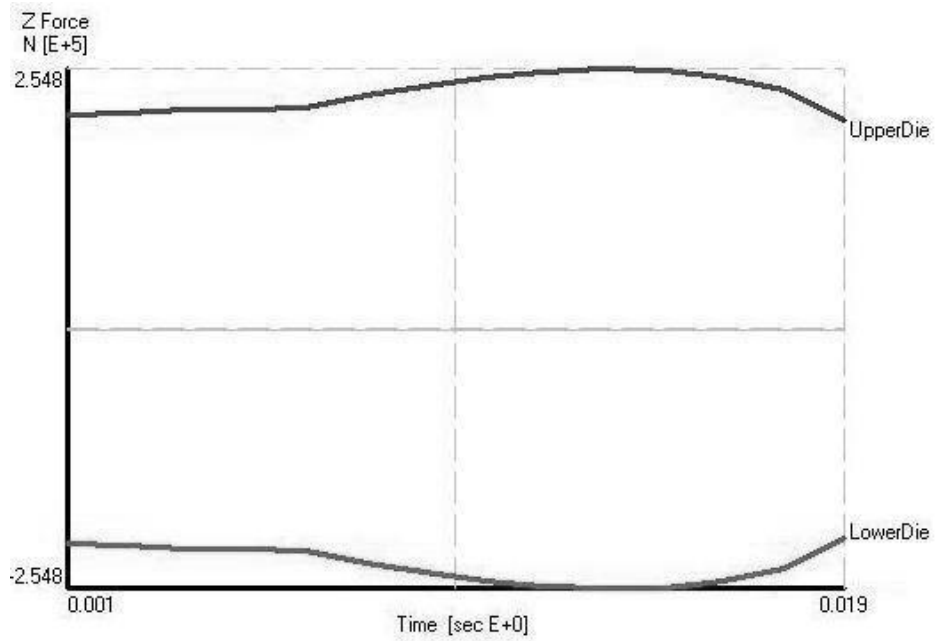


**Figure 3.43 Graphical Output of the Numerical Result for the Process with  $r=10\%$  at  $1100^\circ\text{C}$  for the Specimen with  $h_0=25$  mm**

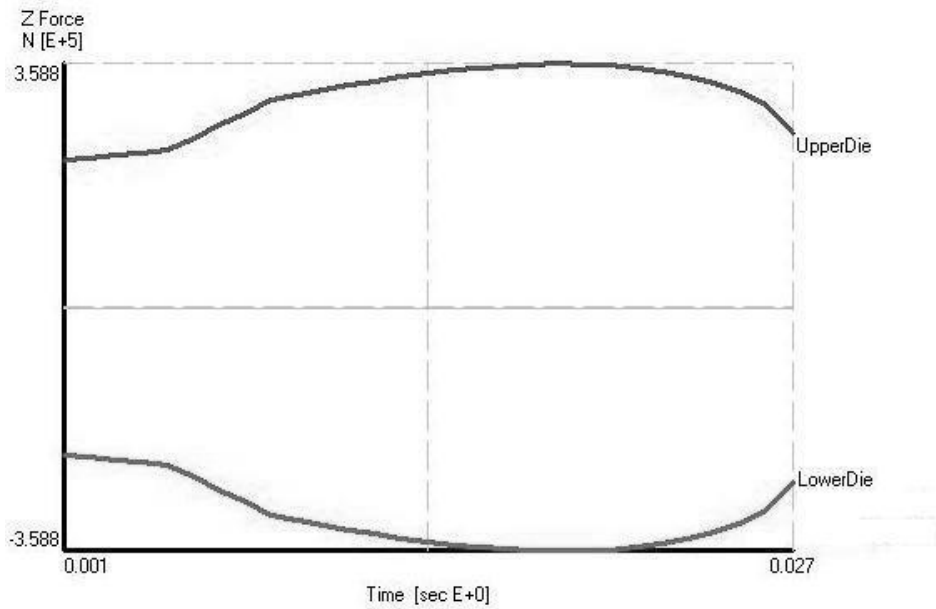


**Figure 3.44 Graphical Output of the Numerical Result for the Process with  $r=20\%$  at  $1100^\circ\text{C}$  for the Specimen with  $h_0=25$  mm**



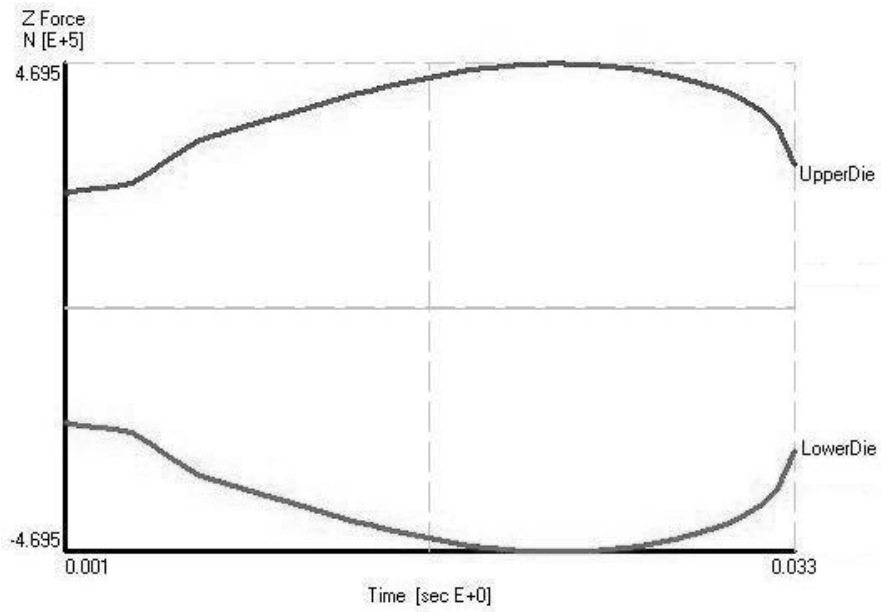


**Figure 3.45 Graphical Output of the Numerical Result for the Process with  $r=30\%$  at  $1100^{\circ}\text{C}$  for the Specimen with  $h_0=25\text{ mm}$**

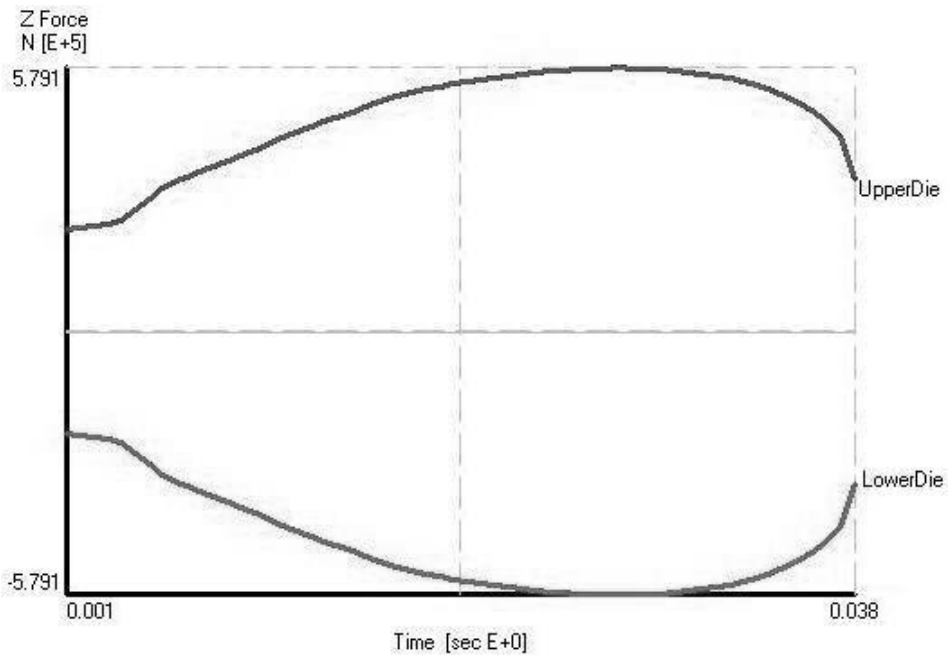


**Figure 3.46 Graphical Output of the Numerical Result for the Process with  $r=40\%$  at  $1100^{\circ}\text{C}$  for the Specimen with  $h_0=25\text{ mm}$**

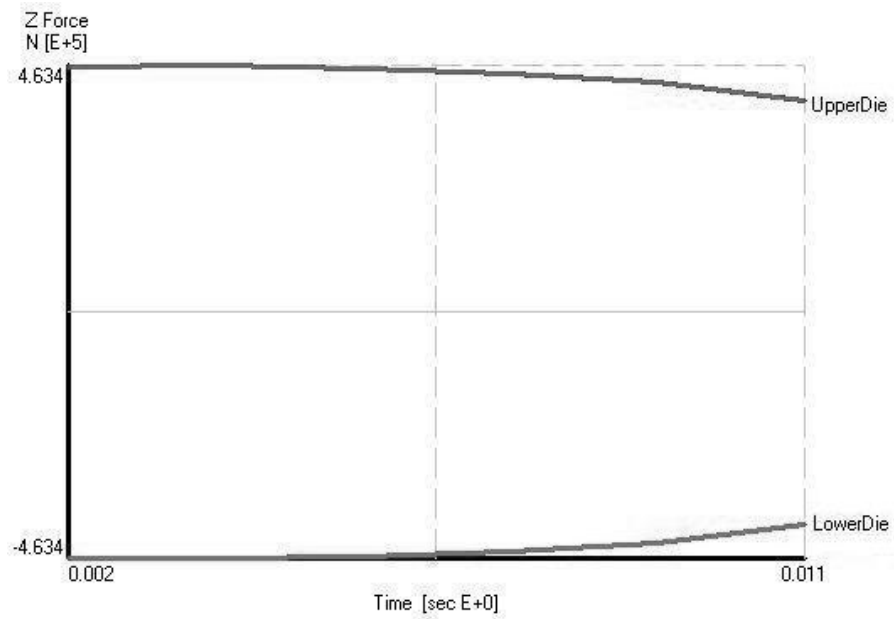


**Figure 3.47 Graphical Output of the Numerical Result for the Process with  $r=5\%$  at  $900^{\circ}\text{C}$  for the Specimen with  $h_0=16,67$  mm**

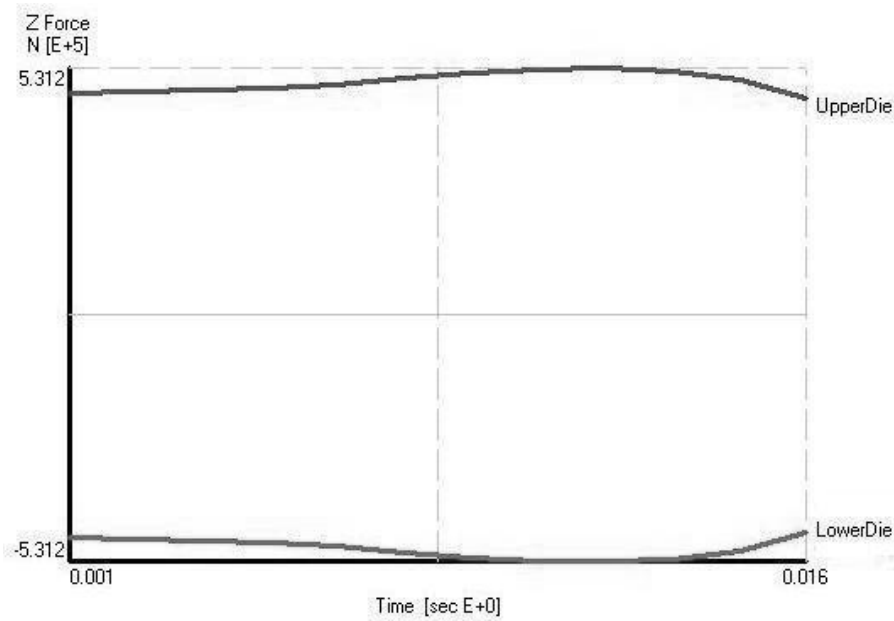


**Figure 3.48 Graphical Output of the Numerical Result for the Process with  $r=10\%$  at  $900^{\circ}\text{C}$  for the Specimen with  $h_0=16,67$  mm**

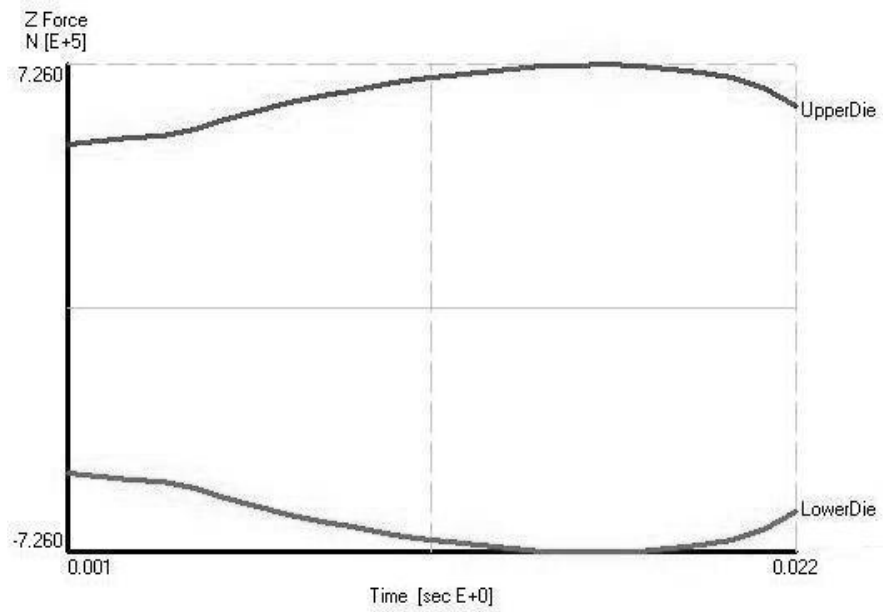


**Figure 3.49 Graphical Output of the Numerical Result for the Process with  $r=20\%$  at  $900^\circ\text{C}$  for the Specimen with  $h_0=16,67\text{ mm}$**

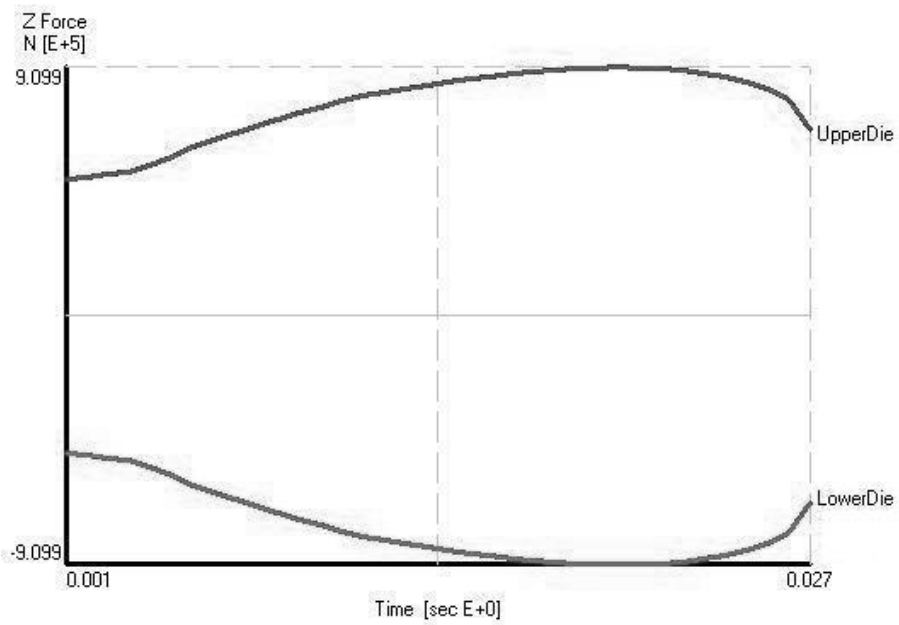


**Figure 3.50 Graphical Output of the Numerical Result for the Process with  $r=30\%$  at  $900^\circ\text{C}$  for the Specimen with  $h_0=16,67\text{ mm}$**

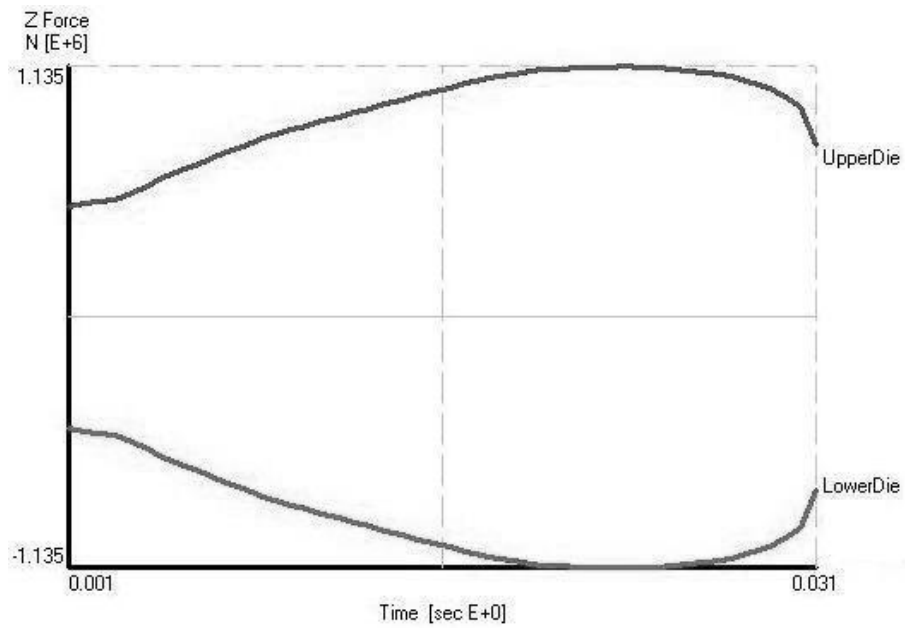


**Figure 3.51 Graphical Output of the Numerical Result for the Process with  $r=40\%$  at  $900^{\circ}\text{C}$  for the Specimen with  $h_0=16,67$  mm**

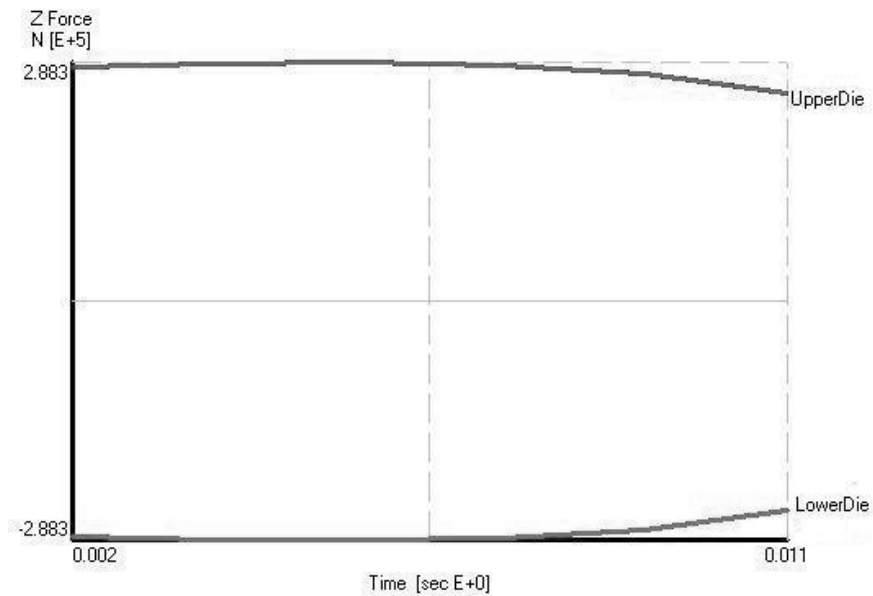


**Figure 3.52 Graphical Output of the Numerical Result for the Process with  $r=5\%$  at  $1000^{\circ}\text{C}$  for the Specimen with  $h_0=16,67$  mm**

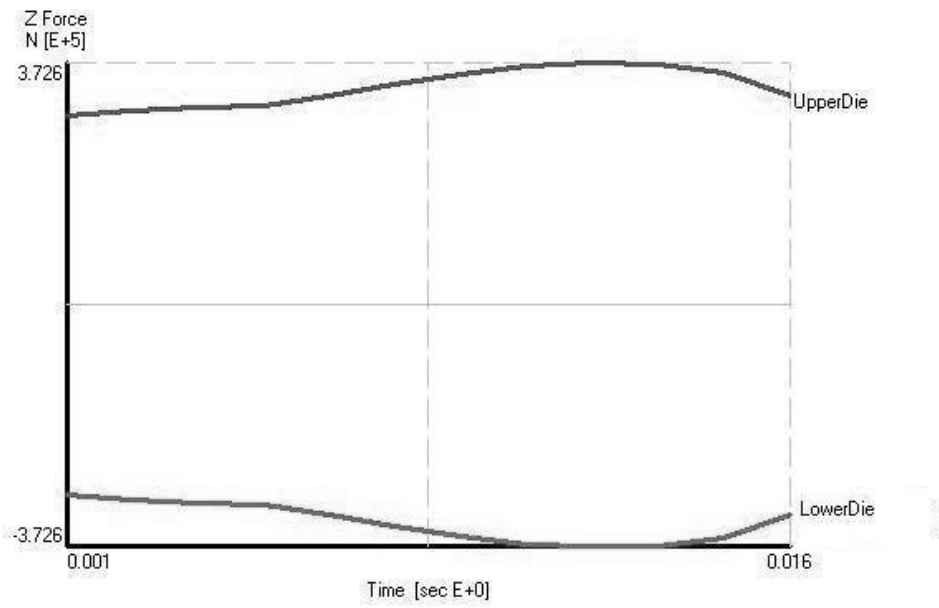


**Figure 3.53 Graphical Output of the Numerical Result for the Process with  $r=10\%$  at  $1000^{\circ}\text{C}$  for the Specimen with  $h_0=16,67\text{ mm}$**

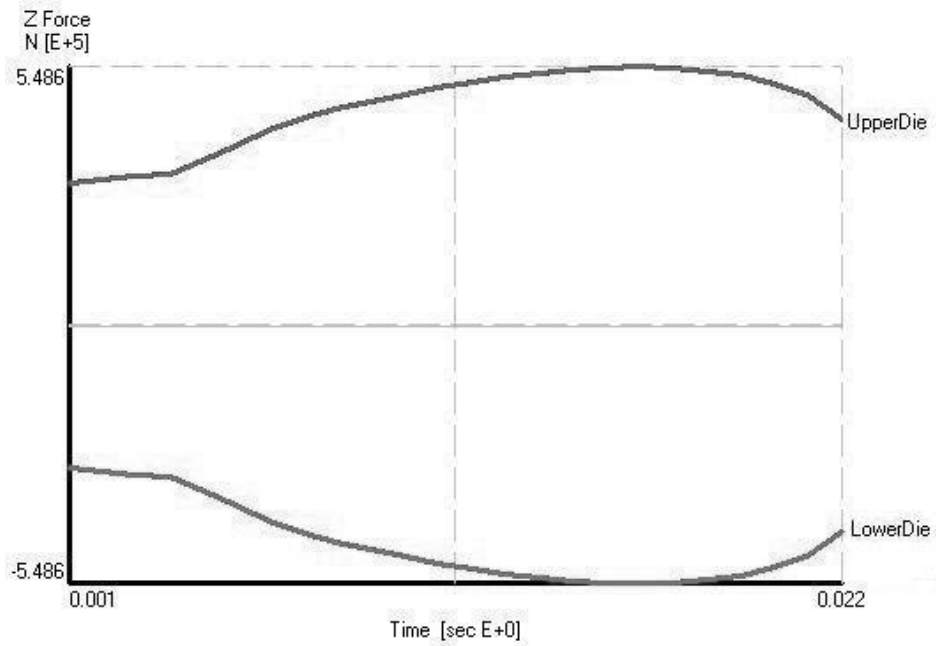


**Figure 3.54 Graphical Output of the Numerical Result for the Process with  $r=20\%$  at  $1000^{\circ}\text{C}$  for the Specimen with  $h_0=16,67\text{ mm}$**

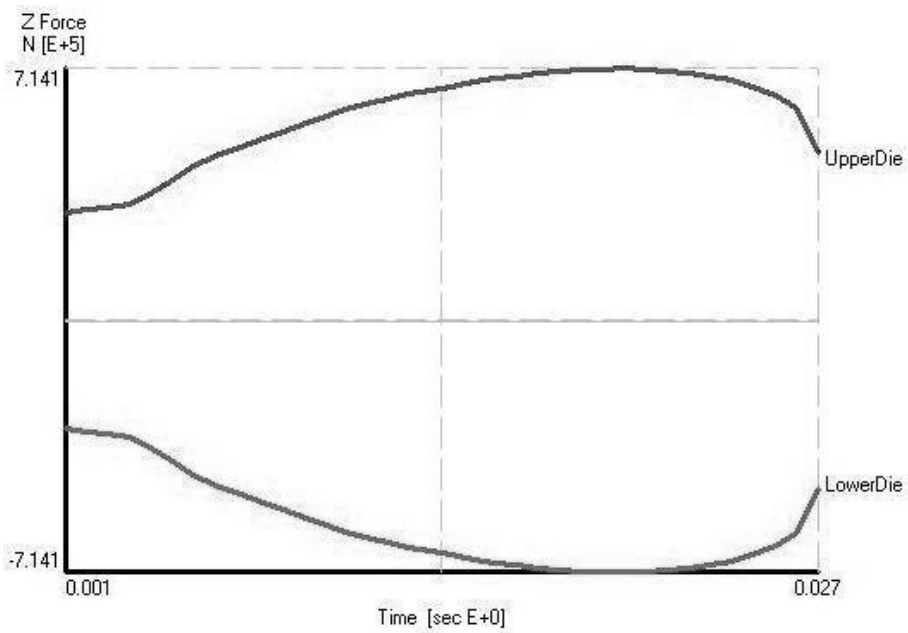


**Figure 3.55 Graphical Output of the Numerical Result for the Process with  $r=30\%$  at  $1000^{\circ}\text{C}$  for the Specimen with  $h_0=16,67\text{ mm}$**

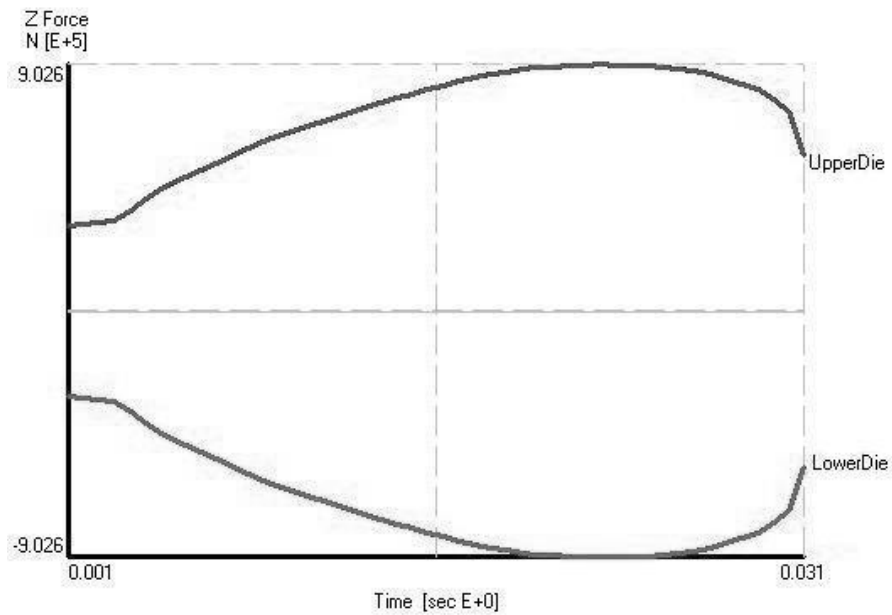


**Figure 3.56 Graphical Output of the Numerical Result for the Process with  $r=40\%$  at  $1000^{\circ}\text{C}$  for the Specimen with  $h_0=16,67\text{ mm}$**

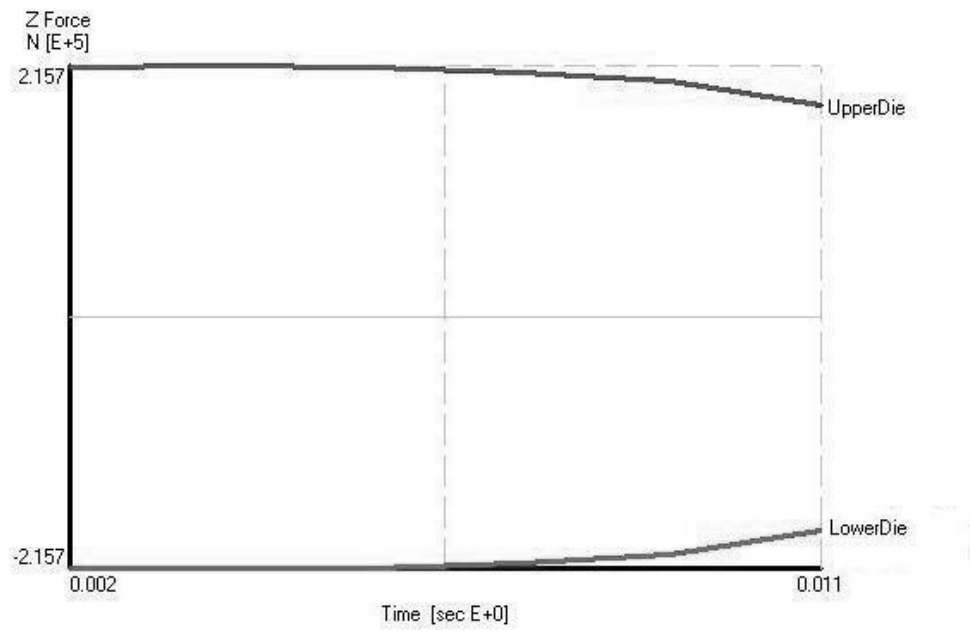


**Figure 3.57 Graphical Output of the Numerical Result for the Process with  $r=5\%$  at  $1100^{\circ}\text{C}$  for the Specimen with  $h_0=16,67$  mm**

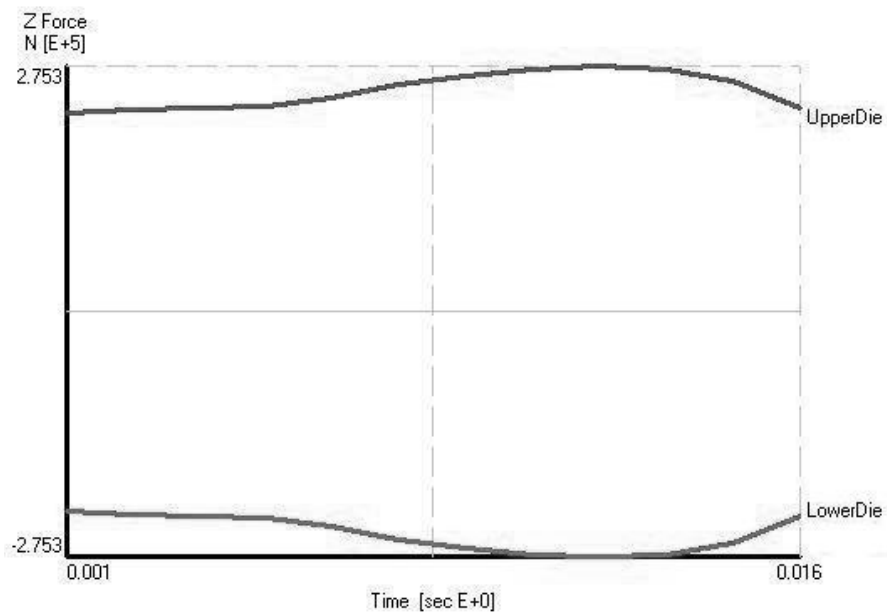


**Figure 3.58 Graphical Output of the Numerical Result for the Process with  $r=10\%$  at  $1100^{\circ}\text{C}$  for the Specimen with  $h_0=16,67$  mm**

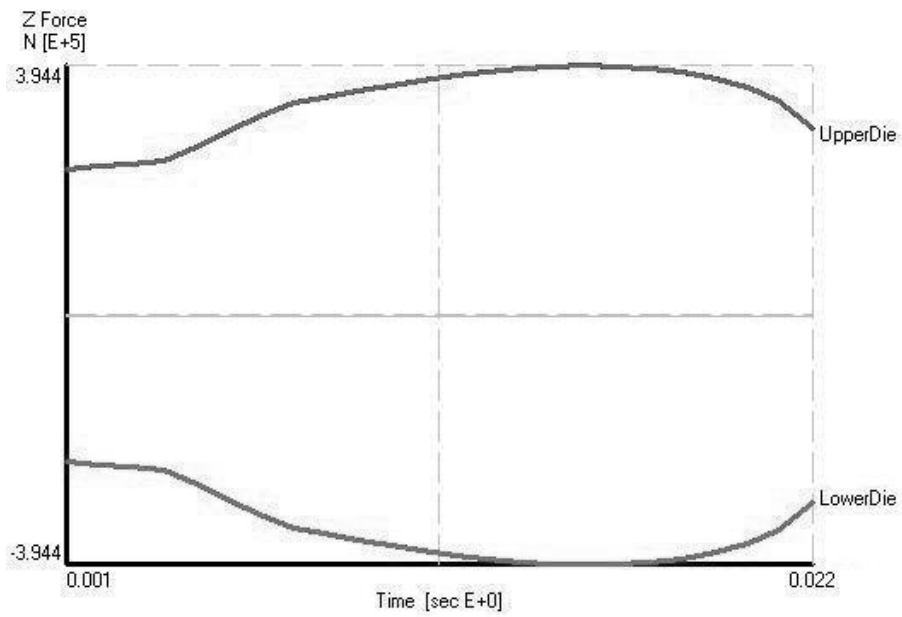


**Figure 3.59 Graphical Output of the Numerical Result for the Process with  $r=20\%$  at  $1100^{\circ}\text{C}$  for the Specimen with  $h_0=16,67$  mm**

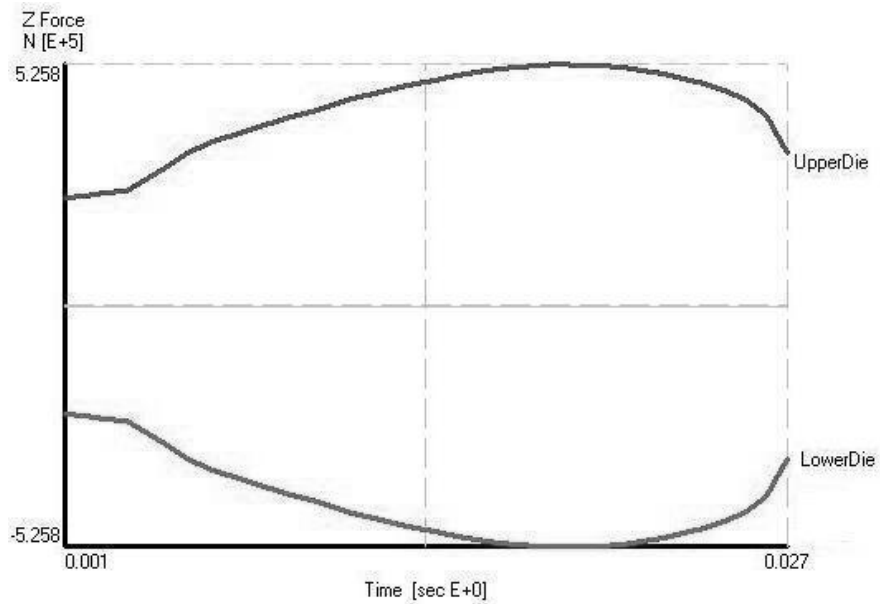


**Figure 3.60 Graphical Output of the Numerical Result for the Process with  $r=30\%$  at  $1100^{\circ}\text{C}$  for the Specimen with  $h_0=16,67$  mm**



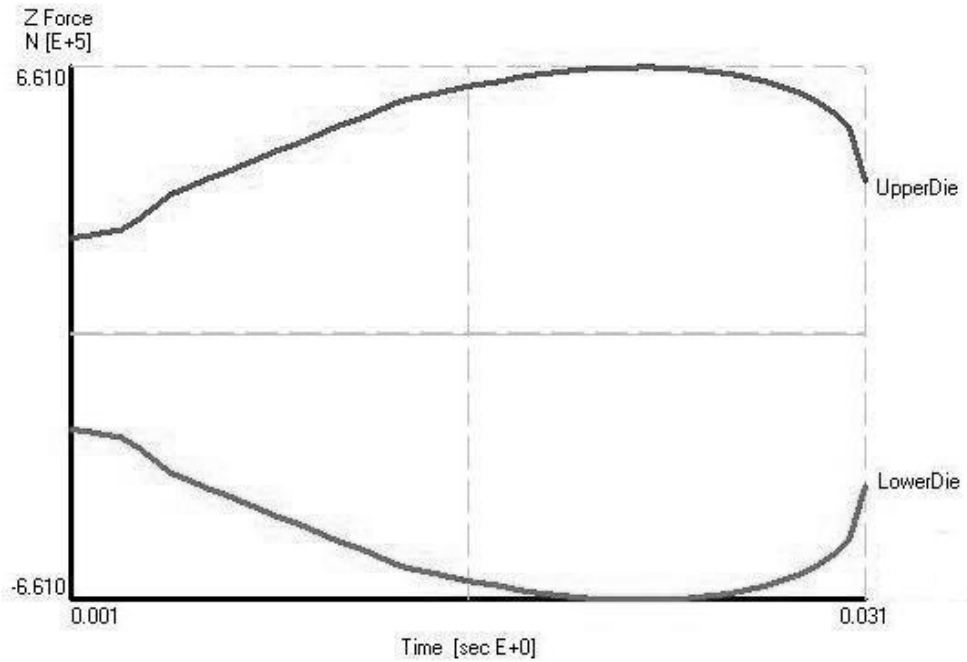


**Figure 3.61 Graphical Output of the Numerical Result for the Process with  $r=40\%$  at  $1100^{\circ}\text{C}$  for the Specimen with  $h_0=16,67\text{ mm}$**

Additionally, the maximum forces evaluated from the numerical studies are given in Table 3.2-3.4.

**Table 3.2 Maximum Force Values (kN) of the Processes at  $900^{\circ}\text{C}$**

	$r=5\%$	$r=10\%$	$r=20\%$	$r=30\%$	$r=40\%$
$h_0=100,00\text{ mm}$	1069,17	1163,07	1546,44	1888,82	2213,83
$h_0=50,00\text{ mm}$	1100,30	1221,17	1627,11	1986,61	2362,19
$h_0=25,00\text{ mm}$	1186,16	1343,34	1820,86	2273,49	2614,06
$h_0=16,67\text{ mm}$	1269,94	1453,32	1996,73	2530,27	3198,18

**Table 3.3 Maximum Force Values (kN) of the Processes at 1000°C**

	<i>r=5%</i>	<i>r=10%</i>	<i>r=20%</i>	<i>r=30%</i>	<i>r=40%</i>
<i>h<sub>0</sub>=100,00 mm</i>	643,5276	773,4781	1114,566	1404,555	1668,088
<i>h<sub>0</sub>=50,00 mm</i>	669,4658	819,6482	1173,705	1499,23	1790,257
<i>h<sub>0</sub>=25,00mm</i>	729,3831	924,9574	1350,085	1747,718	2180,368
<i>h<sub>0</sub>=16,67mm</i>	795,5256	1029,488	1520,24	2005,025	2554,657

**Table 3.4 Maximum Force Values (kN) of the Processes at 1100°C**

	<i>r=5%</i>	<i>r=10%</i>	<i>r=20%</i>	<i>r=30%</i>	<i>r=40%</i>
<i>h<sub>0</sub>=100,00 mm</i>	479,60	561,82	773,74	970,35	1159,44
<i>h<sub>0</sub>=50,00 mm</i>	501,39	604,62	832,36	1054,13	1281,09
<i>h<sub>0</sub>=25,00 mm</i>	546,78	683,21	963,35	1263,19	1577,04
<i>h<sub>0</sub>=16,67mm</i>	591,91	761,29	1098,48	1548,25	1885,71

## CHAPTER 4

### EXPERIMENTAL STUDY

The experimental study has been conducted for the specimens having the initial diameter of 50 mm to apply the Cook and Larke Simple Compression Test at the temperatures of 900°C, 1000°C and 1100°C. After forging of each specimen, compression forces versus crank angle of the forging press are recorded to determine compression force versus axial position of the ram.

#### 4.1 Preparation for the Experiments

##### 4.1.1 Specimens

AISI 1045 steel is used for experiments. Its material properties are given in Appendix B. In METU-BILTIR Center Forging Research and Application Laboratory, the bars with diameter of 50 mm are cut into pieces of which height values are determined according to the aspect ratios ( $d_0/h_0$ ) of 1/2, 1, 2, and 3.

**Table 4.1 Specimen Dimensions According to Selected Aspect Ratios**

$d_0/h_0$	3	2	1	0,5
$d_0$ (mm)	50,00	50,00	50,00	50,00
$h_0$ (mm)	16,67	25,00	50,00	100,00

As described in Chapter 2, the heights of the specimens are reduced by 5%, 10%, 20%, 30% and 40%. In other words, a specimen with an aspect ratio of 0,5 is forged to final heights by this five reduction ratios and the same process will be repeated for

the specimens with aspect ratios 1, 2 and 3. This means  $5 \times 4 = 20$  specimens are needed for each temperature. As discussed previously, the experiments have been done at three temperatures, so by this point  $5 \times 4 \times 3 = 60$  specimens are needed for all temperature. Generally in experiments, more than one test is made for the same condition to reduce the doubts. In these experiments, tests for each condition are repeated three times. As a result, there need to be  $5 \times 4 \times 3 \times 3 = 180$  specimens to be cut.

The bars made of AISI 1045 steel are cut in an automatic saw which is available in METU-BILTIR Center Forging Research and Application Laboratory. Then these specimens are carried to a surface grinding machine to be ground. The specimens which are cut according to the same aspect ratio are loaded onto the table of the grinding machine in order to get the same height value. In Figure 4.1, some specimens are seen while being ground.



**Figure 4.1 Grinding of the Specimens**

### **4.1.2 Forging Dies**

By preparing the G-codes for CAM operations, turning and milling operations are applied in METU-BILTIR Center Forging Research and Application Laboratory. In Figure 4.2, turning operation and in Figure 4.3 CNC milling operation of the lower die are shown.



**Figure 4.2 Turning Operation of the Lower Die**

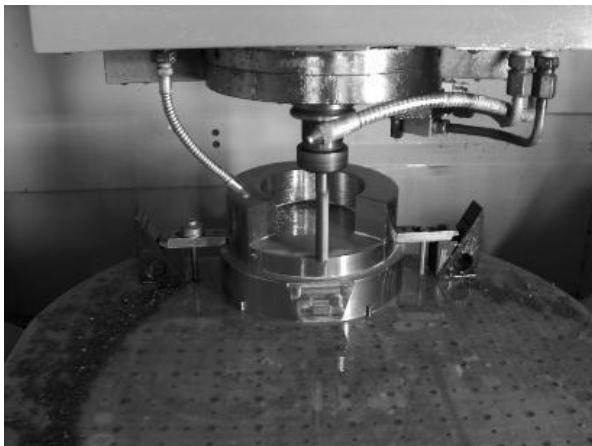


**Figure 4.3 CNC Milling of the Lower Die**

The inserts of the die set after machining operations are shown in Figure 4.4. After manufacturing processes, heat treatment is applied to the die set to get harder structure in order to avoid the failures during forging processes.



**Figure 4.4 Inserts of the Die Set after Machining Operations**

#### **4.1.3 Heating Equipment and the Forging Press**

The specimens are heated in Inductoheat<sup>®</sup> 125 kVA induction heater seen in Figure 4.5 (a) and they are forged in Smeral Brno<sup>®</sup> LZK 1000 forging press shown in Figure 4.5 (b). The feature of the forging press is given in Appendix C.

As seen in Chapter 3, the finite element analyses results showed that using 1000 ton forging press available in METU-BILTIR Center is capable to conduct all the necessary experiments since the required forces have been determined as below 1000 ton.



(a)



(b)

**Figure 4.5 (a) 125 kVA Induction Heater (b) 1000 Ton Capacity Forging Press**

#### **4.1.4 Other Equipment**

The temperatures of the heated billets are measured by a fixed pyrometer seen in Figure 4.6. The temperature measurements of the heated specimens are realized just before they are carried to the forging press. The temperature range of this pyrometer is between 600°C and 1400°C [4].



**Figure 4.6 Fixed Pyrometer**

The dies which are fixed on the anvil and the ram of the forging press are preheated by the flame gun of an LPG tube and the hot specimens are hold with a metal tong seen in Figure 4.7.

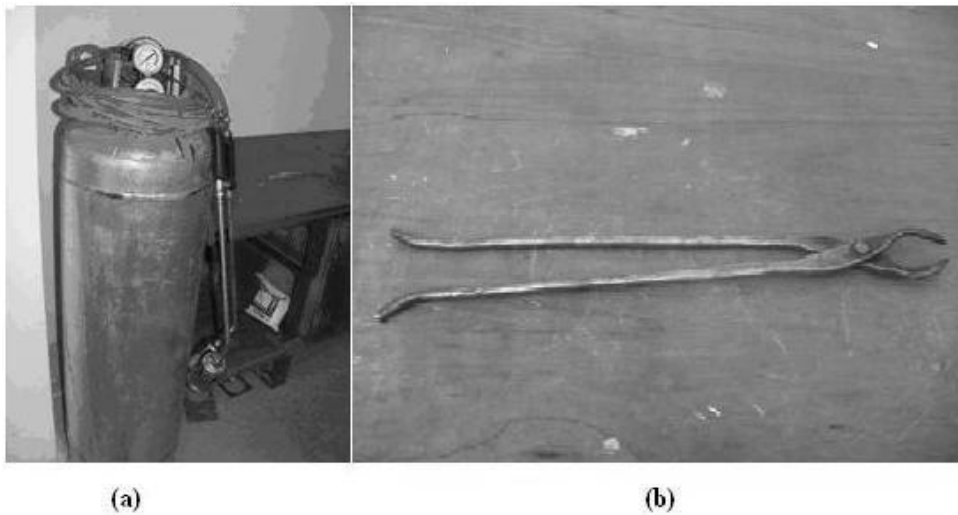


**Figure 4.7 (a) LPG Tube with Flame Gun for Preheating the Dies  
(b) Tong for Holding Hot Specimens**



The dies are generally heated to about 200°C. The die temperatures are measured with a portable pyrometer seen in Figure 4.8. This is useful for measuring the temperatures of the objects which are fixed somewhere and cannot be carried easily like forging dies. The temperature range of this pyrometer is between -32°C and 600°C [4], so this is not suitable for measuring the temperatures of the specimens to be tested in this thesis study.



**Figure 4.8 Portable Pyrometer**

#### **4.2 Data Acquisition System for Recording Load versus Press Crank Angle Values**

As seen in Figure 4.9, the data acquisition system is integrated on the forging press to measure and record the compressive forces vs. the stroke of the ram is. These are used to calculate axial ram position versus the forging load.

When the covers on both sides of the forging press shown in Figure 4.9 are opened, strain gages attached to the columns can be seen. One of these strain gages is shown in Figure 4.10 (a). These strain gages produce analogue signals to be transmitted to DECADE 260<sup>®</sup> unit. Not only these analogue signals are transmitted to the DECADE 260<sup>®</sup> unit but also the digital signals produced by the encoder which is driven by the flywheel of the forging press. A picture of the encoder is seen in Figure 4.10 (b).

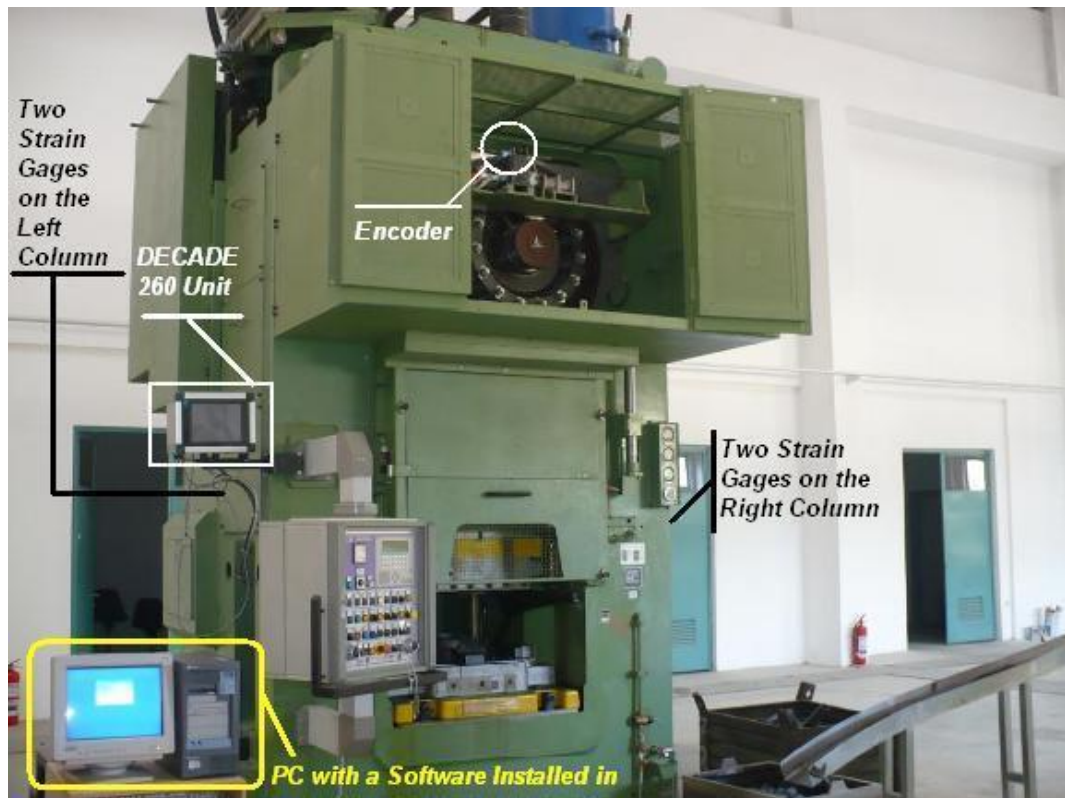
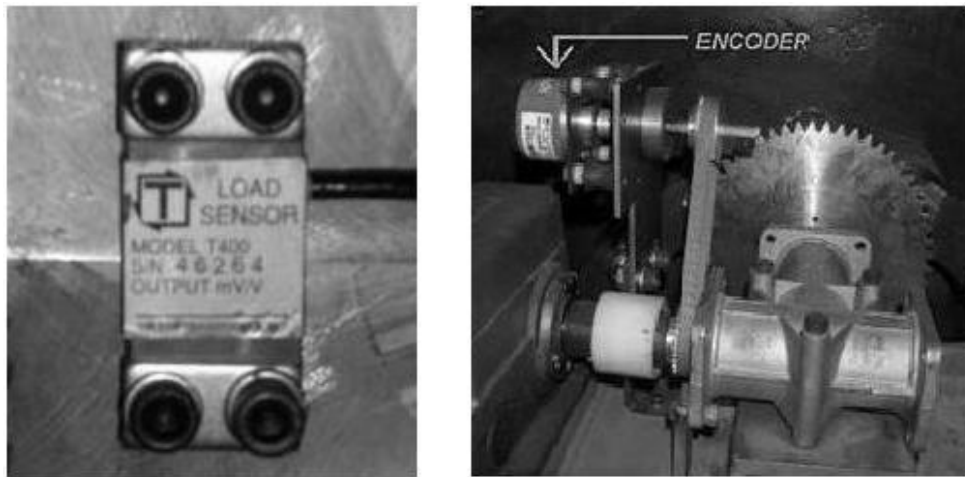


**Figure 4.9** Picture Showing the Elements of the Data Acquisition System



( a )

( b )

**Figure 4.10** (a) One of the Strain Gages Attached to the Forging Press  
 (b) Encoder of the Data Acquisition System

The analogue signals coming from the strain gages are converted to digital signals of load values in terms of tons and raw data coming from the encoder are converted to binary signals of angle values in terms of degrees in the DECADE 260<sup>®</sup> unit which is seen in Figure 4.11. These signals can be transferred to the personal computer (PC), with the software installed in, to monitor the data collected. Working principle of the data acquisition system is simply shown in Figure 4.12.



(a)



(b)

**Figure 4.11 DECADE 260<sup>®</sup> Unit (a) Screen on the Front Side (b) View of the Hardware when the Back Cover is Opened**

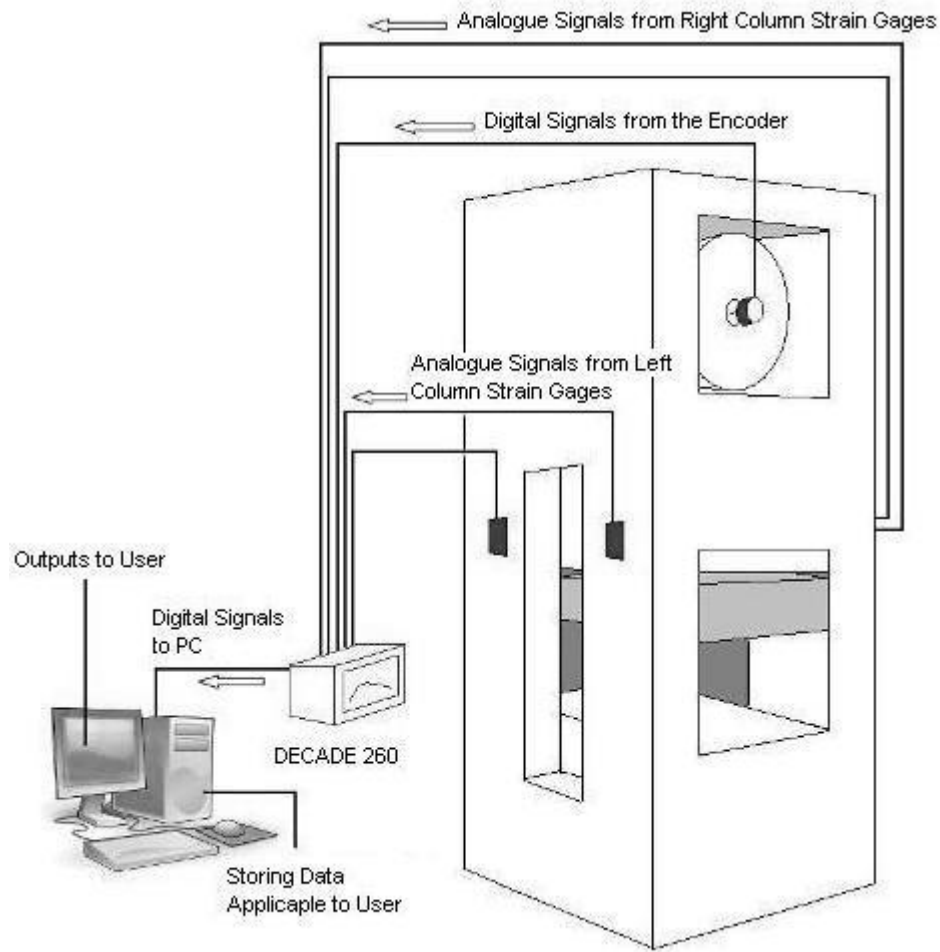


**Figure 4.12 Schematic View Showing the Working Principle of the Data Acquisition System**

### 4.3 Conducting Experiments

The tests for the Cook and Larke Simple Compression Test in METU-BILTIR Center Forging Research and Application Laboratory are applied according to the procedure in Appendix D. First, the forging dies are preheated as shown in Figure 4.13. At the same time, the specimens are begun to be heated in the induction heater as shown in Figure 4.13 (a) to the temperature values to be forged.

The heated specimens are hold with the tong and their temperatures are measured by the pyrometer before upsetting as shown in Figure 4.13 (b) and the observed temperature values are recorded.



**Figure 4.13 Preheating of the Forging Dies**



**( a )**



**( b )**

**Figure 4.14 (a) Heated Specimen Leaving the Induction Heater (b) Measuring the Temperature of a Specimen by a Pyrometer Before Forging Process**

Each specimen is loaded to the lower die to be forged. In Figure 4.15, a specimen with an initial height of 100 mm is seen just before upsetting.



**Figure 4.15 A Specimen Waiting to be Forged Between the Dies**

Just after every forging cycle of the press, the data is recorded by using the PC which is connected to DECADE 260<sup>®</sup> unit. The forged specimens are grouped according to their forging temperatures as seen in Figure 4.16.



**Figure 4.16 Grouped Specimens Waiting for Cooling**

After cooling, the surfaces of the forged specimens are cleaned with a wire brush and the final height of each specimen is measured as shown in Figure 4.17. In Figure 4.18, marked specimens are seen according to their forging temperature level, aspect and reduction ratios and sequence of forging.



**Figure 4.17 Measuring the Final Height of a Specimen**



**Figure 4.18 Grouped Specimens after Measurement**

#### 4.4 Experimental Results

The experimental results for each experimental case with different reduction ratio,  $r$ , and different aspect ratio,  $d_0/h_0$ , are given in Table 4.2. The forging temperatures for each specimen with the die temperatures recorded just before applying test in each experimental case and the data collected by using the acquisition system, which is the maximum force for each test are also shown in the same table. Each experimental case is repeated three times to obtain more reliable results and the averages are used in the comparisons. The comparison of the experimental results and computational results will be given in Chapter 5.

**Table 4.2 The Dimensions, Temperatures and Force Values Measured in the Experiments**

Experimental Case	Specimen No	Initial Height (mm)	Final Height (mm)	Specimen Temperature (°C)	Die Temperature (°C)	Maximum Force (tons)
$r = 5\%$ $d_0/h_0 = 0,5$	1	100,04	95,65	917	225	38,1
	2	100,04	95,67	912	223	37,7
	3	100,04	95,60	920	217	38,0
$r = 5\%$ $d_0/h_0 = 0,5$	4	100,04	95,43	1012	215	18,8
	5	100,04	95,47	1017	214	18,7
	6	100,04	95,44	1013	209	18,6
$r = 5\%$ $d_0/h_0 = 0,5$	7	100,04	95,38	1110	203	16,2
	8	100,04	95,35	1103	200	16,4
	9	100,04	95,37	1108	198	16,5
$r = 10\%$ $d_0/h_0 = 0,5$	10	100,04	90,68	924	226	41,3
	11	100,04	90,66	921	223	41,7
	12	100,04	90,65	913	218	42,0
$r = 10\%$ $d_0/h_0 = 0,5$	13	100,04	90,43	1011	215	27,6
	14	100,04	90,44	1008	213	27,3
	15	100,04	90,47	1003	210	26,9



**Table 4.2 The Dimensions, Temperatures and Force Values Measured in the Experiments (cont'd)**

Experimental Case	Specimen No	Initial Height (mm)	Final Height (mm)	Specimen Temperature (°C)	Die Temperature (°C)	Maximum Force (tons)
r = 10 % d <sub>0</sub> /h <sub>0</sub> =0,5	16	100,04	90,33	1109	209	19,9
	17	100,04	90,31	1103	206	20,1
	18	100,04	90,35	1112	201	19,5
r = 20 % d <sub>0</sub> /h <sub>0</sub> = 0,5	19	100,04	80,55	911	231	55,3
	20	100,04	80,49	915	228	56,0
	21	100,04	80,53	913	224	55,8
r = 20 % d <sub>0</sub> /h <sub>0</sub> = 0,5	22	100,04	80,43	1008	218	38,8
	23	100,04	80,40	1010	215	39,1
	24	100,04	80,35	1013	212	39,7
r = 20 % d <sub>0</sub> /h <sub>0</sub> = 0,5	25	100,04	80,33	1120	207	27,7
	26	100,04	80,31	1123	205	28,1
	27	100,04	80,35	1126	201	27,5
r = 30 % d <sub>0</sub> /h <sub>0</sub> = 0,5	28	100,04	70,40	905	235	68,9
	29	100,04	70,35	908	231	69,1
	30	100,04	70,38	910	228	69,1
r = 30 % d <sub>0</sub> /h <sub>0</sub> = 0,5	31	100,04	70,33	1008	225	51,3
	32	100,04	70,30	1010	223	51,8
	33	100,04	70,31	1015	218	51,2
r = 30 % d <sub>0</sub> /h <sub>0</sub> = 0,5	34	100,04	70,29	1110	214	35,8
	35	100,04	70,29	1115	212	35,7
	36	100,04	70,28	1118	208	36,0
r = 40 % d <sub>0</sub> /h <sub>0</sub> = 0,5	37	100,04	60,41	912	229	82,3
	38	100,04	60,43	915	224	82,0
	39	100,04	60,38	915	222	82,5
r = 40 % d <sub>0</sub> /h <sub>0</sub> = 0,5	40	100,04	60,38	1015	217	61,0
	41	100,04	60,30	1018	213	61,4
	42	100,04	60,29	1020	211	61,7

**Table 4.2 The Dimensions, Temperatures and Force Values Measured in the Experiments (cont'd)**

Experimental Case	Specimen No	Initial Height (mm)	Final Height (mm)	Specimen Temperature (°C)	Die Temperature (°C)	Maximum Force (tons)
r = 40 % d <sub>0</sub> /h <sub>0</sub> = 0,5	43	100,04	60,19	1110	208	39,9
	44	100,04	60,18	1111	204	40,1
	45	100,04	60,18	1113	199	40,3
r = 5 % d <sub>0</sub> /h <sub>0</sub> = 1	46	50,03	47,59	912	233	38,7
	47	50,03	47,57	913	230	39,1
	48	50,03	47,57	915	228	39,3
r = 5 % d <sub>0</sub> /h <sub>0</sub> = 1	49	50,03	47,55	1013	225	23,9
	50	50,03	47,54	1011	220	24,0
	51	50,03	47,55	1011	216	23,8
r = 5 % d <sub>0</sub> /h <sub>0</sub> = 1	52	50,03	47,53	1101	208	17,4
	53	50,03	47,51	1105	205	17,6
	54	50,03	47,50	1106	200	17,7
r = 10 % d <sub>0</sub> /h <sub>0</sub> = 1	55	50,03	45,23	920	229	44,7
	56	50,03	45,21	917	225	44,9
	57	50,03	45,20	915	221	44,3
r = 10 % d <sub>0</sub> /h <sub>0</sub> = 1	58	50,03	45,19	1021	217	28,9
	59	50,03	45,18	1018	213	29,1
	60	50,03	45,18	1010	211	29,2
r = 10 % d <sub>0</sub> /h <sub>0</sub> = 1	61	50,03	45,15	1110	208	19,7
	62	50,03	45,13	1111	204	20,0
	63	50,03	45,10	1105	198	20,2
r = 20 % d <sub>0</sub> /h <sub>0</sub> = 1	64	50,03	40,33	919	236	57,9
	65	50,03	40,31	921	234	58,1
	66	50,03	40,34	917	230	57,5
r = 20 % d <sub>0</sub> /h <sub>0</sub> = 1	67	50,03	40,28	1019	225	42,1
	68	50,03	40,30	1025	222	41,8
	69	50,03	40,27	1013	217	42,3

**Table 4.2 The Dimensions, Temperatures and Force Values Measured in the Experiments (cont'd)**

Experimental Case	Specimen No	Initial Height (mm)	Final Height (mm)	Specimen Temperature (°C)	Die Temperature (°C)	Maximum Force (tons)
r = 20 % d <sub>0</sub> /h <sub>0</sub> = 1	70	50,03	40,21	1121	209	29,7
	71	50,03	40,20	1125	205	29,8
	72	50,03	40,23	1120	200	30,1
r = 30 % d <sub>0</sub> /h <sub>0</sub> = 1	73	50,03	35,40	912	233	72,3
	74	50,03	35,33	915	231	72,5
	75	50,03	35,38	916	227	72,9
r = 30 % d <sub>0</sub> /h <sub>0</sub> = 1	76	50,03	35,31	1010	224	54,5
	77	50,03	35,30	1013	222	54,7
	78	50,03	35,20	1012	217	55,1
r = 30 % d <sub>0</sub> /h <sub>0</sub> = 1	79	50,03	35,29	1119	211	37,9
	80	50,03	35,27	1120	209	40,2
	81	50,03	35,27	1121	203	40,3
r = 40 % d <sub>0</sub> /h <sub>0</sub> = 1	82	50,03	30,25	918	229	87,8
	83	50,03	30,28	917	224	87,5
	84	50,03	30,27	917	221	87,3
r = 40 % d <sub>0</sub> /h <sub>0</sub> = 1	85	50,03	30,19	1015	217	65,9
	86	50,03	30,18	1016	213	66,1
	87	50,03	30,19	1020	209	65,2
r = 40 % d <sub>0</sub> /h <sub>0</sub> = 1	88	50,03	30,15	1110	205	46,9
	89	50,03	30,16	1113	200	46,7
	90	50,03	30,16	1112	197	46,5
r = 5 % d <sub>0</sub> /h <sub>0</sub> = 2	91	25,03	23,83	914	234	42,4
	92	25,03	23,81	915	232	42,6
	93	25,03	23,83	915	228	42,1
r = 5 % d <sub>0</sub> /h <sub>0</sub> = 2	94	25,03	23,79	1017	217	26,9
	95	25,03	23,77	1019	213	27,1
	96	25,03	23,80	1021	209	26,3

**Table 4.2 The Dimensions, Temperatures and Force Values Measured in the Experiments (cont'd)**

Experimental Case	Specimen No	Initial Height (mm)	Final Height (mm)	Specimen Temperature (°C)	Die Temperature (°C)	Maximum Force (tons)
r = 5 % d <sub>0</sub> /h <sub>0</sub> = 2	97	25,03	23,76	1113	205	19,3
	98	25,03	23,76	1113	202	19,1
	99	25,03	23,75	1119	198	19,4
r = 10 % d <sub>0</sub> /h <sub>0</sub> = 2	100	25,03	22,61	917	229	47,9
	101	25,03	22,59	921	226	48,2
	102	25,03	22,62	915	221	47,7
r = 10 % d <sub>0</sub> /h <sub>0</sub> = 2	103	25,03	22,59	1017	217	32,3
	104	25,03	22,58	1020	213	32,4
	105	25,03	22,58	1021	208	32,1
r = 10 % d <sub>0</sub> /h <sub>0</sub> = 2	106	25,03	22,57	1110	202	24,7
	107	25,03	22,55	1008	198	24,5
	108	25,03	22,55	1005	195	24,3
r = 20 % d <sub>0</sub> /h <sub>0</sub> = 2	109	25,03	20,18	921	232	67,4
	110	25,03	20,19	919	228	67,8
	111	25,03	20,21	919	225	68,1
r = 20 % d <sub>0</sub> /h <sub>0</sub> = 2	112	25,03	20,17	1021	221	48,2
	113	25,03	20,15	1022	217	47,9
	114	25,03	20,17	1019	213	47,7
r = 20 % d <sub>0</sub> /h <sub>0</sub> = 2	115	25,03	20,13	1110	209	36,3
	116	25,03	20,11	1113	205	36,7
	117	25,03	20,15	1107	202	36,4
r = 30 % d <sub>0</sub> /h <sub>0</sub> = 2	118	25,03	17,61	922	233	84,7
	119	25,03	17,59	917	230	85,0
	120	25,03	17,61	920	216	84,9
r = 30 % d <sub>0</sub> /h <sub>0</sub> = 2	121	25,03	17,57	1021	211	64,9
	122	25,03	17,56	1018	208	65,1
	123	25,03	17,56	1017	204	65,2

**Table 4.2 The Dimensions, Temperatures and Force Values Measured in the Experiments (cont'd)**

Experimental Case	Specimen No	Initial Height (mm)	Final Height (mm)	Specimen Temperature (°C)	Die Temperature (°C)	Maximum Force (tons)
r = 30 % d <sub>0</sub> /h <sub>0</sub> = 2	124	25,03	17,51	1117	200	45,5
	125	25,03	17,53	1121	197	45,8
	126	25,03	17,53	1119	194	45,9
r = 40 % d <sub>0</sub> /h <sub>0</sub> = 2	127	25,03	15,63	915	235	95,1
	128	25,03	15,61	920	231	95,4
	129	25,03	15,61	920	229	95,5
r = 40 % d <sub>0</sub> /h <sub>0</sub> = 2	130	25,03	15,59	1013	222	81,3
	131	25,03	15,58	1017	220	81,5
	132	25,03	15,58	1017	216	81,6
r = 40 % d <sub>0</sub> /h <sub>0</sub> = 2	133	25,03	15,55	1111	207	57,3
	134	25,03	15,56	1113	204	57,2
	135	25,03	15,56	1117	199	57,1
r = 5 % d <sub>0</sub> /h <sub>0</sub> = 3	136	16,69	15,94	918	233	46,3
	137	16,69	15,91	921	231	46,6
	138	16,69	15,89	922	227	46,6
r = 5 % d <sub>0</sub> /h <sub>0</sub> = 3	139	16,69	15,87	1021	224	27,9
	140	16,69	15,86	1018	222	28,1
	141	16,69	15,87	1022	217	28,0
r = 5 % d <sub>0</sub> /h <sub>0</sub> = 3	142	16,69	15,85	1119	211	19,2
	143	16,69	15,86	1115	209	18,9
	144	16,69	15,84	1122	203	19,0
r = 10 % d <sub>0</sub> /h <sub>0</sub> = 3	145	16,69	15,33	923	226	53,9
	146	16,69	15,35	916	223	54,1
	147	16,69	15,29	920	218	54,2
r = 10 % d <sub>0</sub> /h <sub>0</sub> = 3	148	16,69	15,27	1019	215	37,3
	149	16,69	15,25	1022	213	37,4
	150	16,69	15,25	1020	210	37,4

**Table 4.2 The Dimensions, Temperatures and Force Values Measured in the Experiments (cont'd)**

Experimental Case	Specimen No	Initial Height (mm)	Final Height (mm)	Specimen Temperature (°C)	Die Temperature (°C)	Maximum Force (tons)
r = 10 % d <sub>0</sub> /h <sub>0</sub> = 3	151	16,69	15,19	1115	209	27,6
	152	16,69	15,17	1120	206	27,8
	153	16,69	15,17	1119	201	27,5
r = 20 % d <sub>0</sub> /h <sub>0</sub> = 3	154	16,69	13,41	917	236	74,2
	155	16,69	13,40	919	234	74,0
	156	16,69	13,39	919	230	73,9
r = 20 % d <sub>0</sub> /h <sub>0</sub> = 3	157	16,69	13,36	1015	225	54,6
	158	16,69	13,35	1018	222	54,8
	159	16,69	13,36	1016	217	54,5
r = 20 % d <sub>0</sub> /h <sub>0</sub> = 3	160	16,69	13,34	1115	209	40,9
	161	16,69	13,32	1118	205	41,1
	162	16,69	13,32	1117	200	41,3
r = 30 % d <sub>0</sub> /h <sub>0</sub> = 3	163	16,69	11,75	915	229	95,1
	164	16,69	11,73	920	226	95,3
	165	16,69	11,74	919	221	95,4
r = 30 % d <sub>0</sub> /h <sub>0</sub> = 3	166	16,69	11,71	1021	217	75,1
	167	16,69	11,71	1020	213	74,9
	168	16,69	11,72	1020	207	75,0
r = 30 % d <sub>0</sub> /h <sub>0</sub> = 3	169	16,69	11,69	1118	202	57,1
	170	16,69	11,70	1121	198	56,9
	171	16,69	11,69	1116	195	56,9
r = 40 % d <sub>0</sub> /h <sub>0</sub> = 3	172	16,69	10,23	915	233	121,5
	173	16,69	10,21	917	231	121,7
	174	16,69	10,21	921	228	121,8
r = 40 % d <sub>0</sub> /h <sub>0</sub> = 3	175	16,69	10,17	1018	224	96,9
	176	16,69	10,17	1017	222	97,0
	177	16,69	10,18	1020	216	97,1

**Table 4.2 The Dimensions, Temperatures and Force Values Measured in the Experiments (cont'd)**

Experimental Case	Specimen No	Initial Height (mm)	Final Height (mm)	Specimen Temperature (°C)	Die Temperature (°C)	Maximum Force (tons)
r = 40 % d <sub>0</sub> /h <sub>0</sub> = 3	178	16,69	10,15	1119	211	70,0
	179	16,69	10,13	1121	205	70,1
	180	16,69	10,14	1121	203	69,9

## CHAPTER 5

### DISCUSSION AND CONCLUSION

#### 5.1 Comparison of Experimental and Numerical Results

For the comparison of experimental and numerical studies, graphical interpretations of yield stress curves for each temperatures are necessary. Since both experimental and numerical studies are realised according to the constant reduction method of the Cook and Larke Simple Compression Test [15], the yield stress curves for AISI 1045 steel at different temperatures are obtained with respect to this method. For this purpose, the mean stress is calculated from the load and the current cross-sectional area which is calculated by the assumption of uniform diameter and constant volume. Then, the true stress values are determined by using the following equation;

$$\sigma_t = \sigma_e (1 + \epsilon_e) \quad (5.1)$$

Where  $\sigma_t$  is the true (mean) stress,  $\sigma_e$  is the engineering stress and  $\epsilon_e$  is the engineering strain.

The maximum force values for 900°C, 1000°C and 1100°C have been given in Tables 3.1, 3.2 and 3.3 respectively for the numerical analyses. On the other hand, the maximum force values obtained in the experimental study have been given in Table 4.2. The engineering stress and strain values are calculated from the initial and final height and force values given in these tables. The average force and height values are utilized for each experimental case.



The Cook and Larke Simple Compression Test procedure has been firstly applied for 900°C. The true stress values are plotted for each experimental case (i.e reduction ratio and aspect ratio) as shown in Figure 5.1. Then, extrapolating to zero aspect ratio for each reduction ratio gives the true yield stress. The true stress values and corresponding true strain values,  $\epsilon_t$ , are given in Table 5.1. The true strain values are calculated by the following equation;

$$\epsilon_t = \ln ( 1 + \epsilon_e ) \quad (5.2)$$

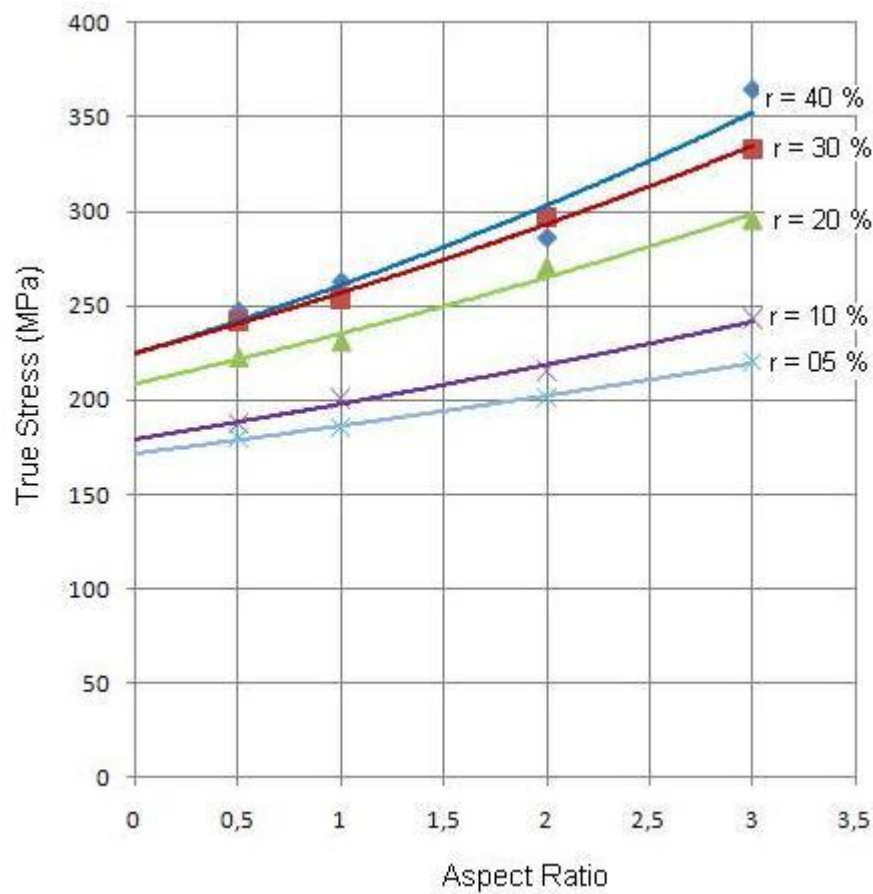


**Figure 5.1 Plotting and Curve Fitting of True Stresses versus Aspect Ratios for the Experimental Study at 900°C**

**Table 5.1 True Stress Values Obtained from the Graph in Figure 5.1  
and Calculated True Strains**

<b>TRUE STRESS (MPa)</b>	<b>TRUE STRAIN (%)</b>
171,59	0,05
179,56	0,11
208,64	0,22
224,90	0,36
224,44	0,51

Using these true stress values, when plotted with respect to true strain, the yield stress curve is obtained as shown in Figure 5.2. The same procedure have been repeated for the experimental analysis for 900°C and 1000°C and numerical study for 900°C, 1000°C and 1100°C. The application of this procedure to the experimental and numerical studies mentioned recently are shown in Figures and the true stress values obtained from the true stress versus aspect ratio graphics are given in Tables

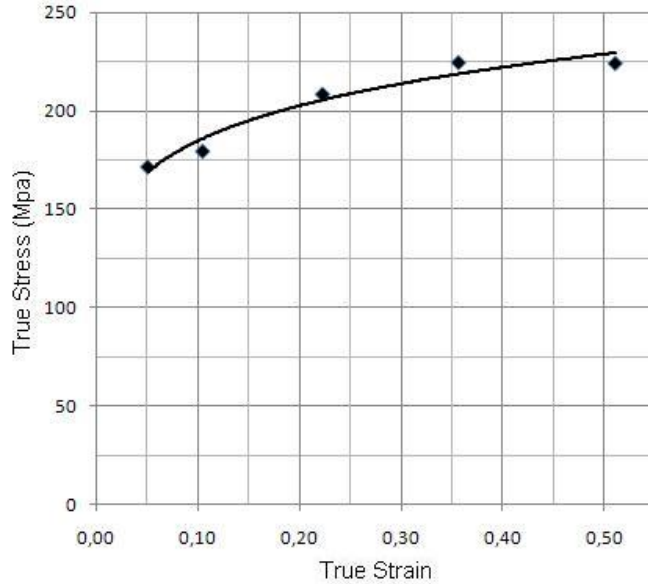


**Figure 5.2 True Stress versus True Strain Curve for Experimental Study at  
900°C**

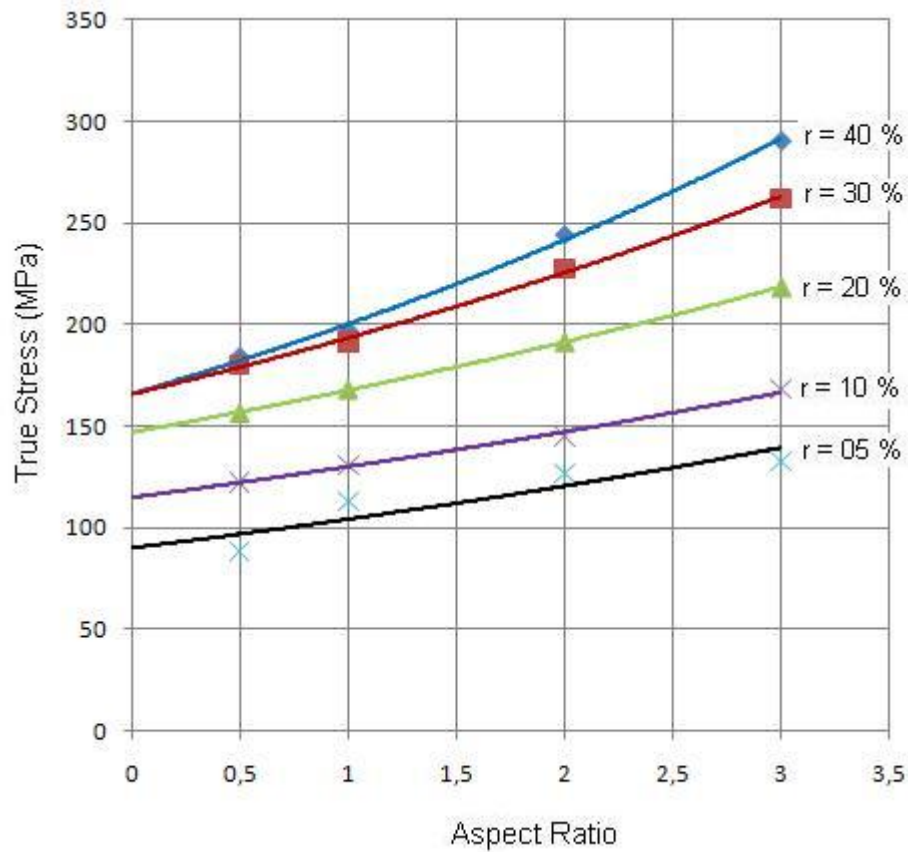


**Figure 5.3 Plotting and Curve Fitting of True Stresses versus Aspect Ratios for the Experimental Study at 1000°C**

**Table 5.2 True Stress Values Obtained from the Graph in Figure 5.3 and Calculated True Strains**

TRUE STRESS (MPa)	TRUE STRAIN (%)
90,15	0,05
114,97	0,11
146,96	0,22
165,83	0,36
165,98	0,51

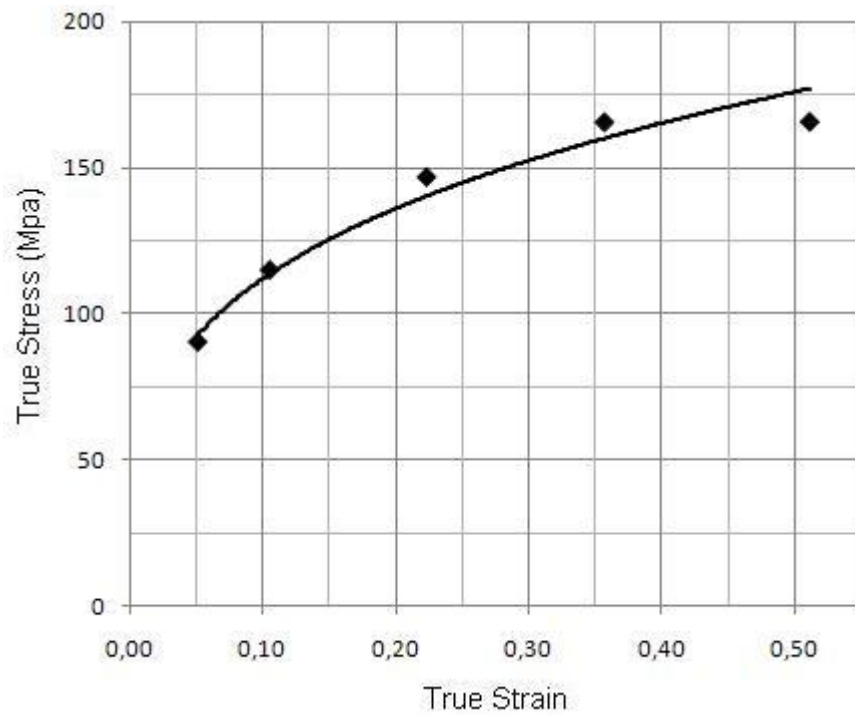


**Figure 5.4 True Stress versus True Strain Curve for Experimental Study at 1000°C**

In Figure 5.13, true stress vs. true strain curves obtained from all studies are shown together. In Figure 5.14, true stress vs. true strain curves obtained from simple compression and simple tension tests at room temperature are additionally given with the ones already available in Figure 5.13. Simple compression and simple tension tests at room temperature are performed on a DARTEC<sup>®</sup> testing machine available in Material Testing Laboratory of METU Mechanical Engineering Department.

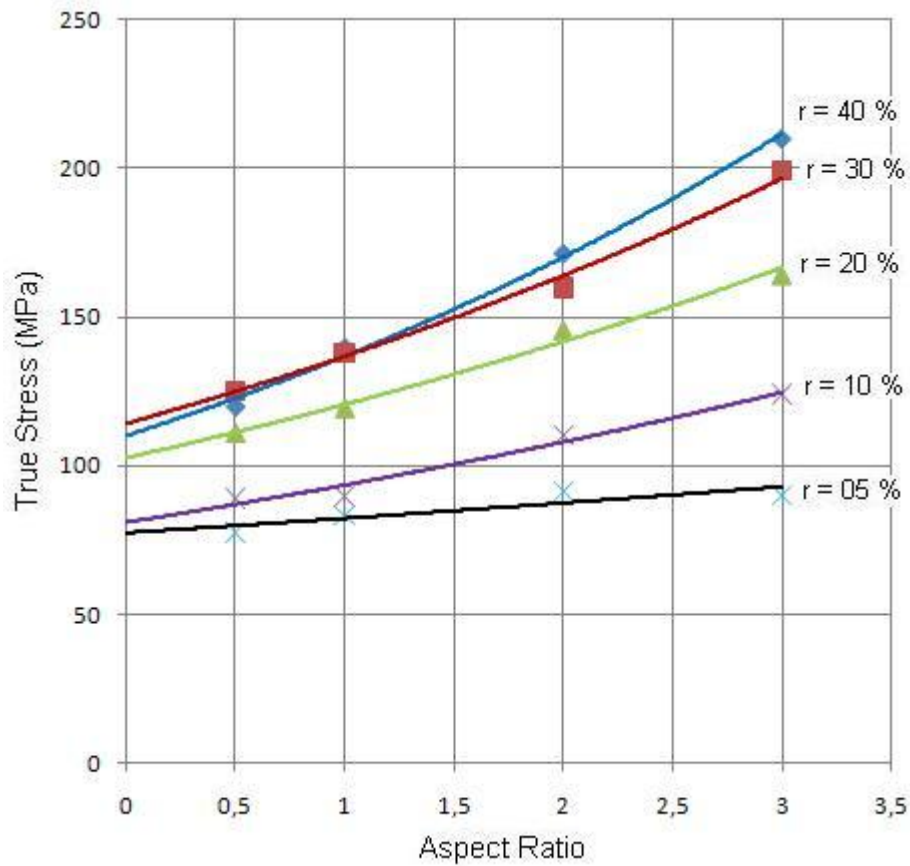


**Figure 5.5 Plotting and Curve Fitting of True Stress versus  $d_0/h_0$  for the Experimental Study at 1100°C**

**Table 5.3 True Stress Values Obtained from the Graph in Figure 5.5 and Calculated True Strains**

TRUE STRESS (MPa)	TRUE STRAIN (%)
77,47	0,05
80,97	0,11
102,64	0,22
114,12	0,36
110,07	0,51

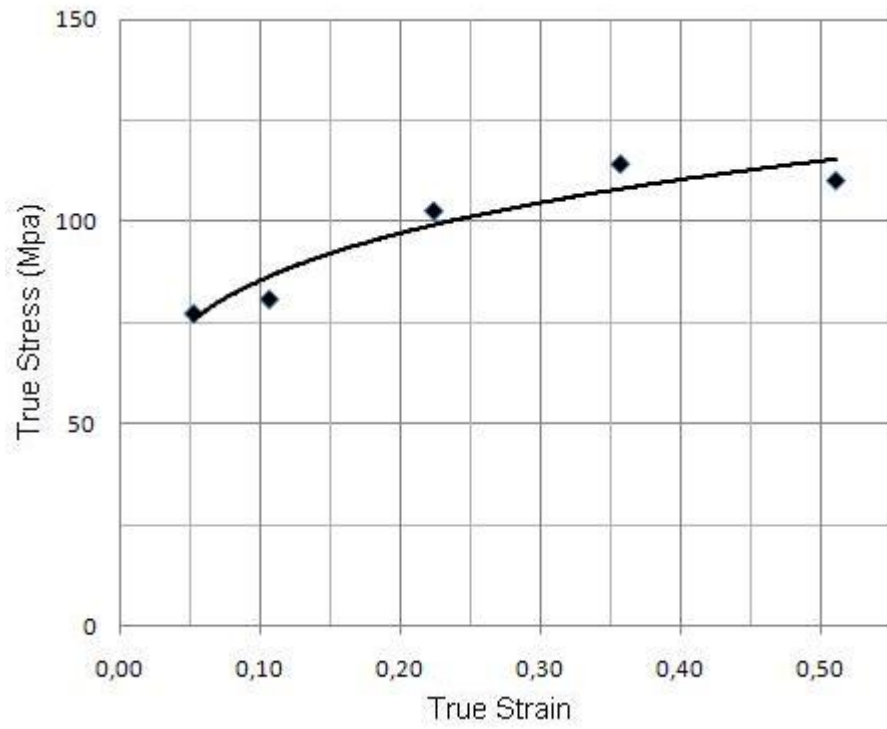


**Figure 5.6 True Stress versus True Strain Curve for Experimental Study at 1100°C**

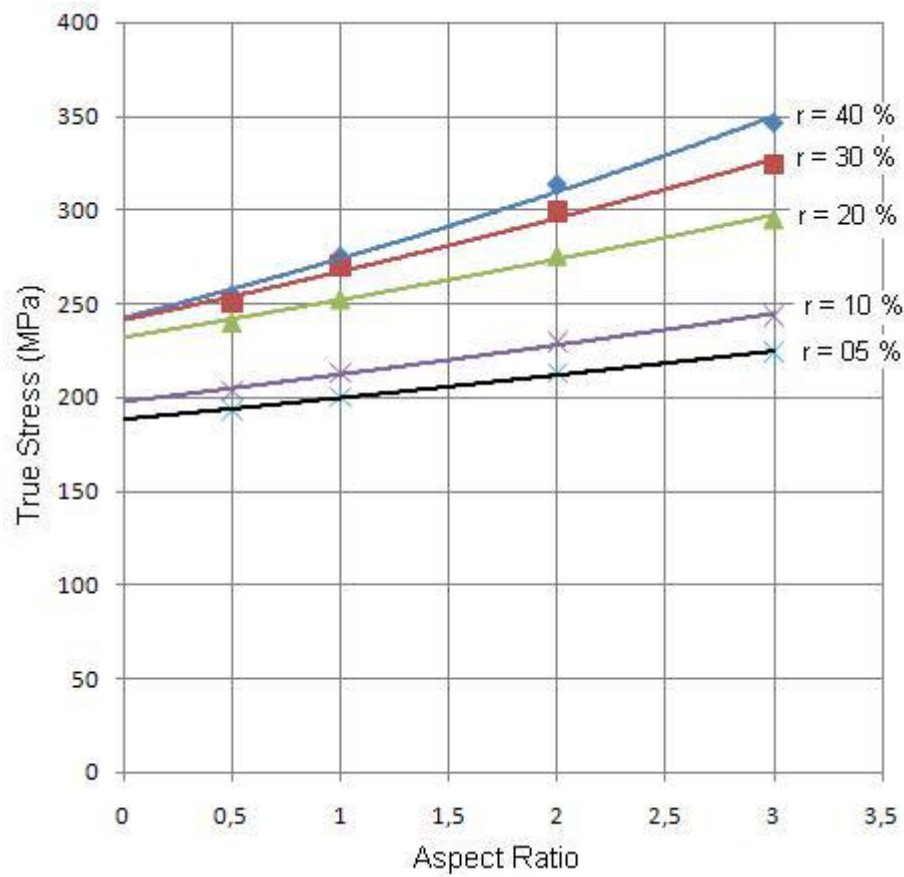


**Figure 5.7 Plotting and Curve Fitting of True Stress versus  $d_0/h_0$  for the Numerical Study at 900°C**

**Table 5.4 True Stress Values Obtained from the Graph in Figure 5.7 and Calculated True Strains**

TRUE STRESS (MPa)	TRUE STRAIN (%)
188,37	0,05
197,82	0,11
232,17	0,22
241,39	0,36
242,62	0,51

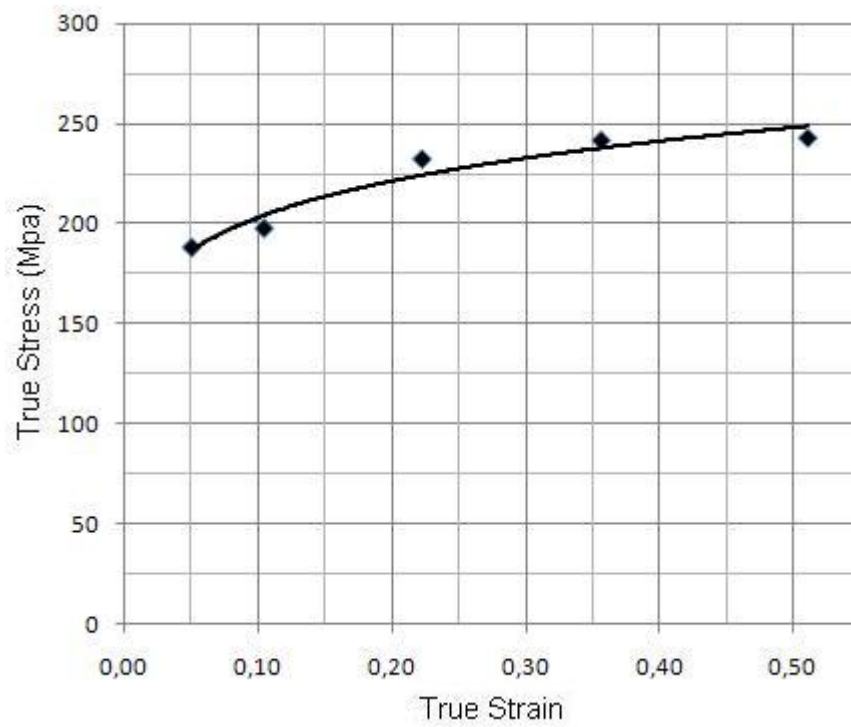


**Figure 5.8 True Stress versus True Strain Curve for Numerical Study at 900°C**



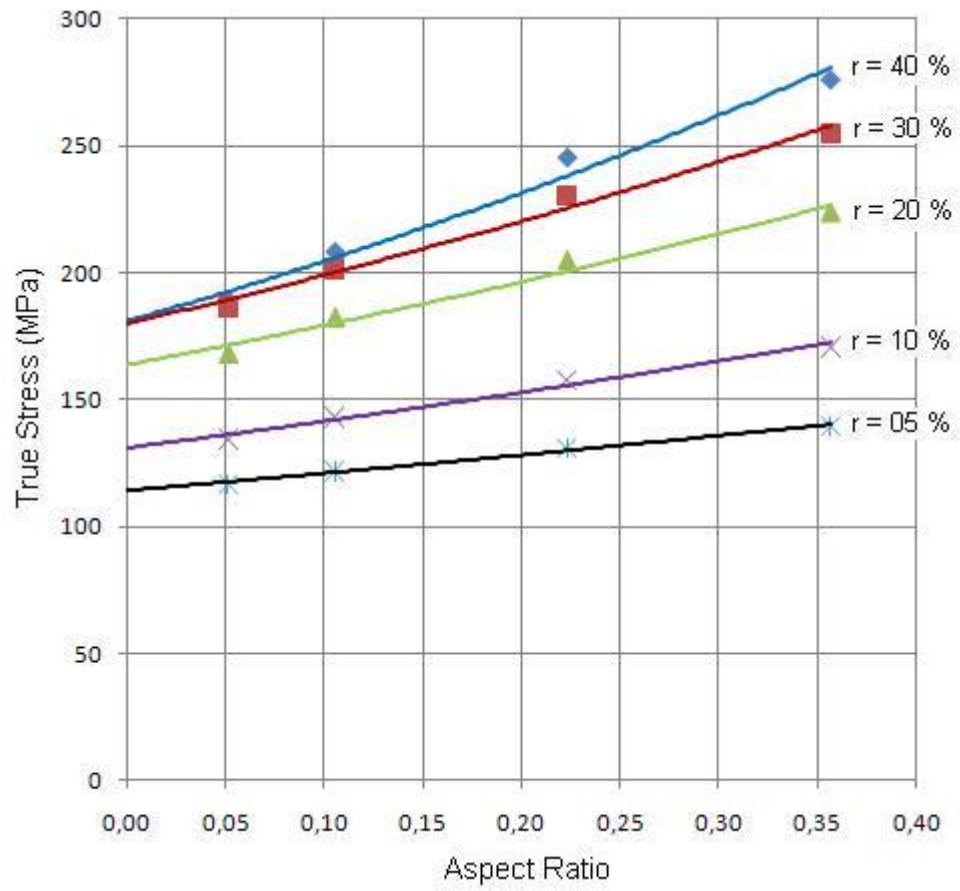


**Figure 5.9 Plotting and Curve Fitting of True Stress versus  $d_0/h_0$  for the Numerical Study at 1000°C**

**Table 5.5 True Stress Values Obtained from the Graph in Figure 5.9 and Calculated True Strains**

TRUE STRESS (MPa)	TRUE STRAIN (%)
114,15	0,05
130,91	0,11
163,56	0,22
179,86	0,36
180,81	0,51

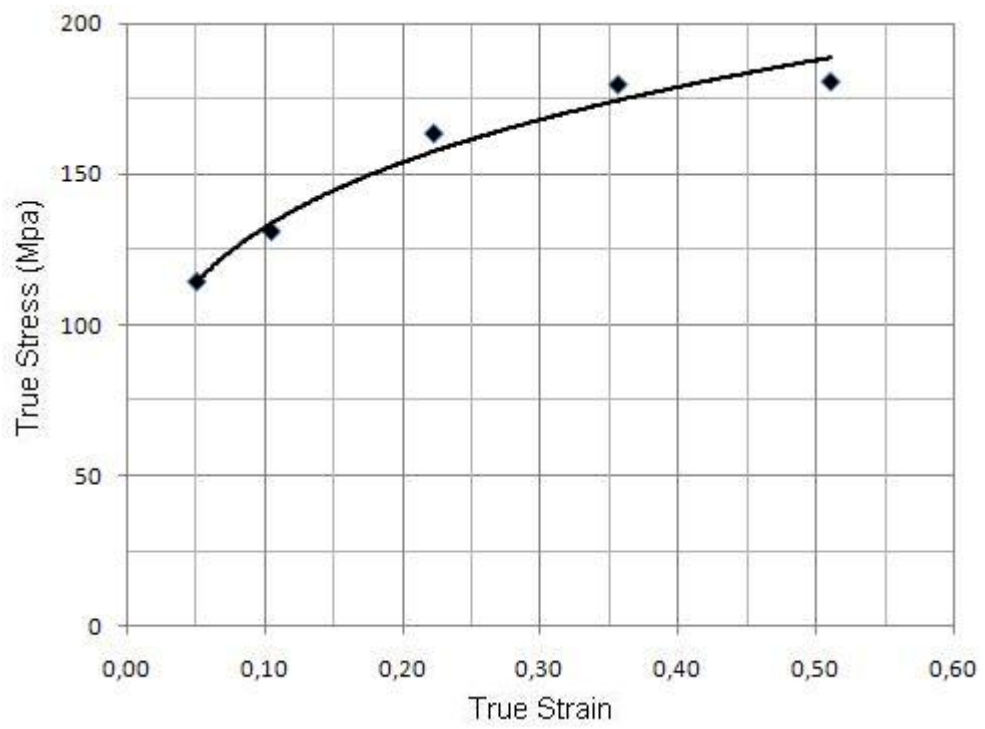


**Figure 5.10 True Stress versus True Strain Curve for Numerical Study at 1000°C**

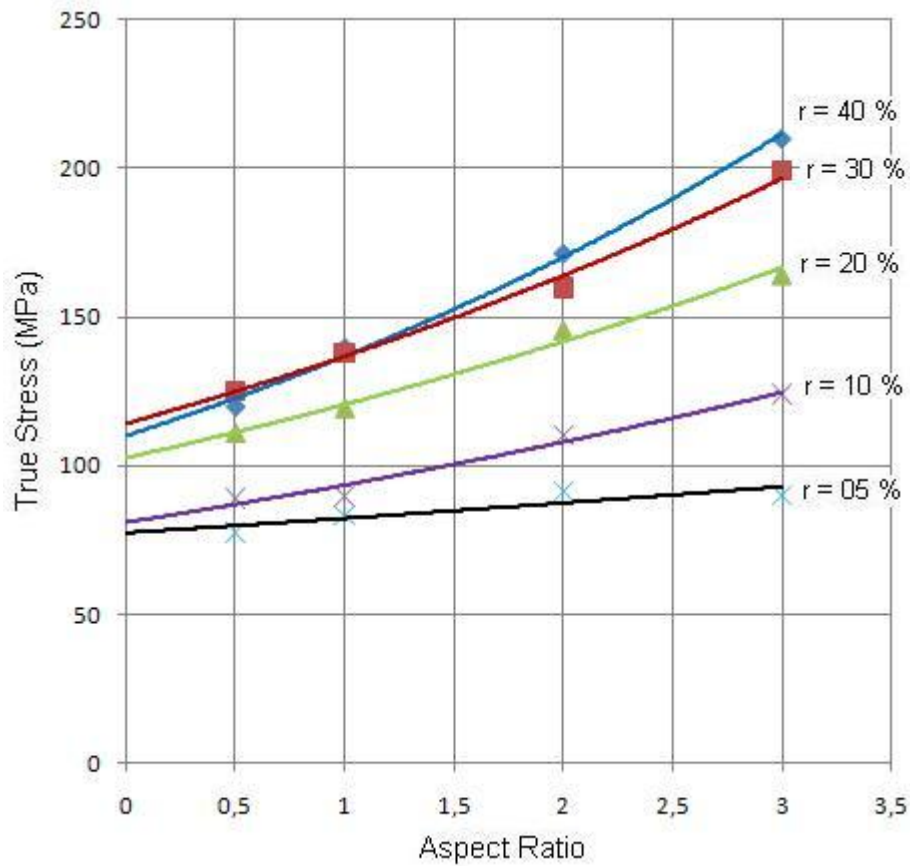


**Figure 5.11 Plotting and Curve Fitting of True Stress versus  $d_0/h_0$  for the Numerical Study at 1100°C**

**Table 5.6 True Stress Values Obtained from the Graph in Figure 5.11 and Calculated True Strains**

TRUE STRESS (MPa)	TRUE STRAIN (%)
84,78	0,05
94,76	0,11
113,94	0,22
123,07	0,36
122,35	0,51

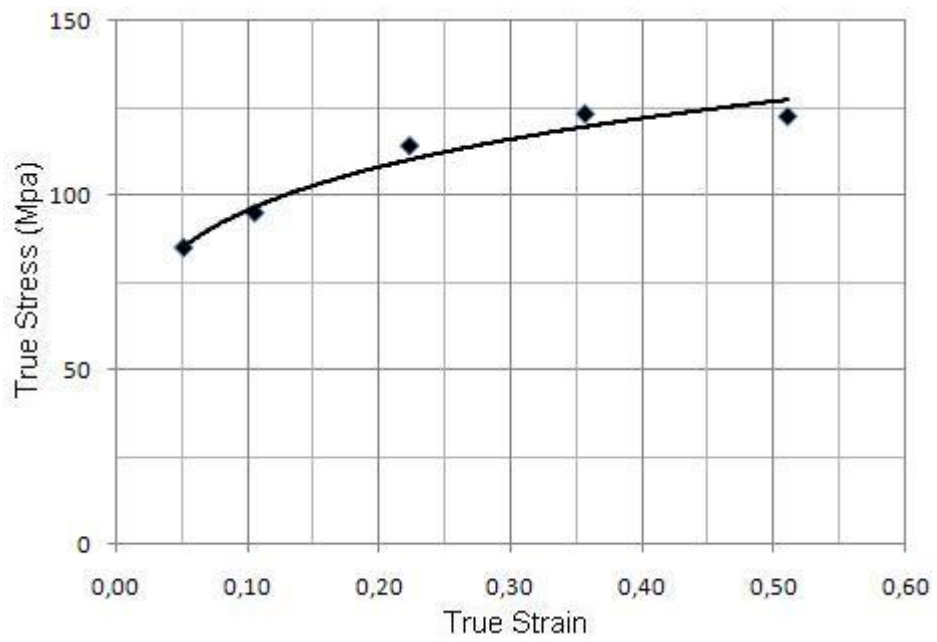


**Figure 5.12 True Stress versus True Strain Curve for Numerical Study at 1100°C**

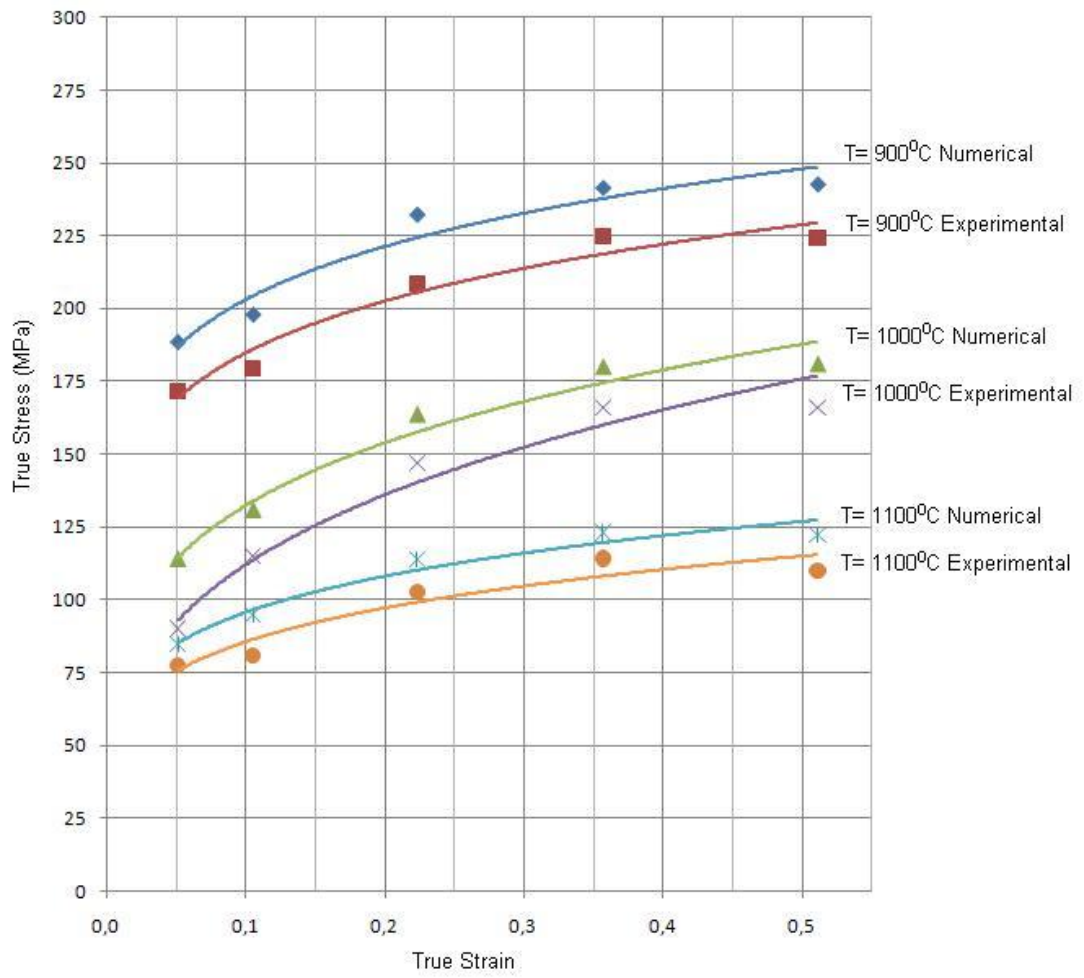


**Figure 5.13 True Stress versus True Strain Curves Obtained from all Numerical and Experimental Studies**

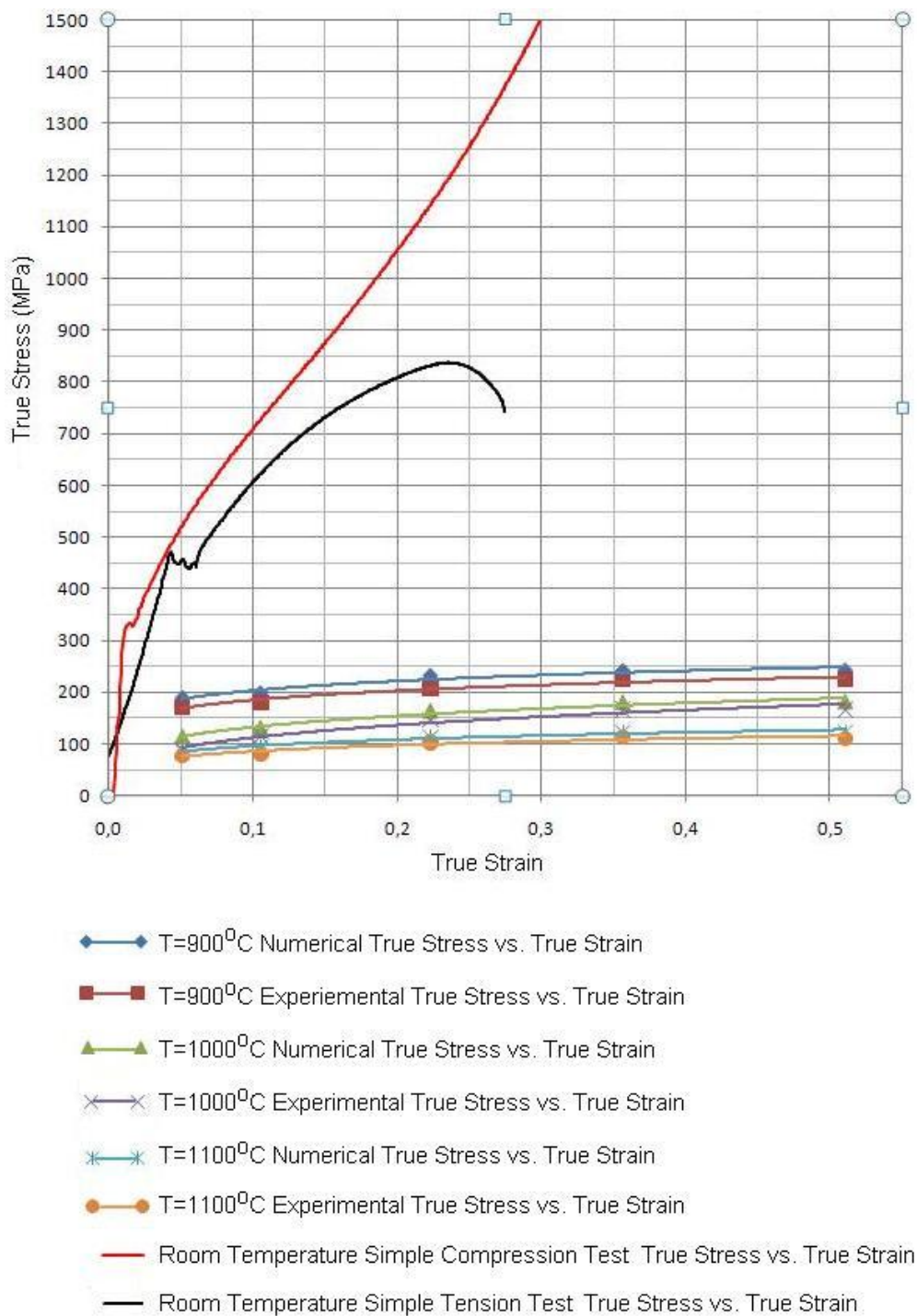


**Figure 5.14 True Stress versus True Strain Values Obtained from Numerical and Experimental Studies with the Ones Obtained from Material Tests at Room Temperature**

## **5.2 General Conclusion**

General conclusions can be summarized as follows:

- It has been shown that the forging press with the data acquisition system can be used as a material testing equipment to obtain stress-strain curves.
- A modular die set has been designed and manufactured to conduct the Cook and Larke Simple Compression Test on the 1000 ton forging press.
- The yield stress curves obtained from the experimental studies are similar to the numerical studies.

## **5.3 Future Works**

The Cook and Larke Simple Compression Test on the forging press can be applied to the specimens of other materials with different dimensions at various elevated temperatures.

## REFERENCES

- [1] Degarmo, E. Paul., Black, J T., Kohser, Ronald A. "Materials and Processes in Manufacturing" Ninth Edition, Wiley, 2003, ISBN 0 471 65653 4T.
- [2] Öztürk, H., "Analysis and Design for Aluminum Forging Process", M. Sc. Thesis, Middle East Technical University, Turkey, 2008.
- [3] Maşat, M., "Design and Implementation of Hot Precision Die for a Spur Gear", M. Sc. Thesis, Middle East Technical University, Turkey, 2007.
- [4] Saraç S., "Design and Thermo-mechanical Analysis of Warm Forging Process and Dies", M. Sc. Thesis, Middle East Technical University, Turkey, 2007.
- [5] Özcan M. C., "Thermo-mechanically Coupled Numerical and Experimental Study on 7075 Aluminum Forging Process and Dies" M. Sc. Thesis, Middle East Technical University, Turkey, 2008.
- [6] Halisçelik M., "Elastic-plastic Finite Element Analysis of Semi-hot Forging Dies" M. Sc. Thesis, Middle East Technical University, Turkey, 2009.
- [7] Kutlu A. E., "Analysis and Design of Preforms for Non-axisymmetric Press Forgings" M. Sc. Thesis, Middle East Technical University, Turkey, 2001.
- [8] Aktakka G., "Analysis of Warm Forging Process" M. Sc. Thesis, Middle East Technical University, Turkey, 2006.
- [9] Civelekoğlu B., "Analysis of Forging for Three Different Alloy Steels" M. Sc. Thesis, Middle East Technical University, Turkey, 2003.
- [10] Karacaovalı H., "Analysis of Roll-Forging Process" M. Sc. Thesis, Middle East Technical University, Turkey, 2005.
- [11] Cora Ö. N., "Friction Analysis in Cold Forging" M. Sc. Thesis, Middle East Technical University, Turkey, 2004.
- [12] Abachi S., "Wear Analysis of Forging Dies" M. Sc. Thesis, Middle East Technical University, Turkey, 2004.



- [13] Gülbahar S., "Preform Design for Forging of Heavy Vehicle Steering Joint" M. Sc. Thesis, Middle East Technical University, Turkey, 2004.
- [14] Johnson, W., Mellor, P.B. "Engineering Plasticity" Van Nostrand Reinhold Co., London, 1973, ISBN 0 442 04151 9
- [15] Ford, H., Alexander, J. M., "Advanced Mechanics of Materials" Second Edition, John Wiley & Sons Ltd., 1977.
- [16] A. P. Singh, K. A. Padmanabhan "Axi-symmetric Compression of Solid Cylinders – Part I Slow Loading Conditions", Journal of Materials Science, 26, (1991) 5481-5487.
- [17] J. K. Banerjee "Barreling of Solid Cylinders Under Axial Compression", Journal of Engineering Materials and Technology, Vol 107, (2002) 138-144.
- [18] A. P. Singh, K. A. Padmanabhan "Axi-symmetric Compression of Solid Cylinders – Part II Rapid Loading Conditions", Journal of Materials Science, 26, (1991) 5488-5494.
- [19] F. Chen, C. Chen "On the Non Uniform Deformation of the Cylinder Compression Test", Transactions of ASME, Journal of Engineering Materials and Technology, Vol. 122, (2000), 192-197.
- [20] Instruction Manual of Smeral Brno<sup>®</sup> LZK 1000
- [21] ProEngineer WildFire 5.0<sup>®</sup>
- [22] Simufact.forming 8.1<sup>®</sup> User's Manual
- [23] Durukan İ., "Effects of Induction Heating Parameters on Forging Billet Temperature", M. Sc. Thesis, Middle East Technical University, Turkey, 2008.

## **APPENDIX A**

### **TECHNICAL DRAWINGS OF THE DIE SET**

The technical drawings of the Upper Die, Lower Die and the Inserts are given in Figures A1-A6.

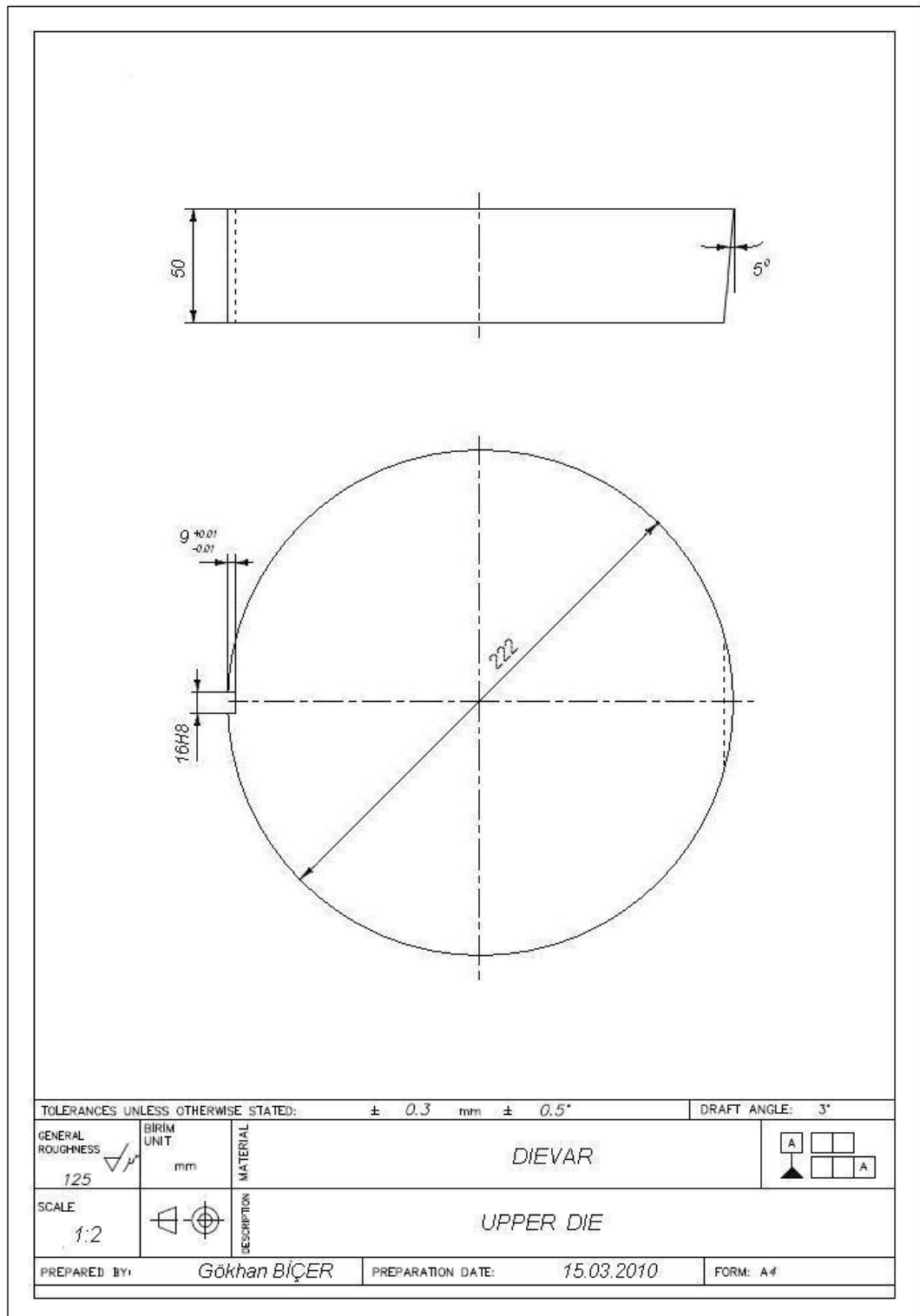


**Figure A.1 Technical Drawing of the Upper Die**

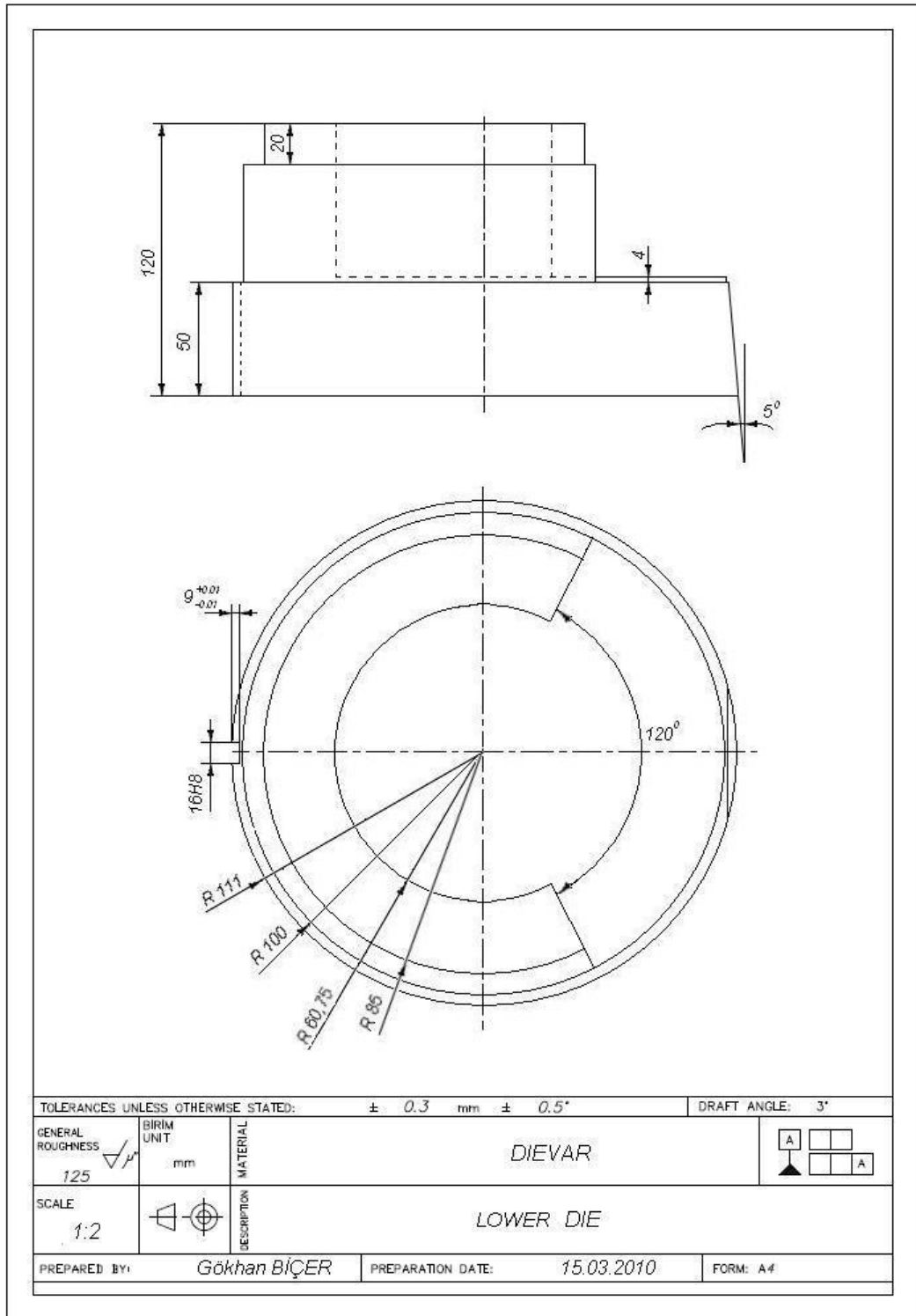


**Figure A.2 Technical Drawing of the Lower Die**

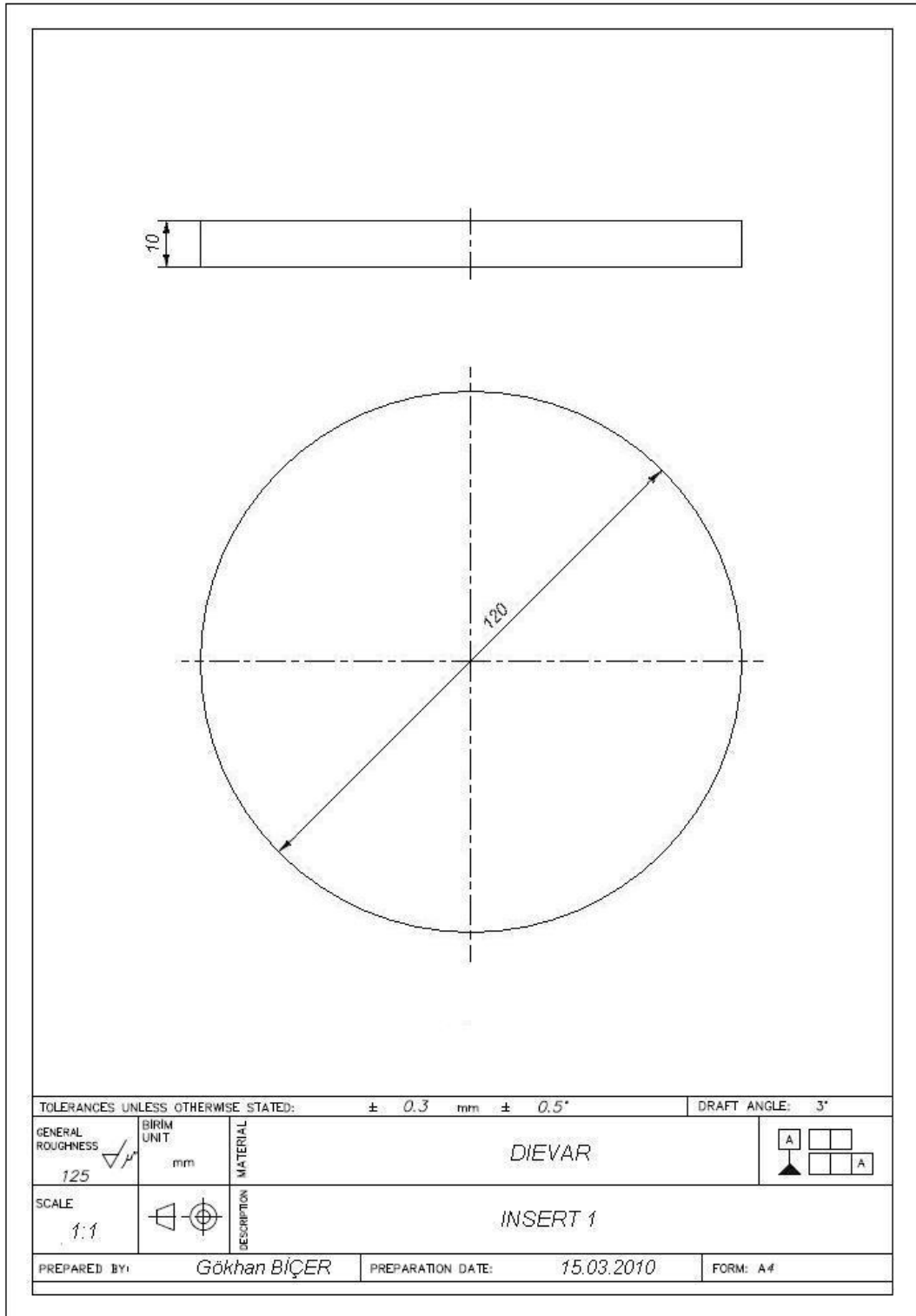
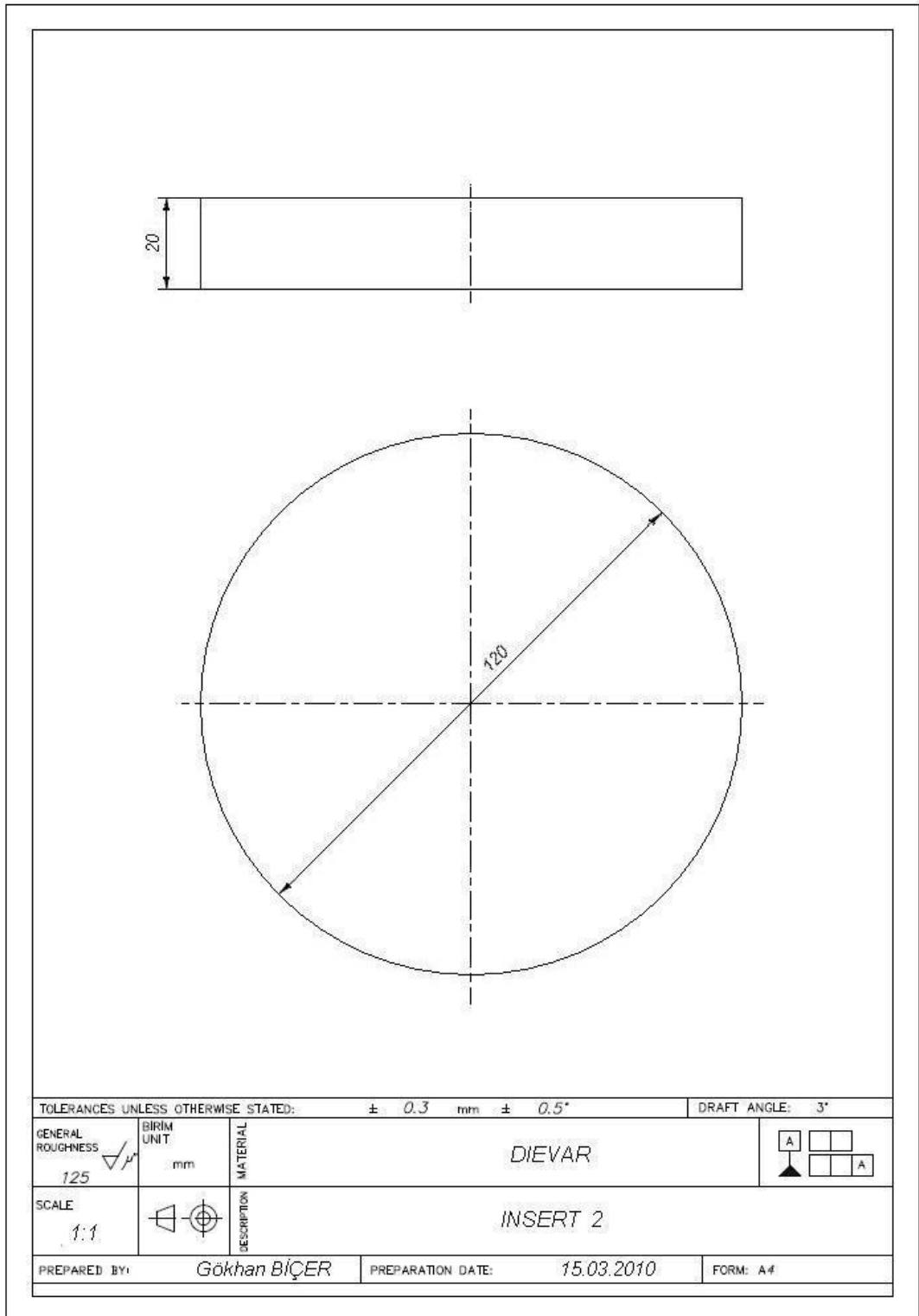
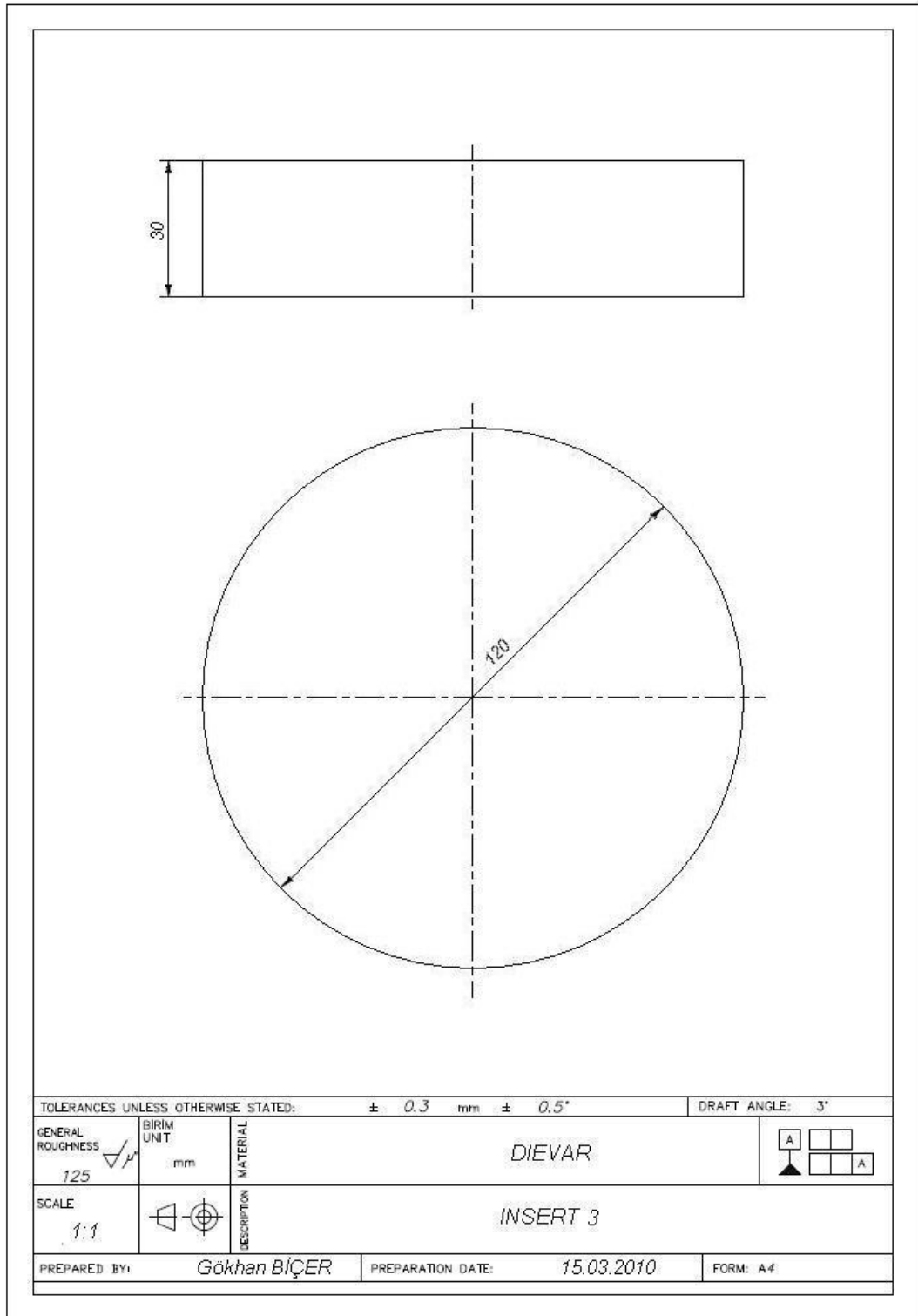


Figure A.3 Technical Drawing of the Insert with 10 mm Height



**Figure A.4 Technical Drawing of the Insert with 20 mm Height**



**Figure A.5 Technical Drawing of the Insert with 30 mm Height**

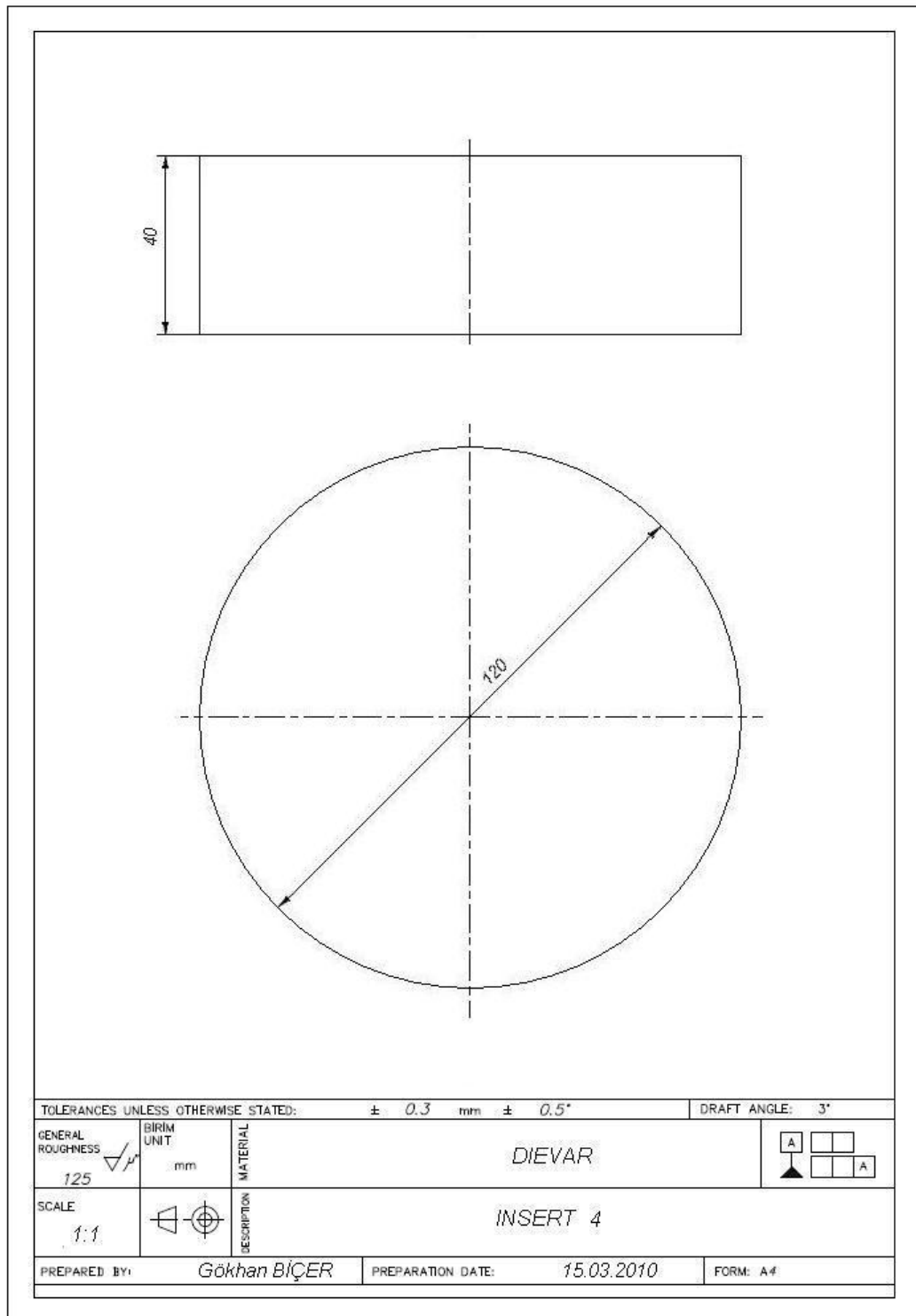


**Figure A.6 Technical Drawing of the Insert with 40 mm Height**



## APPENDIX B

### PROPERTIES OF AISI 1045 STEEL

The properties of AISI 1045 steel are given below [23]

#### **Composition (%):**

0,42-0,50 C

98,51-98,98 Fe

0,6-0,9 Mn

Max 0,04 P

Max 0,05 S

#### **Physical Properties:**

Density: 7870 kg/mm<sup>3</sup>

Hardness: 170 HB

#### **Mechanical Properties at Room Temperature:**

Yield Strength: 485 MPa

Ultimate Tensile Strength: 515 MPa

Modulus of Elasticity: 200 GPa

Poisson's Ratio: 0,29

#### **Thermal Properties:**

Specific Heat Conductivity: 486 J/kg°C at 100°C

Thermal Conductivity: 51,9 W/mK

## APPENDIX C

### TECHNICAL INFORMATION OF SMERAL BRNO LZK 1000<sup>®</sup> HOT FORGING PRESS

Technical Information of the forging press used in the study is given as follows [20]

**Nominal Forging Force:** 10MN (approximately)

**Ram Stroke:** 220 mm

**Shut Height:** 620 mm

**Ram Resetting:** 10 mm

**Rod Length:** 750 mm

**Crank Radius:** 110 mm

**Number of Strokes at Continuous Run:** 100 min<sup>-1</sup>

**Main Motor Input:** 55 kW

**Maximum Stroke of the Upper Ejector:** 40 mm

**Maximum Stroke of the Lower Ejector:** 50 mm

**Maximum Force of the Upper Ejector:** 60 kN

**Maximum Force of the Lower Ejector:** 150 kN

## **APPENDIX D**

### **MANUAL FOR THE APPLICATION OF THE COOK AND LARKE SIMPLE COMPRESSION TEST AT METU-BILTIR CENTER FORGING RESEARCH AND APPLICATION LABORATORY**

Before the application of this procedure; the systems, machinery and the equipment to be used for the tests must be checked and necessary precautions for the labor safety must be taken.

#### **D.1 Main Steps for the Test**

1. If necessary, put the proper inserts into the cavity of the lower forging die according to the final height to be gotten after forging the specimens.
2. If the gap between die surfaces when the ram is at its bottom dead point is greater than the desired value, adjust the ram to this value.
3. Hold the heated billet with a tong and put it in front of the fixed pyrometer. Read the temperature of the billet and record it.
4. Put the heated billet on the lower die.
5. If necessary, measure the temperatures of the dies with the portable pyrometer and record it.
6. Press the pedal of the press to apply the forging process.
7. Take away the forged specimen from the press.
8. Record the data by using the software installed in the computer connected to the data acquisition system.

9. Apply the last six steps above until the forging processes to get one final height value for a group of specimens with the same initial height finishes.
10. For getting the following final height for the group of specimens with the same height value, repeat the steps from 1 to 9.

## **D.2 Applying the Cook and Larke Simple Compression Test for Specimens with Initial Diameter of 50 mm and the Height of 100 mm.**

This section contains applications for the specimens with initial diameter 50 mm and initial height 100 mm to be forged to final height values 95 mm, 90 mm, 80 mm, 70 mm and 60 mm respectively.

1. Adjust the ram to 1 mm.
2. Hold the heated billet with a tong and put it in front of the fixed pyrometer. Read the temperature of the billet and record it.
3. Put the heated billet on the lower die.
4. If necessary, measure the temperature of the dies with the portable pyrometer and record it.
5. Press the pedal of the press to apply the forging process.
6. Take away the forged specimen away from the press.
7. Record the data by using the software installed in the PC.
8. Apply the last six steps until the forging process to 95 mm height finishes.
9. Adjust the ram to 6 mm.
10. Hold the heated billet with a tong and put it in front of the fixed pyrometer. Read the temperature of the billet and record it.
11. Put the heated billet on the lower die.
12. If necessary, measure the temperature of the dies with the portable pyrometer and record it.
13. Press the pedal of the press to apply the forging process.
14. Take away the forged specimen away from the press.

15. Record the data by using the software installed in the PC.
16. Apply the last six steps until the forging process to 90 mm height finishes.
17. Put the insert with 10 mm height into the cavity of the lower die.
18. Hold the heated billet with a tong and put it in front of the fixed pyrometer.  
Read the temperature of the billet and record it.
19. Put the heated billet on the insert in the lower die.
20. If necessary, measure the temperature of the dies with the portable pyrometer and record it.
21. Press the pedal of the press to apply the forging process.
22. Take away the forged specimen away from the press.
23. Record the data by using the software installed in the PC.
24. Apply the last six steps until the forging process to 80 mm height finishes.
25. Take out the insert with 10 mm height and put the insert with 20 mm height into the cavity of the lower die.
26. Hold the heated billet with a tong and put it in front of the fixed pyrometer.  
Read the temperature of the billet and record it.
27. Put the heated billet on the insert in the lower die.
28. If necessary, measure the temperature of the dies with the portable pyrometer and record it.
29. Press the pedal of the press to apply the forging process.
30. Take away the forged specimen away from the press.
31. Record the data by using the software installed in the PC.
32. Apply the last six steps until the forging process to 70 mm height finishes.
33. Take out the insert with 20 mm height and put the insert with 30 mm height into the cavity of the lower die.
34. Hold the heated billet with a tong and put it in front of the fixed pyrometer.  
Read the temperature of the billet and record it.
35. Put the heated billet on the insert in the lower die.
36. If necessary, measure the temperature of the dies with the portable pyrometer and record it.

37. Press the pedal of the press to apply the forging process.
38. Take away the forged specimen away from the press.
39. Record the data by using the software installed in the PC.
40. Apply the last six steps until the forging process to 60 mm height finishes.